SIDE CHANNEL SPILLWAYS

by

T.D. TIMM

A Thesis
presented in partial fulfilment of the
requirements for the degree of
MASTER OF SCIENCE
in
Civil Engineering
at the
University of Cape Town,
June, 1977.

Supervisor: Professor F.A. Kilner

To my mother

ACKNOWLEDGEMENTS

I should like to acknowledge the assistance received from my supervisor, Professor F.A. Kilner, and to thank him for his encouragement throughout this project

My thanks also to the workshop personnel for their assistance in the construction of the models and to Mrs. Gillian Rootman for giving up so much of her time to type this thesis.

SYNOPSIS

The design of side channel spillways has been discussed in detail by a number of investigators. In this thesis the most important works have been summarised, discussed and in some cases expanded in an attempt to give a concise account of the existing theories.

Model tests were carried out on a side channel spillway of general type as well as on the proposed Mtata dam spillway and the results are presented and discussed.

Charts were drawn up and a procedure was recommended for the design of side channel spillways in an attempt to provide a designer with a simple method of design which he can use with confidence.

CONTENTS

1. INTRODUCTION

The side channel spillway is a type of hydraulic structure which has many applications, especially with earth wall dams. The most obvious difference from other spillways is that the spillway crest is usually perpendicular to the dam wall. Water flowing over the spillway crest is collected in a channel running along its length which carries the water away.

The depth of flow in this receiving channel cannot be calculated in the usual way as the flow is not constant along its length. Indeed, water is added continuously along its length. This is an example of what is known as spatially varied flow.

Spatially varied flow occurs in a large variety of hydraulic structures and the discharge may increase or decrease in the direction of flow. Decreasing discharge is found mainly with side-weirs where water flowing along a pipe or channel is lost along its length due to spilling over a weir in its side. Increasing discharge is found in wash-water troughs in filters, effluent channels round sewage tanks, roof gutters, and side channel spillways. This thesis will deal mainly with the flow of water in the receiving channel of a side channel spillway.

This type of structure is particularly useful with earth wall dams where a conventional spillway cannot be used because of settlement of the wall. To be able to use a conventional free overfall spillway, the wall below the entire crest must be constructed in concrete. In most dams, the spillway is of considerable length and the use of the earth wall is thus negated. Another solution is the use of a bellmouth spillway but these are of limited capacity and for large dams, the only alternative is the side channel spillway.

Side channel spillways must be classified into two types, single sided and double sided spillways. Typical examples of each of these are shown in figures 1 and 2.

Traditionally, these structures were of the single sided type as shown in figure 1. The spillway is built at one end of the dam wall, running approximately along a contour of the hillside where the water is

TYPYICAL SIDE-CHANNEL SPILLWAYS.

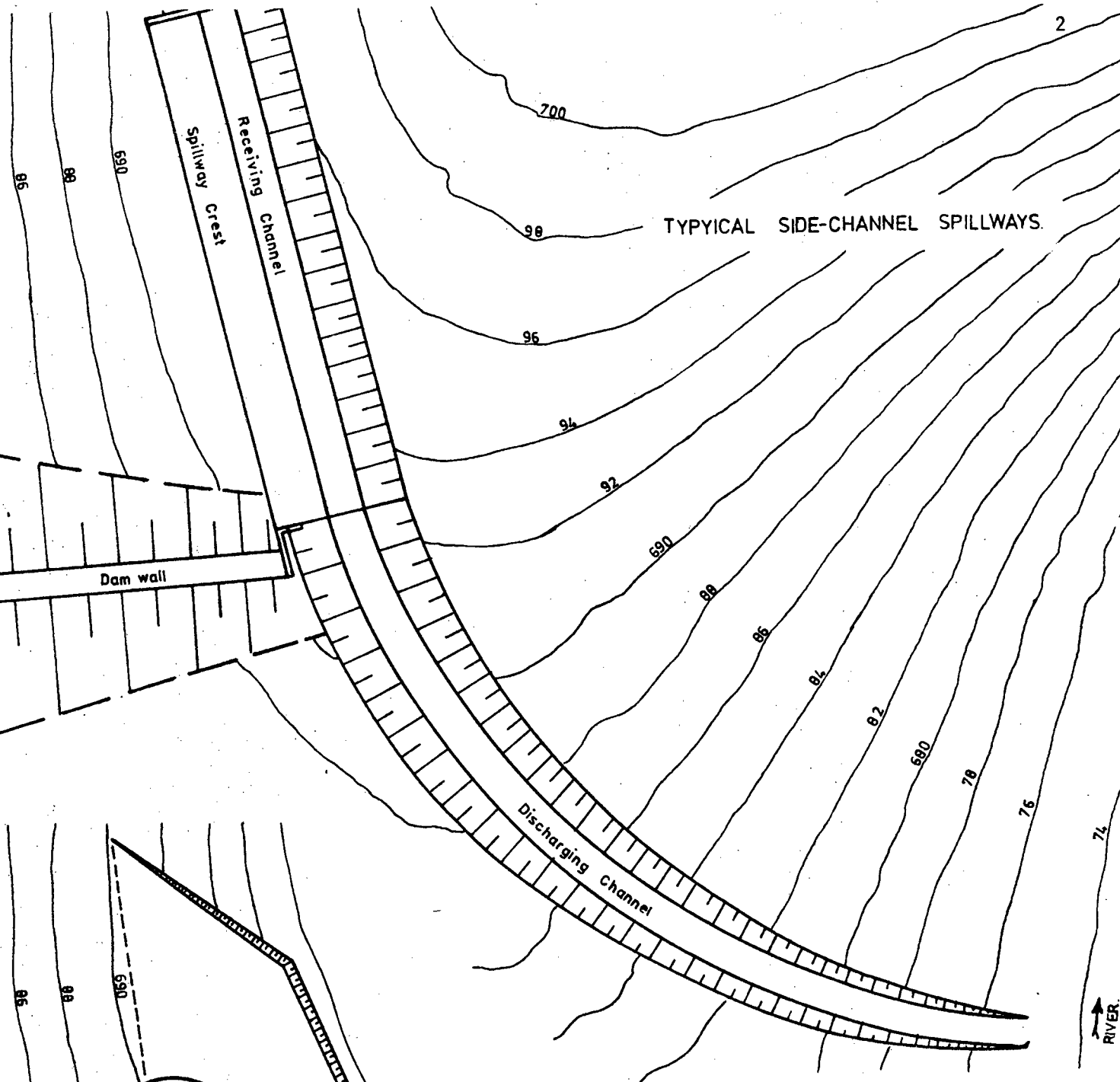

FIGURE 1 : Single sided spillway.

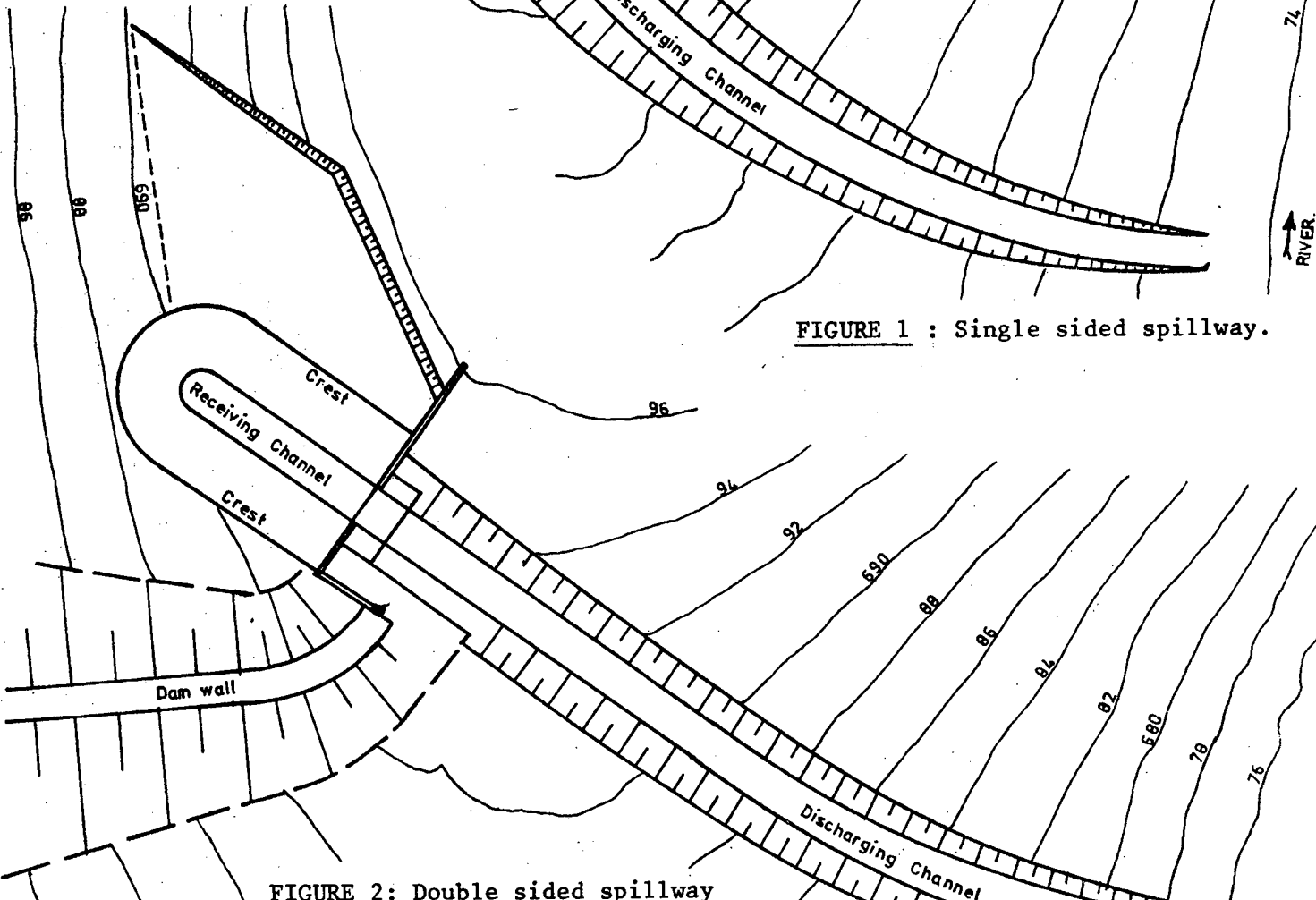

FIGURE 2: Double sided spillway

shallow. The receiving channel is excavated into the hillside and a relatively small amount of concrete is required. Usually a discharging channel or chute is required to carry the water back to the riverbed.

More recently, the double sided spillways have become popular. The main advantage of this type is that for the same length of spillway crest, the receiving channel is only half the length. The disadvantage of this type is that in order to allow the water to flow over both sides, the structure must be moved into deeper water resulting in a higher concrete structure, or else the approaches must be excavated out on the upper side. Either of these configurations results in increased cost which must be compared with the cost of the single sided type before deciding which to construct.

A list follows of some of the better known side channel spillways together with their dates of construction and capacities where these are available.

Solingen, Germany	1902	
Quielle, France	1904	
New Croton, New York City	1906	
Wachusett, Boston, Mass.	1906	
Rochebut, France	1909	
Cold Springs, Oregon	1910	
Conconully, Washington	1910	
Croton Falls, New York City	1910	
Sweetwater, San Diego, Calif.	1911	
Ashokan, New York City	1912	
Mauer, Germany	1912	
Oakley, Idaho	1913	
Moehne, Germany	1913	
Klingenberg, Bohemia	1914	
Cedar Lake, Seattle, Wash.	1914	
Morena, San Diego, Calif.	1915	
Arrowrock, Idaho	1915	1133 cumecs
Don Pedro, California		
Burrinjuck, N.S. Wales	1916	
Teiton, Washington		
McKay, Oregon		
Nooitgedacht, Carolina, E. Tvl.	1962	1586 cumecs
Nuane, Lobatsi, Botswana	1965	850 cumecs
Mtata, Transkei,	under construction	2430 cumecs

2. SYMBOLS

All symbols used are defined in the text where they first appear but are listed below for easy reference. It should be noted that where material has been quoted from other published works symbols sometimes have different meanings but these are clearly defined in the text.

A	cross-sectional area of flow
b	base width of a trapezoidal or rectangular channel
B	width of water surface
d	water depth
d_c	critical depth
d_o	normal depth
f	Darcy-Weisbach friction factor
F	frictional drag per unit area of channel wall
Fr	Froude Number
g	acceleration due to gravity
H_o	water depth at upstream end of channel
IM	hydraulically mild slope with lateral *inflow* along its length
IS	hydraulically steep slope with lateral *inflow* along its length
L	horizontal length of receiving channel
M	momentum
n	Manning's friction factor
p	wetted perimeter
P	static pressure
q	lateral inflow per unit length of channel
Q	total discharge at any point x, = qx
R	hydraulic radius = A/p
S_o	uniform invert slope of channel
S_f	head lost by friction per unit length
V	horizontal velocity of water
w	specific weight of water
x	horizontal distance from upstream end
x_c	horizontal distance to the control point
y	vertical distance of water surface from a horizontal datum
α	energy coefficient
α_{mn}	accelerating force on water prism mn
β	momentum correction factor
θ	angle of side wall of channel to vertical

3. HYDRAULIC THEORY

3.1 The Basic Equation

Although a number of semi-empirical equations had been used previously, the first correct theoretical analysis of this problem was done in 1926 by Hinds[1] who made use of the principle of conservation of linear momentum to find a differential equation which described the water surface profile in a side channel spillway. In this analysis, the effect of friction was neglected, but this was later remedied by Faure[3] and Camp[5] who derived equations including this effect.

Camp's equation was derived as follows: For a rectangular flume of width b (figure 3), consider two vertical cross-sections at sections m and n, a distance Δx apart. The momentum at section m, for the mass per second, is

$$M_m = \frac{QwV}{g} \qquad \ldots\ldots (1)$$

in which Q, the discharge at section m, equals qx; q is the constant increment of inflow per unit length; w is the unit weight of water; g is the acceleration due to gravity; and V is the horizontal component of the mean velocity at section m. The momentum at section n for the mass per second is

$$M_n = \frac{(Q + q\Delta x)w(V + \Delta V)}{g} \qquad \ldots\ldots (2)$$

The change in momentum in the distance Δx is

$$\Delta M = \frac{w}{g} [Q\Delta V + q\Delta x(V + \Delta V)] \qquad \ldots\ldots (3)$$

or, neglecting the product $\Delta x\Delta V$ and expressing equation 3 in terms of differentials

$$dM = \frac{w}{g} (QdV + qVdx) \qquad \ldots\ldots (4)$$

since

$$\frac{dM}{dt} = \frac{dM}{dx}\,\frac{dx}{dt} = V\,\frac{dM}{dx},$$

$$\frac{dM}{dt} = \frac{w}{g} \left(VQ\,\frac{dV}{dx} + qV^2\right) \qquad \ldots\ldots (5)$$

in which dM is the change in momentum in the time dt.

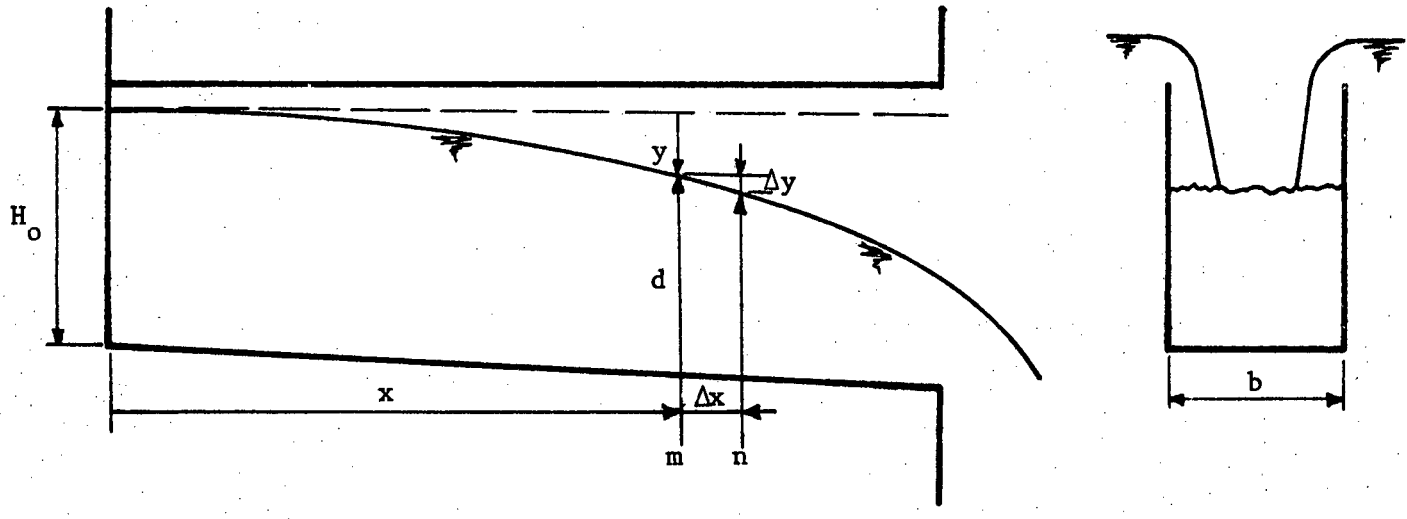

Figure 3

Equation (5) gives the time rate of change of linear momentum at any section, m, for the mass of water flowing per second. This is equal to the net force in the direction of x producing the change. The net force in the direction of x acting upon the volume of water between sections m and n is the difference between the static pressures less the friction force. The static pressures at sections m and n are

$$P_m = \frac{bwd^2}{2} \quad \ldots\ldots \quad (6)$$

$$P_n = \frac{bw}{2}(d - \Delta y + S_o\Delta x)^2 = \frac{bw}{2}(d^2 - 2d\Delta y + 2dS_o\Delta x) \quad \ldots\ldots \quad (7)$$

in which S_o = the slope of the bottom. The horizontal component of the static pressure on the bottom is

$$P_b = bw\left(\frac{2d - \Delta y + S_o\Delta x}{2}\right) S_o\Delta x = wbdS_o\Delta x \quad \ldots\ldots \quad (8)$$

The net static pressure on the water prism mn is the summation of equations (6), (7) and (8), or

$$P_m - P_n + P_b = wbd\Delta y \quad \ldots\ldots \quad (9)$$

It will be noted that the slope of the bottom has no effect upon the value of the net pressure. It may be shown also that a changing width b has no influence on the value of this force.

The friction drag is

$$P_F = F(b + 2d)\Delta x = \frac{Fbd\Delta x}{R} \quad \ldots\ldots \quad (10)$$

in which F = frictional drag per unit area of channel wall, and R = the hydraulic radius at section m. The equivalent water head on the area bd corresponding to the friction drag P_F is

$$\text{Head} = \frac{P_F}{wbd} = \frac{Fbd\Delta x}{wbdR} = \frac{F\Delta x}{wR} \quad \ldots\ldots \quad (11a)$$

and from the Darcy-Weisbach formula, this lost head is also given by

$$\text{Lost head} = \frac{f\Delta xV^2}{2Rg} \quad \ldots\ldots \quad (11b)$$

Hence, from equation (11),

$$F = \frac{wfV^2}{2g} \quad \ldots\ldots \quad (12)$$

in which f = the Darcy-Weisbach friction factor.
From equations (10) and (12)

$$P_F = \frac{wfV^2}{2g} \frac{bd}{R} \Delta x \quad \ldots\ldots \quad (13)$$

The net accelerating force on the water prism mn, from equation (9) and (13),

$$\alpha_{mn} = wbd\Delta y - \frac{wfV^2}{2g} \frac{bd}{R} \Delta x$$

and since the volume of water between sections m and n is

$$bd\Delta x = \frac{\Delta x}{V} Q \quad \ldots\ldots \quad (15)$$

The accelerating force on the water flowing per second (that is, Q) is

$$\frac{V}{\Delta x} (wbd\Delta y - \frac{wfV^2}{2g} \frac{bd}{R} \Delta x) = wQ \frac{\Delta y}{\Delta x} - \frac{wQfV^2}{2gR} \quad \ldots\ldots \quad (16)$$

Expressing equation (16) in terms of differentials and equating to equation (5):

$$\frac{dy}{dx} - \frac{fV^2}{2gR} = \frac{1}{g} (V \frac{dV}{dx} + q \frac{V^2}{Q}) \quad \ldots\ldots \quad (17)$$

This equation is general for any shape of channel, and it is identical with Hinds' original equation except for the friction term.

It should be noted that the friction factor used in the original publication is the American friction factor which is four times that used here. The friction term in Camp's paper therefore read:

$$\frac{fV^2}{8gR}$$

This equation can be written in a more familiar and convenient form if a number of substitutions are made.

$$V = \frac{Q}{A} \quad \ldots\ldots (18)$$

$$\frac{dV}{dx} = \frac{q}{A} - \frac{Q}{A^2}\frac{dA}{dx} \quad \ldots\ldots (19)$$

$$= \frac{q}{A} - \frac{Q}{A^2}\frac{dA}{dd}\cdot\frac{dd}{dx} \quad \ldots\ldots (20)$$

$$= \frac{q}{A} - \frac{QB}{A^2}\frac{dd}{dx} \quad \ldots\ldots (21)$$

where A is the cross-sectional area and B the width of the water surface at a distance x from the upstream end. The water depth measured from the bottom of the channel is d and the depth at the upstream end is H_o, therefore

$$y = H_o + S_o x - d \quad \ldots\ldots (22)$$

$$\frac{dy}{dx} = S_o - \frac{dd}{dx} \quad \ldots\ldots (23)$$

If equations (18), (21) and (23) are substituted into equation (17)

$$S_o - \frac{dd}{dx} = \frac{1}{g}\left[\frac{Q}{A}\left(\frac{q}{A} - \frac{QB}{A^2}\frac{dd}{dx}\right) + \frac{qQ}{A^2}\right] + \frac{fQ^2}{2gRA^2} \quad \ldots\ldots (24)$$

This can be rearranged to give

$$\frac{dd}{dx} = \frac{S_o - \frac{fQ^2}{2gA^2R} - \frac{2qQ}{gA^2}}{1 - \frac{Q^2B}{gA^3}} \quad \ldots\ldots (25)$$

It can be recognised that $fQ^2/2gA^2R = S_f$, the friction slope or the head lost per unit length, and $Q^2B/gA^3 = Fr^2$ where Fr is the well known Froude

The equation can therefore be written as

$$\frac{dd}{dx} = \frac{S_o - S_f - \frac{2qQ}{gA^2}}{1 - Fr^2} \quad \ldots\ldots \quad (26)$$

This equation is based on the assumptions that the incoming water has no momentum component in the direction parallel to the channel, and that the effect of unequal velocity distribution in the channel is negligible.

In Hinds' example, these were reasonable assumptions, but Farney and Markus[11] studied a side channel spillway with an L-shaped crest where the water entered over the upstream section as well as along the length of the channel. In this case the incoming water had appreciable momentum in the direction of flow and the velocity variations near the upstream end were pronounced. Hinds' assumptions could therefore not be made. This was remedied by the inclusion of a momentum correction factor, β. This factor varied from near unity at the downstream end to a maximum at the upstream end, and was found empirically. Although it may be necessary to include this factor with spillways of this type, it is usually ignored where there is no inflow over the upstream end, as β is then, for practical purposes, equal to unity along the whole channel.

The general equation, including the momentum correction factor, is

$$\frac{dd}{dx} = \frac{S_o - S_f - \frac{2q^2x\beta}{gA^2} - \frac{V^2}{g}\frac{d\beta}{dx}}{1 - \frac{q^2x^2B\beta}{gA^3}} \quad \ldots\ldots \quad (27)$$

If β is assumed to be unity, then this equation obviously reduces to the one above. The derivation of this equation has appeared in a number of references, for example Chow,[20] and will not be given here.

K Smith[15] used the energy principle (see figure 4) to derive a very similar equation, namely

$$\frac{dd}{dx} = \frac{S_o - S_f - \frac{2q^2x\alpha}{gA^2}}{1 - \frac{q^2x^2B\alpha}{gA^3}} \quad \ldots\ldots \quad (28)$$

where α is the energy coefficient.

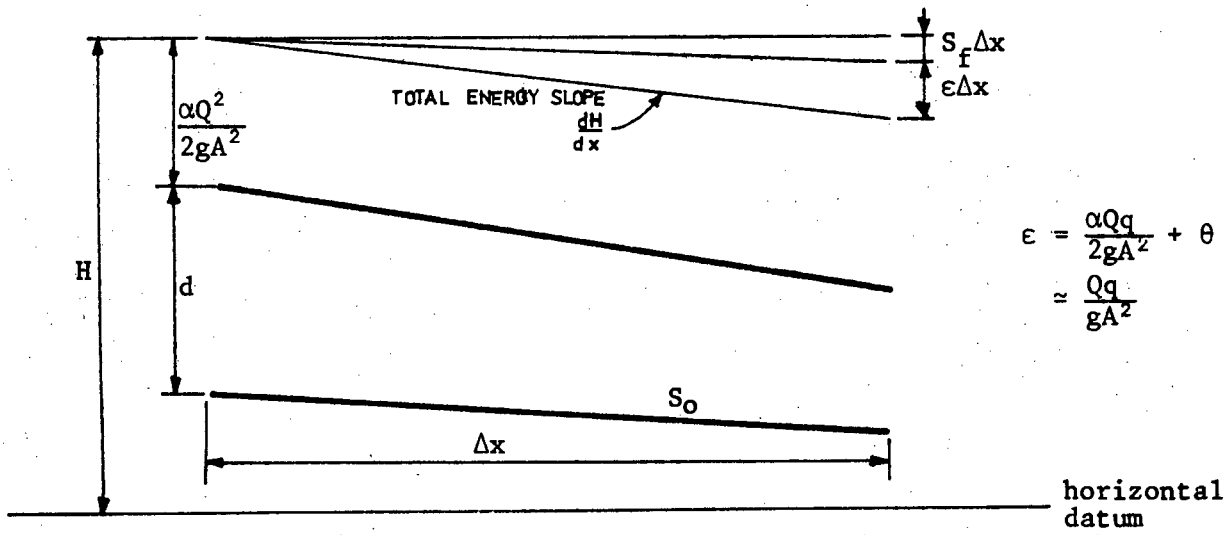

Figure 4

Although this is very similar to the equation above, it does not have a term accounting for the variation of α with x. In a discussion on Smith's paper, Babb and Ross[15] gave a more rigorous analysis to get

$$\frac{dd}{dx} = \frac{S_o - S_f - \frac{3}{2}\frac{q^2 x \alpha}{gA^2} - \theta - \frac{V^2}{2g}\frac{d\alpha}{dx}}{1 - \frac{q^2 x^2 B \alpha}{gA^3}} \quad \ldots\ldots \quad (29)$$

where θ represents the dissipated energy. To determine θ it is necessary to compare this equation with the momentum equation above. If α and β are unity, then $\theta = q^2x/2gA^2$

Babb and Ross also presented some experimental values for α and β which they obtained from velocity patterns measured at three cross-sections of their model channel. These results are shown in figure 5.

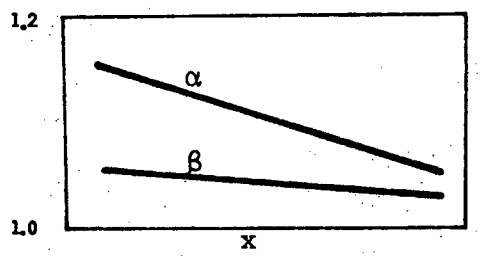

Figure 5

They used these values of α and β to calculate the water surface profile and compared this to that obtained by assuming both coefficients equal to unity. From the relatively small differences between the two profiles, they concluded that this is a satisfactory approximation in most applications. These coefficients will therefore be ignored in the following discussion.

Equation (26), in whatever form it is written, can not be solved directly but must be integrated numerically for a particular case, starting from some known point.

3.2 The Control Point

If, for a certain flow condition, the channel slope is mild (to be defined later), then the known point will be at the end of the channel and will depend on downstream conditions. If there is a free outfall or if the invert slope becomes steep at the end of the spillway, and the channel is not drowned, then the depth at the downstream end, will be critical. This is the usual case.

However, if the channel is "steep", then supercritical flow will occur in the lower section of the receiving channel and the control point will move to where the water surface crosses the critical depth line. This point can be found and can be used as the starting point for the numerical integration of the equation.

At this point, the depth is equal to the critical depth so the Froude number is equal to unity. However, this makes the denominator of equation (26) equal to zero. As dd/dx cannot be infinite, the numerator must also be zero at this point.

Keulegan,[9] studied the possibility of this slope being infinite but showed that it would have to occur in the form of a negative hydraulic jump. However, just as in a normal hydraulic jump energy is lost, so in a negative hydraulic jump, energy is gained. This is impossible in a real channel so one can conclude that the slope must be finite and to solve for the critical point, one must solve the simultaneous equations

$$1 - Fr^2 = 0 \qquad \ldots\ldots (30)$$

$$S_o - S_f - \frac{2q^2x}{gA^2} = 0 \qquad \ldots\ldots (31)$$

i.e. one must find the point where the lines described by these two equations cross.

The first is the well known critical depth line and is calculated in the same way as with conventional channel flow except that the flow varies along the channel. The critical depth therefore also varies from zero at the upstream end (if there is no flow over the upstream end) to a maximum at the end of the spillway.

Fox and Goodwill[18] called the line described by equation (31) the "energy balance line", but Professor Kilner prefers to talk of the "pseudo normal depth line" because of the similarity in behaviour to the normal depth line in non-spatially varied flow.

Fox and Goodwill claim that the concept of normal depth is meaningless in spatially varied flow, but this is only true if one limits the definition of normal depth to being the depth to which the water will tend in a long uniform channel. However, as described below, the interaction of this line with the water surface and with the critical depth line, is very similar to that found in non-spatially varied flow. As the latter is simply a special case of spatially varied flow with zero inflow ($q = 0$) it seems reasonable to extend the idea of the normal depth line to the general case. For the purposes of this thesis, therefore, the line defined by equation (31) will be called the normal depth line. The interaction of these lines as shown in figure 6, can be easily seen. From equation (30), for rectangular channels,

$$1 - \frac{q^2x^2}{gb^2d_c^3} = 0 \qquad \ldots\ldots (32)$$

where d_c is the critical depth. It can therefore be seen that

$$d_c = K_1 x^{\frac{2}{3}} \qquad \ldots\ldots (33)$$

Similarly, from equation (31), neglecting friction,

$$S_o - \frac{2q^2x}{gb^2d_o^2} = 0 \qquad \ldots\ldots (34)$$

where d_o is the normal depth

$$d_o = k_2 x^{\frac{1}{2}} \qquad \ldots\ldots (35)$$

thus $$\frac{d_o}{d_c} = \frac{k_2 x^{\frac{1}{2}}}{k_1 x^{\frac{2}{3}}} \propto \frac{1}{x^{\frac{1}{6}}} \qquad \ldots\ldots (36)$$

As x tends to zero, d_o/d_c becomes very large. It can thus be concluded that the normal depth is always greater than the critical depth near the upstream end. Further downstream, however, the difference in powers has a progressively increasing effect until the two lines eventually cross and the normal depth is thereafter below the critical depth line.

The crossing point of these two lines is found for rectangular channels, ignoring friction, by equating equations (33) and (35). Ignoring the solution at x = 0, only one solution can be found, namely

$$x_c = \left(\frac{K_2}{K_1}\right)^6 \qquad \left(\frac{k_2}{k_1}\right)^6$$

It can therefore be concluded that suggestions which have been made, that these two lines could cross again, are unfounded in the case of prismatic channels. Only with severe changes of cross section and invert slope, is more than one control point possible.

In short channels, these curves are often terminated before they cross. Beyond the spillway, in the discharging channel, these curves can be represented by two straight lines, being the critical depth line and the normal depth line as defined in conventional channel flow.

Even if there is a change in slope at the end of the receiving channel, the critical depth line is continous, having only an abrupt change in the gradient at the end of the spillway. The normal depth line, however, is dependent on both the invert slope and on the lateral inflow so it consists of two discrete lines with a definite vertical shift at the end of the spillway. If these two sections are joined by a vertical line at this point, then in the case of a steep discharging channel, the water surface, the critical depth line, and the normal depth line once again all intersect at this, the control point.

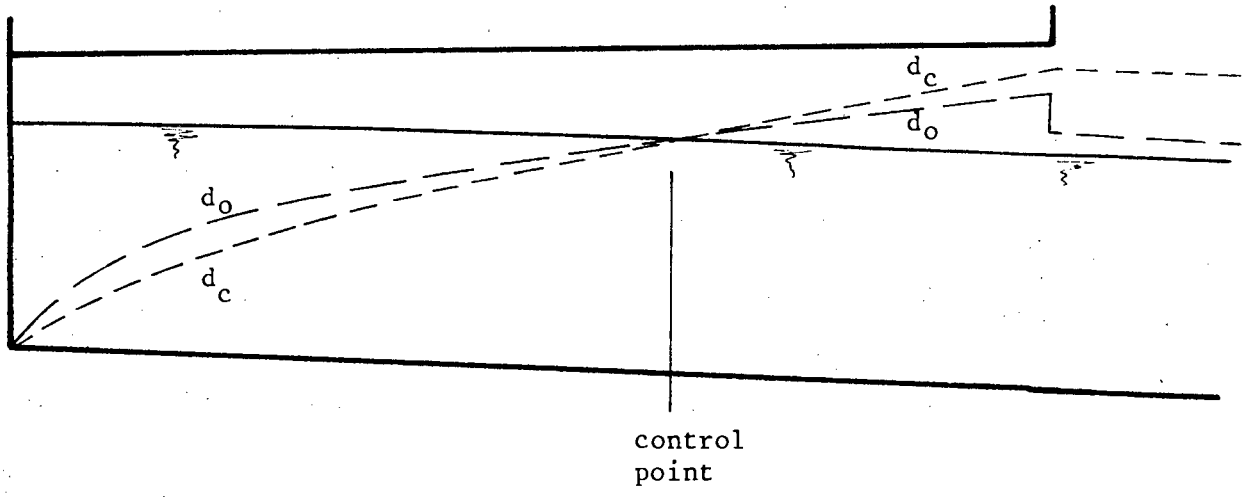

Figure 6a : A Natural Control Point.

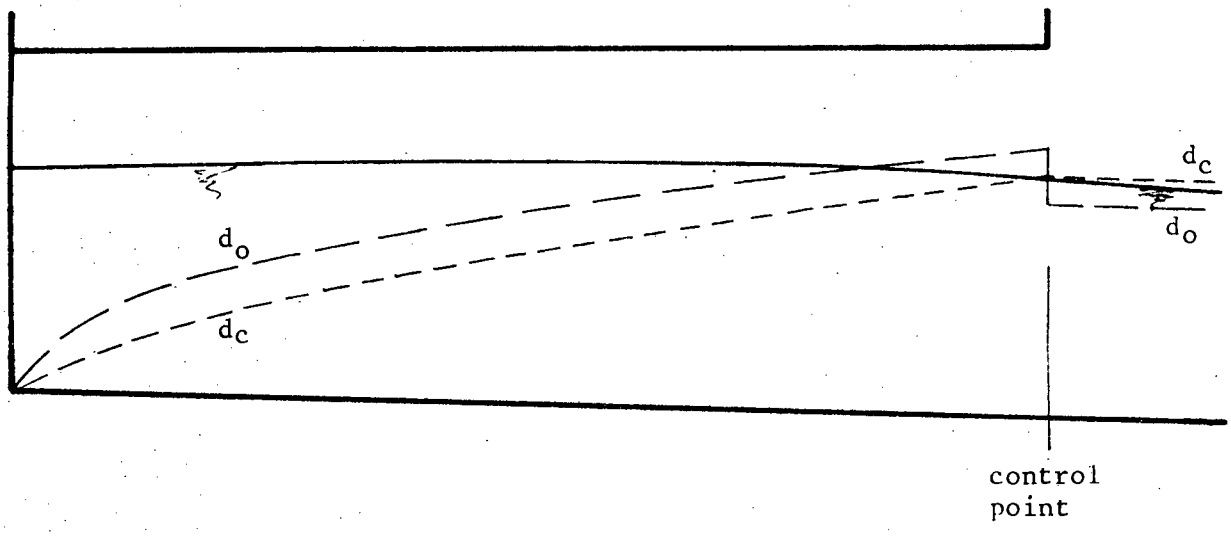

Figure 6b : An Artificial Control Point.

We can thus define two types of control point.

(i) A Natural Control Point is one at which the normal depth line and the critical depth line intersect, and are continuous. (Figure 6a).

(ii) An Artificial Control Point is one at which the normal depth line and the critical depth line intersect due to a vertical shift in the normal depth line. This shift may be due to a sudden cessation of lateral inflow or due to a discontinuity in the channel. (Figure 6b).

3.3 Surface Profiles

Before any calculations of water surface profiles are done, it is possible, as in the case of conventional channel flow, to comment on their general form and to identify various shapes.

Looking at equation (25) it can be seen that:

(i) If d tends to infinity, dd/dx tends to S_o and the water surface is horizontal.

(ii) If d tends to d_c, the critical depth, dd/dx tends to infinity, thus profiles tend to cross the critical depth line at a very large angle. (This is not true at a natural control point where $d_o = d_c$).

(iii) If d tends to d_o, the normal depth, dd/dx tends to zero (except where $d_o = d_c$). It should be noted that this will not result in a profile asymptotic to the normal depth line as in conventional channel flow.

(iv) If x tends to zero, dd/dx tends to S_o. The water surface is thus horizontal at the upstream end.

Because of the importance of the critical and normal depths in the dd/dx equation, channel slopes are classified, as in conventional channel flow, in the following manner.

If the normal depth is less than the critical depth, the channel is STEEP. If the normal depth is greater than the critical depth, the channel is MILD.

To differentiate from conventional flow, these slopes are referred to by the symbols IM and IS respectively. It should be remembered that the criterion for slope classification is a hydraulic one and all slopes, whatever their gradient, are mild near their upstream end. Because side channel spillways are relatively short, only this upstream section usually exists, and steep slopes are rare. It should also be noted, that because of the extra term in the numerator of equation (25), the normal depth is raised in spatially varied flow, and thus many slopes which would be steep in conventional flow, become mild.

For both mild and steep slopes, there are three zones as in conventional channel flow.

Zone 1 : The water surface is above both the critical and the normal depth lines.

Zone 2 : The water surface is between the critical and the normal depth lines.

Zone 3 : The water surface is below both the critical and the normal depth lines.

As in conventional channel flow, only one particular type of water surface profile is possible in each zone for each type of slope. Each profile has a code consisting of a letter denoting the type of slope and a number denoting the zone in which the water surface occurs. The sign of dd/dx in each zone can be calculated and, combined with the limiting conditions given earlier, gives the general shape of each of the six possible profiles which are shown in figure 7. Practical examples of how they can occur are shown in figure 8.

Horizontal and adverse slopes are a particular case of the mild slope and have the same profiles but because the normal depth is infinite in these cases, there can be no M1 profile.

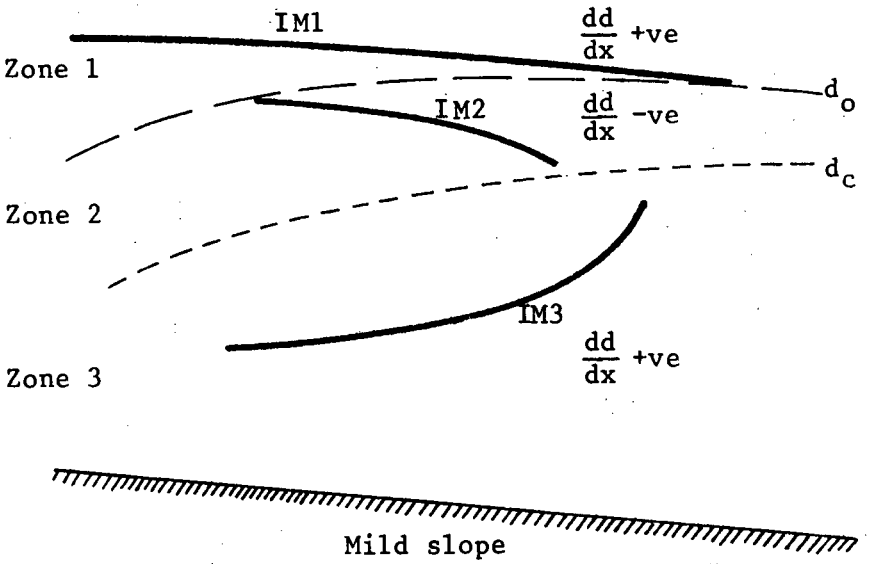

NOTE: The water surface always crosses the d_o line at $dd/dx = S_o$. i.e. parallel to the bottom.

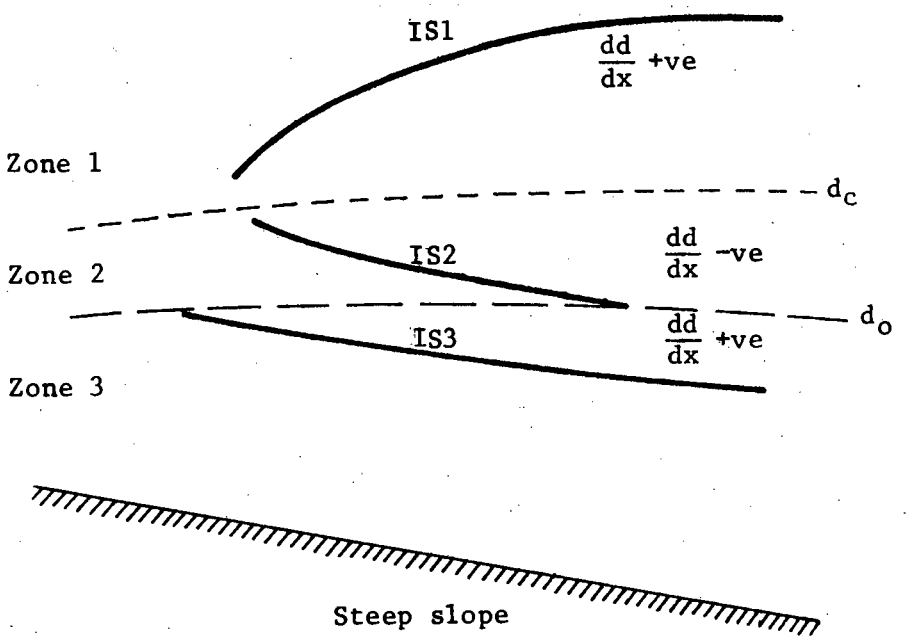

Figure 7 : Types of water surface profile

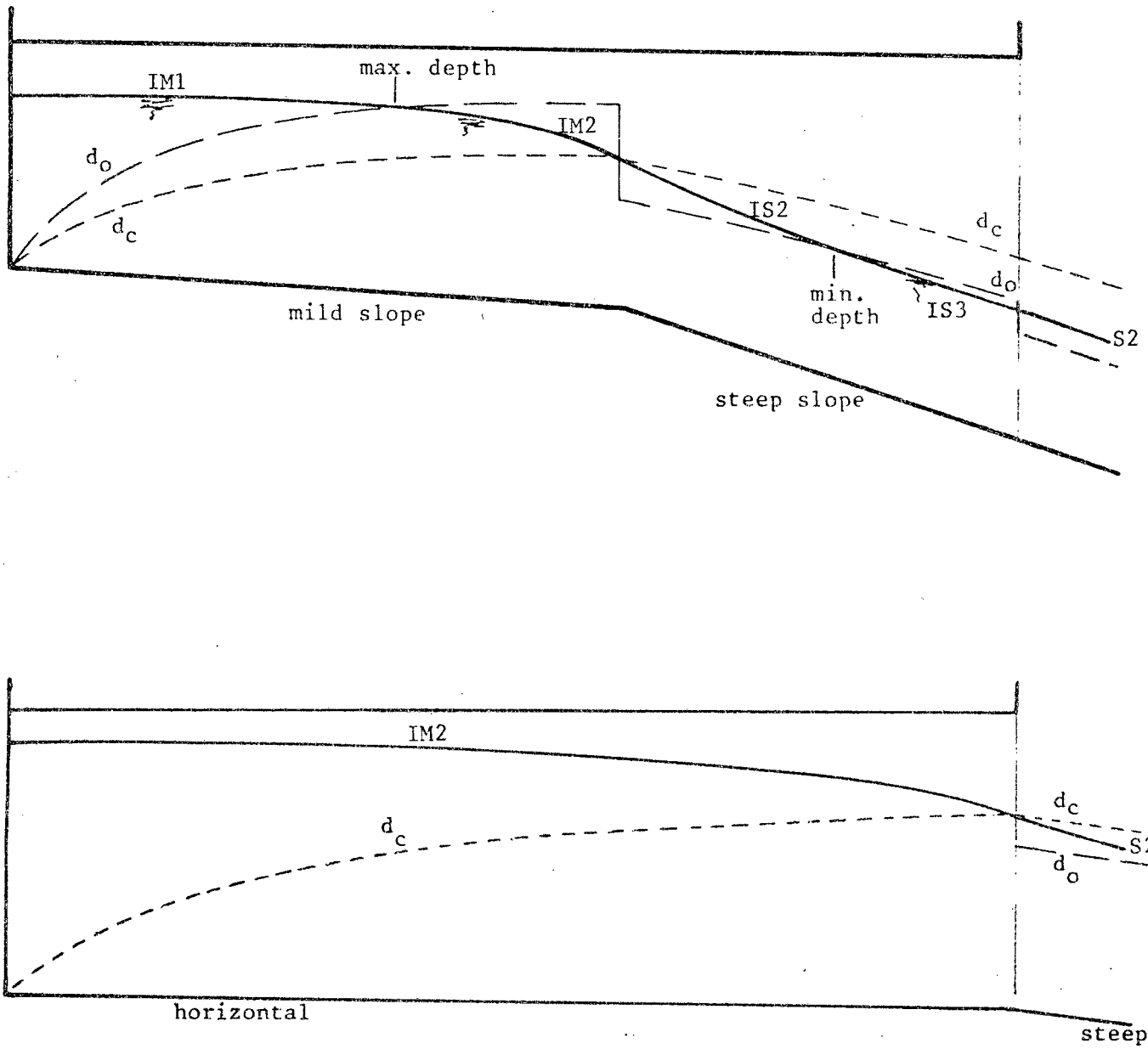

FIGURE 8a : Examples of how different profiles can occur.

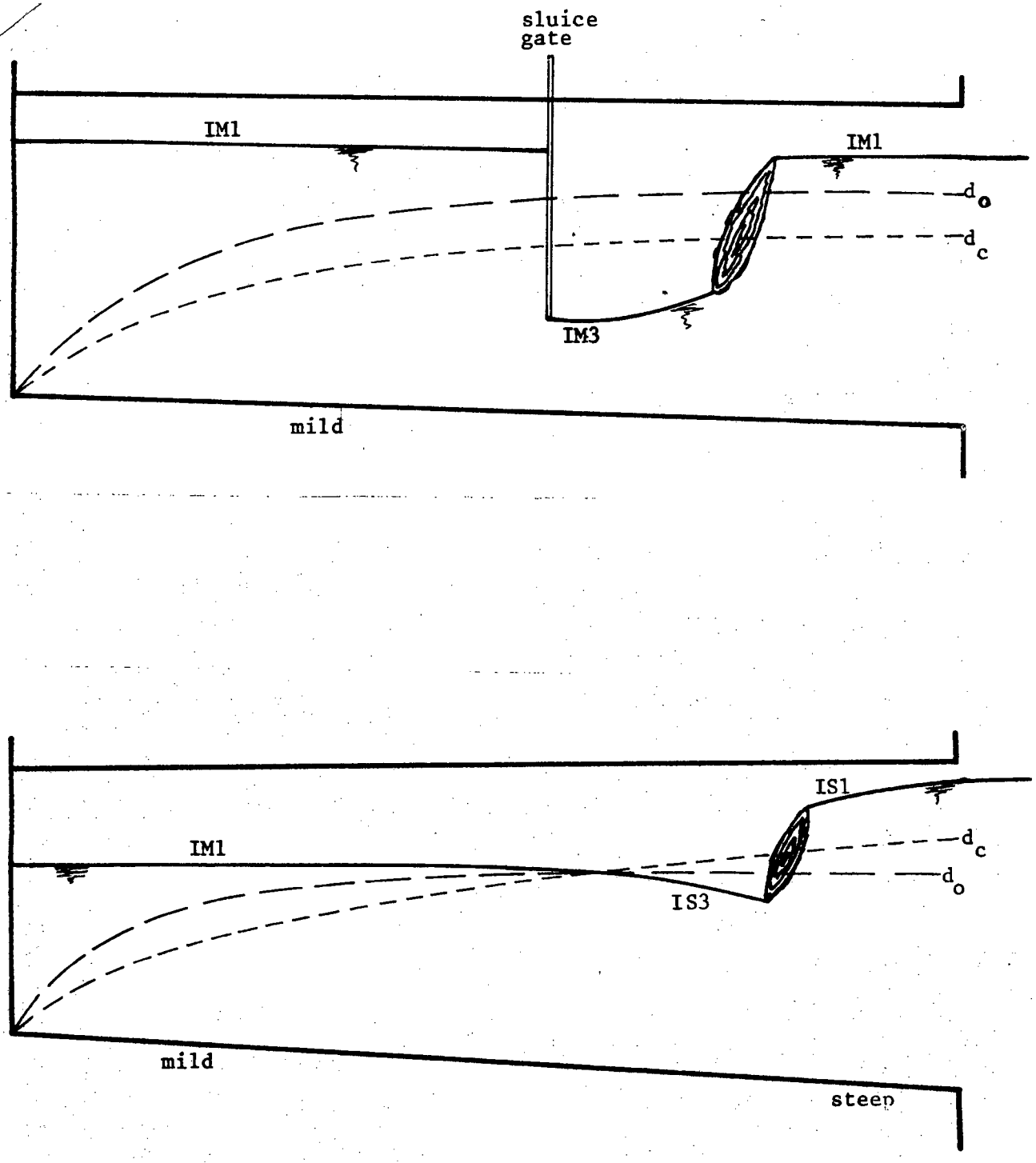

FIGURE 8b : Examples of how different profiles can occur.

3.4 Solution of the Differential Equation

Once the control point has been found, it is possible to find numerically, the solution of the differential equation (25). However, a problem arises in the fact that the control point is a singular point where the water surface slope dd/dx, cannot be easily evaluated.

At an artificial control point, the denominator of equation (25) is zero, while at a natural control point, both the denominator and numerator are zero. It is therefore often necessary to make some sort of approximation at this point. This will be discussed in more detail later.

Finding the control point and solving the equation, if done without the use of a computer, is a long and tedious process, and numerous attempts have been made at finding a quick solution. Some of the methods proposed will be discussed below.

Hinds[1] rewrote equation (17) to make it applicable, approximately, to finite values of Δx in the form

$$\Delta y = \frac{Q_1}{g} \frac{(V_1+V_2)}{(Q_1+Q_2)} \left[\Delta V + \frac{qV_2\Delta x}{Q_1}\right] \quad \ldots\ldots \quad (37)$$

or

$$\Delta y = \frac{Q_2}{g} \frac{(V_1+V_2)}{(Q_1+Q_2)} \left[\Delta V + \frac{qV_1\Delta x}{Q_2}\right] \quad \ldots\ldots \quad (38)$$

where Q_1 and Q_2 are the flows at either end of Δx and $\Delta V = V_2 - V_1$. He suggested also a method of locating the control point. He illustrated his method by means of the following example.

L = 400ft, b = 10ft, side slopes = 2:1, q = 40 cub. ft./sec, S_o = 0,15. The critical velocities and discharges corresponding to a number of depths are calculated as shown in table I. Hydraulic radii are computed at the same time for use in estimating friction losses. From table I, values of the critical depths and velocities may be taken and used in table II, which gives in column (13) the drop in water surface necessary to maintain flow at the critical depth throughout the full length of the channel. Starting from an arbitrary water surface elevation at some station, a profile of the channel, for critical flow at all points, can be plotted, as shown in figure 9. A tangent parallel to the bottom of the actual channel may then be drawn to the resulting bottom line of the

TABLE 1.—COMPUTATIONS FOR CRITICAL DEPTHS.
FOR CHANNEL IN FIG. 9

(Bottom width, 10 ft.; side slopes, $\frac{1}{2}$: 1)

Depth, in feet, d.	Area, in square feet, A.	Top width, in feet, T.	Velocity head, $\frac{A}{2T}$	Critical velocity, in feet per second.	Discharge, Q.	Hydraulic radius, in feet.
2	22	12	0.92	7.68	169	1.52
4	48	14	1.71	10.49	504	2.53
6	78	16	2.44	12.53	978	3.33
8	112	18	3.11	14.15	1 585	4.01
10	150	20	3.75	15.58	2 330	4.63
12	192	22	4.36	16.75	3 216	5.22
14	238	24	4.96	17.86	4 252	5.70
16	288	26	5.54	18.88	5 440	6.29
18	342	28	6.11	19.82	6 780	6.82
20	400	30	6.67	20.71	8 284	7.31
22	462	32	7.22	21.55	9 960	7.81
24	528	34	7.76	22.34	11 800	8.29
26	598	36	8.31	23.12	13 820	8.77
28	672	38	8.84	23.84	16 020	9.26

TABLE 2.—COMPUTATIONS FOR LOCATING CONTROL.
FOR CHANNEL IN FIG. 9

(Bottom width, 10 ft.; side slopes, $\frac{1}{2}$: 1.)

$$\Delta y = \frac{Q_1 (V_1 + V_2)}{g (Q_1 + Q_2)} \left\{ \Delta V + \frac{b V_2 \Delta x}{Q_1} \right\}$$

x	Δx	Q	$Q_1 + Q_2$	d_c	V_c	$V_1 + V_2$	ΔV	$\frac{b V_2 \Delta x}{Q_1}$	$\Delta V + \frac{b V_2 \Delta x}{Q_1}$	Δy	h_f*	$\Delta y + h_f$
(1)	(2)	(3)	(4)	(5)	(6)	(7)	(8)	(9)	(10)	(11)	(12)	(13)
0												
10	10	400	400	3.4	10.0	10.0	10.0				0.03	
25	15	1 000	1 400	6.2	12.5	22.5	2.5	18.8	21.3	4.25	0.04	4.29
50	25	2 000	3 000	9.2	14.9	27.4	2.4	14.9	17.3	4.91	0.08	4.99
100	50	4 000	6 000	13.5	17.6	32.5	2.7	17.6	19.3	6.77	0.15	6.92
150	50	6 000	10 000	16.9	19.3	36.9	1.7	9.6	11.3	5.21	0.15	5.36
200	50	8 000	14 000	19.7	20.6	39.9	1 3	6.8	8.1	4.33	0.15	4.48
250	50	10 000	18 000	22.1	21.6	42.2	1.0	5.4	6.4	3.74	0.15	3.89
300	50	12 000	22 000	24.2	22.4	44.0	0.8	4.5	5.3	3.30	0.15	3.45
350	50	14 000	26 000	26.2	23.2	45.6	0.6	3.8	4.6	3.04	0.15	3.19
400	50	16 000	30 000	28.0	23.8	47.0	0.6	3.4	4.0	2.79	0.15	2.88
....	.....	.....	.....	.....	.....	.....	.....	.....	.....	38.28	1.17	39.45

*h_f = friction loss, computation not shown.

TABLE 3.—COMPUTATIONS FOR BACK-WATER CURVE.
FOR CHANNEL IN FIG. 9.
(Bottom width, 10 ft.; side slopes, $\frac{1}{2}$: 1.)

x.	Δx.	Bottom elevation.	Trial Δy.	Surface elevation.	Depth, d.	Area, A.	Discharge, Q.	Velocity, V.	$Q_1 + Q_2$.	$\frac{Q_1}{g(Q_1+Q_2)}$.	$V_1 + V_2$.	ΔV.	$\frac{b V_2 \Delta x}{Q_1}$	$\Delta V + \frac{b V_2 \Delta x}{Q_1}$	Δy_m*	h_f.	$\Delta y_m + h_f$	Error.	Notes.
(1)	(2)	(3)	(4)	(5)	(6)	(7)	(8)	(9)	(10)	(11)	(12)	(13)	(14)	(15)	(16)	(17)	(18)	(19)	(20)
164		49.10	....	66.80	17.70	333.6	6 560	19.70	.....	.....	.....	....	.....	.....	....	....	....	....	.....
200	36	48.70	4.10	63.70	19.00	370.5	8 000	21.59	14 560	0.0171	41.29	1.89	3.55	5.44	3.82	0.12	3.94	0.16	.....
			4.50	62.30	18.60	359.0	.....	22.27	.....	.....	41.97	2.57	.....	6.12	4.40	....	4.52	0.02	
			4.45	62.25	18.65	360.4	.....	22.22	.....	.....	41.90	2.50	.....	6.05	4.34	....	4.46	0.01	O. K.
250	50	36.20	6.15	56.20	20.00	400.0	10 000	25.00	18 000	0.0173	47.20	2.80	4.44	7.24	5.92	0.18	6.10	0.05	
			6.22	56.18	19.98	397.9	.....	25.13	.....	.....	47.33	2.93	.....	7.37	6.03	....	6.21	0.01	O. K.
300	50	28.70	6.03	49.50	20.80	424.5	12 000	28.29	22 000	0.0170	53.42	3.16	4.19	7.35	6.08	0.24	6.32	0.29	
			6.40	49.78	21.08	431.4	.....	27.81	.....	.....	52.04	2.66	.....	6.85	6.16	....	6.42	0.02	
			6.39	49.79	21.09	431.7	.....	27.79	.....	.....	52.02	2.66	.....	6.85	6.16	....	6.40	0.01	O. K.
350	50	21.20	6.51	43.23	22.03	463.0	14 000	30.24	26 000	0.0168	58.08	2.45	3.97	6.42	6.24	0.30	6.54	0.02	
			6.48	43.26	22.06	463.9	.....	30.18	.....	.....	57.97	2.39	.....	6.36	6.18	....	6.48	0.00	O. K.
400	50	13.50	6.78	36.53	23.03	495.5	16 000	32.29	30 000	0.0166	62.47	2.11	3.73	5.89	6.10	0.35	6.45	0.28	
			6.92	36.34	22.84	489.2	.....	32.71	.....	.....	62.89	2.53	.....	6.31	6.58	....	6.93	0.01	O. K.

*$\Delta y = \frac{Q_1 (V_1 + V_2)}{g (Q_1 + Q_2)} \left\{ \Delta V + \frac{b V_2 \Delta X}{Q_1} \right\}$ = Column (11) × Column (12) × Column (15).....(24)

TABLE 3.—(*Continued.*)

x.	Δx.	Bottom elevation.	Trial Δy.	Surface elevation.	Depth, d.	Area, A.	Discharge, Q.	Velocity, V.	$Q_1 + Q_2$.	$\frac{Q_2}{g(Q_1+Q_2)}$.	$V_1 + V_2$.	ΔV.	$\frac{b V_1 \Delta x}{Q_2}$	$\Delta V + \frac{b V_1 \Delta x}{Q_2}$	Δy_m*	h_f†	$\Delta y_m + h_f$	Error.	Notes.
(1)	(2)	(3)	(4)	(5)	(6)	(7)	(8)	(9)	(10)	(11)	(12)	(13)	(14)	(15)	(16)	(17)	(18)	(19)	(20)
164		49.10	....	66.80	17.70	333.6	6 560	19.70	.....	.....	.....	....	.....	.....	....	....	....	....	.....
200	36	48.70	4.10	63.70	19.00	370.5	8 000	21.59	14 560	0.0171	41.29	1.89	3.55	5.44	3.82	0.12	3.94	0.16	.....
			4.50	62.30	18.60	359.0	.....	22.27	.....	.....	41.97	2.57	.....	6.12	4.40	....	4.52	0.02	
			4.45	62.25	18.65	360.4	.....	22.22	.....	.....	41.90	2.50	.....	6.05	4.34	....	4.46	0.01	O. K.
250	50	36.20	6.15	56.20	20.00	400.0	10 000	25.00	18 000	0.0173	47.20	2.80	4.44	7.24	5.92	0.18	6.10	0.05	
			6.22	56.18	19.98	397.9	.....	25.13	.....	.....	47.33	2.93	.....	7.37	6.03	....	6.21	0.01	O. K.
300	50	28.70	6.03	49.50	20.80	424.5	12 000	28.29	22 000	0.0170	53.42	3.16	4.19	7.35	6.08	0.24	6.32	0.29	
			6.40	49.78	21.08	431.4	.....	27.81	.....	.....	52.04	2.66	.....	6.85	6.16	....	6.42	0.02	
			6.39	49.79	21.09	431.7	.....	27.79	.....	.....	52.02	2.66	.....	6.85	6.16	....	6.40	0.01	O. K.
350	50	21.20	6.51	43.23	22.03	463.0	14 000	30.24	26 000	0.0168	58.08	2.45	3.97	6.42	6.24	0.30	6.54	0.02	
			6.48	43.26	22.06	463.9	.....	30.18	.....	.....	57.97	2.39	.....	6.36	6.18	....	6.48	0.00	O. K.
400	50	13.50	6.78	36.53	23.03	495.5	16 000	32.29	30 000	0.0166	62.47	2.11	3.73	5.89	6.10	0.35	6.45	0.28	
			6.92	36.34	22.84	489.2	.....	32.71	.....	.....	62.89	2.53	.....	6.31	6.58	....	6.93	0.01	O. K.

*$\Delta y = \frac{Q_2 (V_1 + V_2)}{g (Q_1 + Q_2)} \left\{ \Delta V + \frac{b V_1 \Delta X}{Q_2} \right\}$ = Column (11) × Column (12) × Column (15).....(25)

†h_f = friction head, computations not shown.

critical depth channel, and the control point will be located at this point of tangency. The back water curve may then be calculated both ways as illustrated in table III and plotted as shown in figure 9. Equation (37) is used in the upper part of table III, and equation (38) in the lower part, in order to take advantage of as many constant terms as possible.

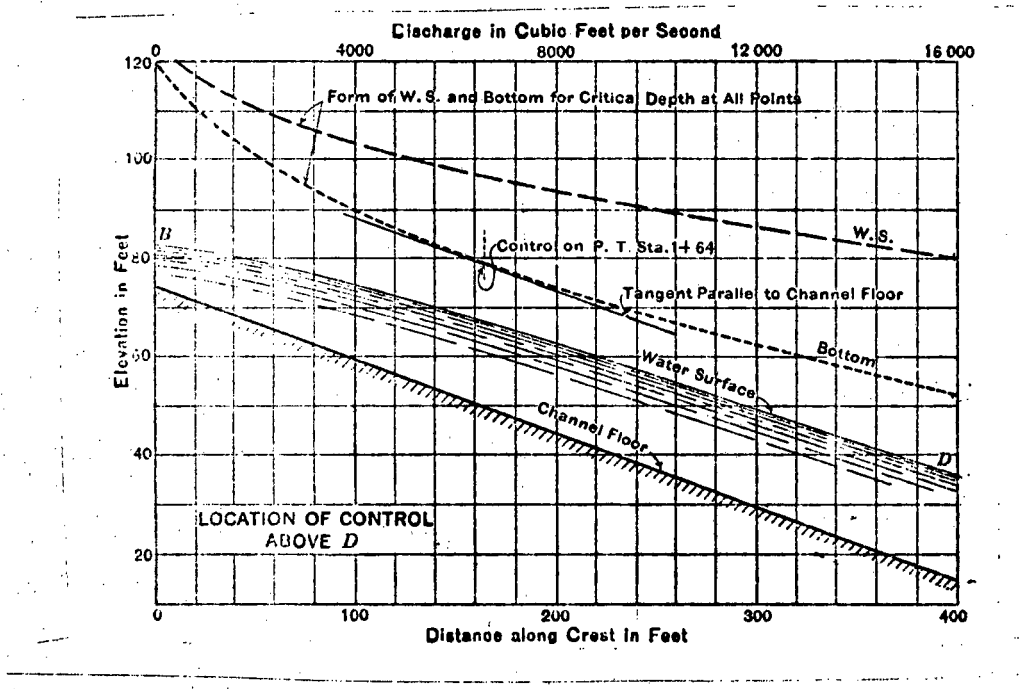

Figure 9

Hinds' method is long and tedious, and a quicker solution was necessary. Camp[5] did some useful work towards this end.

Equation (25) was solved approximately, for rectangular channels, to give

$$\frac{x^2}{d} - \frac{gb^2}{2q^2}(H_o^2 - d^2) = \frac{S_o x g b^2 \bar{d}}{q^2} - \frac{fx^3}{24\bar{R}\bar{d}} \qquad \ldots\ldots \quad (39)$$

where H_o is the value of d at x = 0 and $\bar{R}$ and $\bar{d}$ are, respectively, the average hydraulic radius and the average depth throughout the distance x. This equation can be rewritten in the form

$$H_o = \sqrt{d^2 + \frac{2Q^2}{gb^2d} - 2S_o x\bar{d} + \frac{fxQ^2}{12gb^2\bar{R}\bar{d}}} \quad \ldots\ldots \quad (40)$$

This equation can be used to solve for the depth at the upstream end if the depth at any other point is known. Equation (39) can be rearranged to read

$$\left(\frac{d}{H_o}\right)^3 + A\left(\frac{d}{H_o}\right) + B = 0 \quad \ldots\ldots \quad (41)$$

where $$B = \frac{2Q^2}{gb^2H_o^3} \quad \ldots\ldots \quad (42)$$

$$A = \frac{fH_o xB}{24\bar{R}\bar{d}} - \frac{2S_o x\bar{d}}{H_o^2} - 1 \quad \ldots\ldots \quad (43)$$

The solution of equation (41) may be obtained graphically from figure 10. Equation (40) may be written in terms of the critical depth as follows:

$$H_o = \sqrt{3d_c^2 - 2S_o x_c\bar{d} + \frac{fx_c d_c^3}{12\bar{R}\bar{d}gb^2}} \quad \ldots\ldots \quad (44)$$

For this case, the coefficients of equation (41) are:

$$B_c = 2\left(\frac{d_c}{H_o}\right)^3 \quad \ldots\ldots \quad (45)$$

$$A_c = -3\left(\frac{d_c}{H_o}\right)^3 \quad \ldots\ldots \quad (46)$$

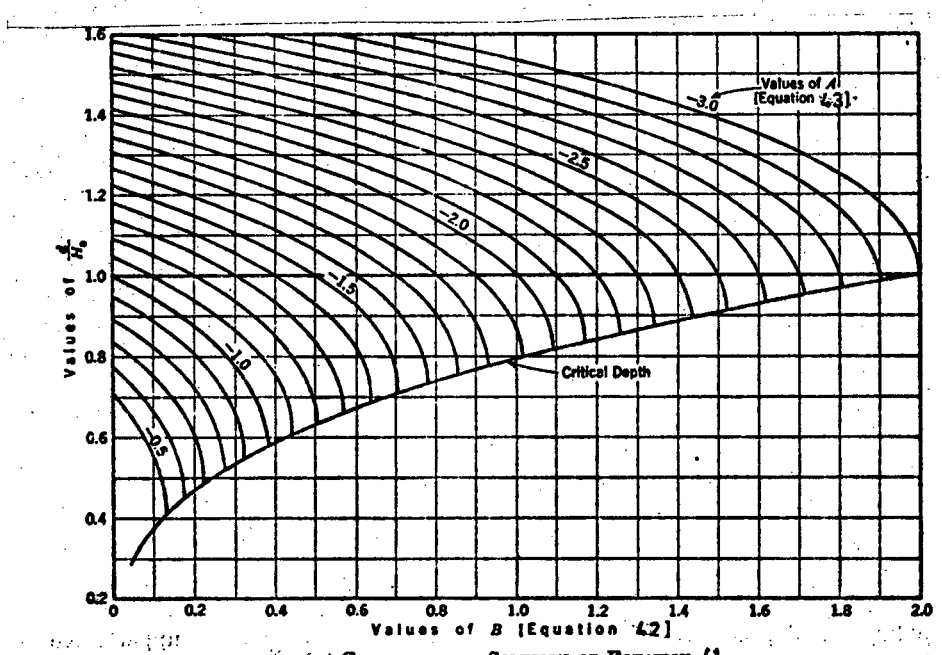

GRAPH FOR THE SOLUTION OF EQUATION 41.

This chart provides a relatively simple method of finding the water surface profile in a rectangular channel and it is unfortunate that a similar analysis cannot be done for trapezoidal channels.

A further limitation of this chart, as drawn by Camp, is that it is applicable only to channels of mild invert slope. The chart is not extended below the critical depth line to include supercritical flow, and the limiting values of A and B limit d_c/H_o to values smaller than unity. However, with sloping channels, this value is often exceeded, and thus a severe and unnecessary limitation is imposed.

Looking at equations (23) and (24) it can be seen that the upstream end ($x = 0$) of all channels is represented by the point $A = -1$, $B = 0$. If friction is ignored, all horizontal channels are represented by the line $A = -1$. As the invert slope is increased, the control point moves from the $A = -1$ line, up the critical depth line and even for mild slopes, moves off the chart as drawn by Camp. All water surface profiles are thus represented by a curved line extending from the point $A = -1$, $B = 0$ to the critical depth line and, in the case of steep slopes, crossing it. Camp's chart has thus been redrawn in figure 11 with extended limits. To avoid compressing that section represented by Camp's chart into an insignificant and useless corner of the larger chart, it has been necessary to use log scales.

Although this method appears to give a simple solution to the problem, its accuracy is greatly dependent on the accuracy of the assumed value of $\bar{d}$ in the second term of equation (44). This value is not easily estimated with accuracy when the depth is known at only one point, especially with relatively steep invert slopes, where the water surface is deepest in the centre and becomes shallower towards each end. It is therefore necessary to use an itterative procedure. An initial estimate of $\bar{d}$ must be made so that a value of H_o can be calculated. This is then used together with the chart to obtain the depths at a number of points. These depths are then used to obtain a better estimate of $\bar{d}$ and the process is repeated till a sufficiently accurate result has been obtained. A quicker method, however, might be first to find H_o using Li's method (to be discussed), and then proceding to Camp's charts.

RECTANGULAR SIDE-CHANNEL SPILLWAYS

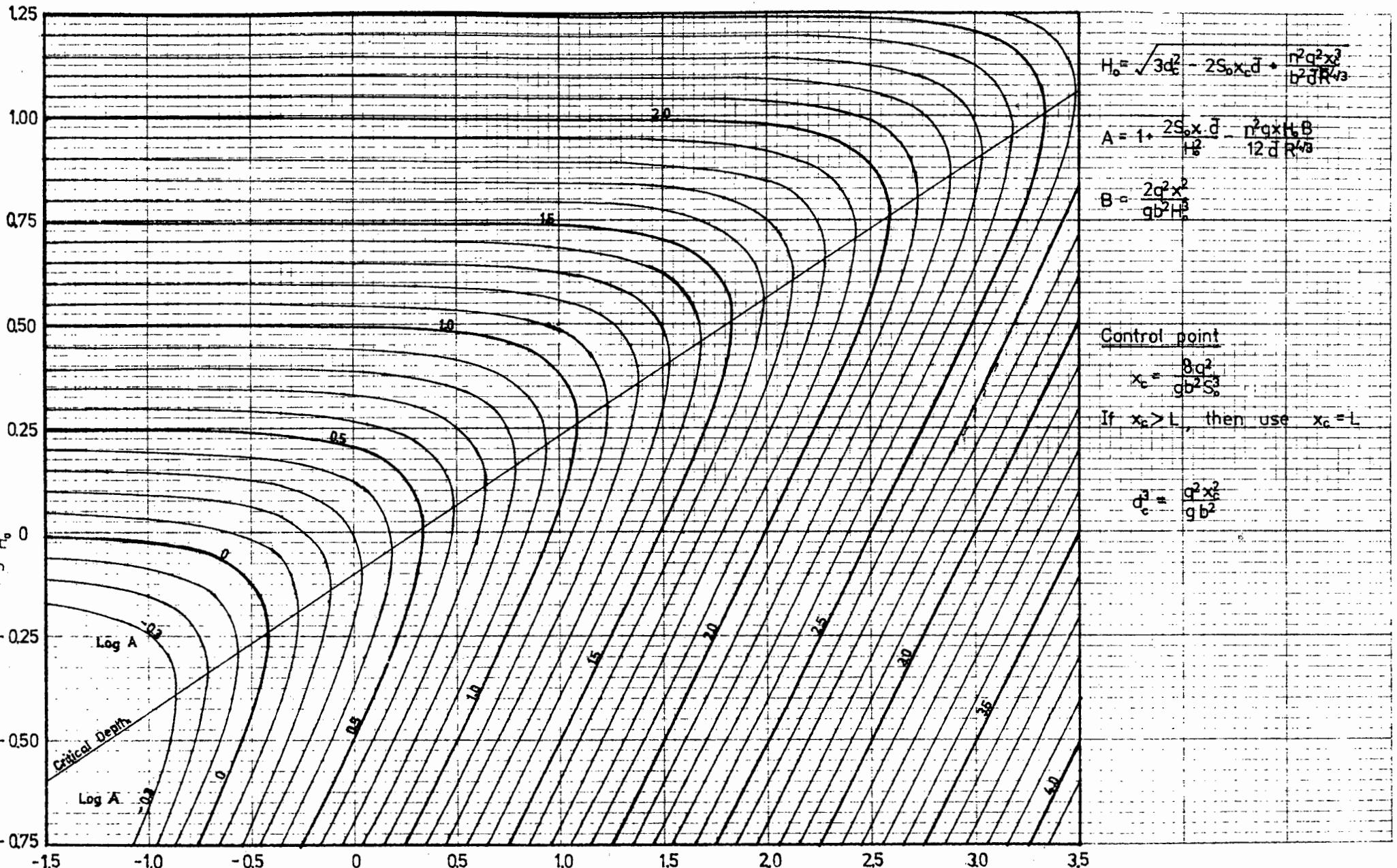

$$H_o = \sqrt{3d_c^2 - 2S_o x_c \bar{d} + \frac{n^2 q^2 x_c^3}{b^2 \bar{d} R^{4/3}}}$$

$$A = 1 + \frac{2S_o x \cdot \bar{d}}{H_o^2} - \frac{n^2 g x H_o B}{12 \bar{d} R^{4/3}}$$

$$B = \frac{2q^2 x^2}{g b^2 H_o^3}$$

Control point

$$x_c = \frac{8q^2}{g b^2 S_o^3}$$

If $x_c > L$, then use $x_c = L$

$$d_c^3 = \frac{q^2 x_c^2}{g b^2}$$

Wen-Hsiung Li,[10] presented an interesting paper which was devoted mainly to the development of methods of finding the depth at the upstream end of the channel. This is usually the most important depth for design purposes as here the water surface level is highest, even though the water is deeper downstream.

Two shortcomings of this work are that the effects of friction have been ignored throughout, and that his graphs are applicable only to channels of a particular shape. He has presented charts for rectangular and triangular channels only, but he has for other shaped channels, presented an empirical equation which combines the results from these two charts.

An advantage of this work is that it is not limited to channels with free outfall at the downstream end but allows for submergence and the formation of hydraulic jumps. Li has isolated four different flow conditions which are shown in figure 12. Each type is represented by a particular section of his chart on which he plots F_o, the Froude number at the downstream end, against G, which is equal to S_oL/Y_o for rectangular channels and equal to $2S_oL/Y_o$ for triangular channels. Y_o is the water depth at the downstream end. Detailed versions of this chart are shown in figures 13 and 14, where a set of curves has been drawn with Y_u/Y_o as parameter. Y_u is the depth at the upstream end. However, before looking at these charts, the general sketch in figure 12 will be discussed in more detail. Section A and figure 12a represent channels of mild slope where the Froude number increases along the channel. Horizontal channels are represented by the line G = 0 and channels with free outfall by the line $F_o = 1$. (If $G < 2$). Their intersection therefore represents all horizontal channels with free outfall.

Section B represents channels which are submerged to a greater depth so that the Froude number, according to Li, first increases and then decreases. The boundary between these two sections is given as $G = \frac{2}{3}(1 + 2F_o^2)$ for rectangular channels and $G = \frac{4}{5}(1 + \frac{3}{2}F_o^2)$ for triangular channels.

Section C represents steep channels (i.e. with supercritical flow) which are submerged to such an extent that a hydraulic jump occurs within

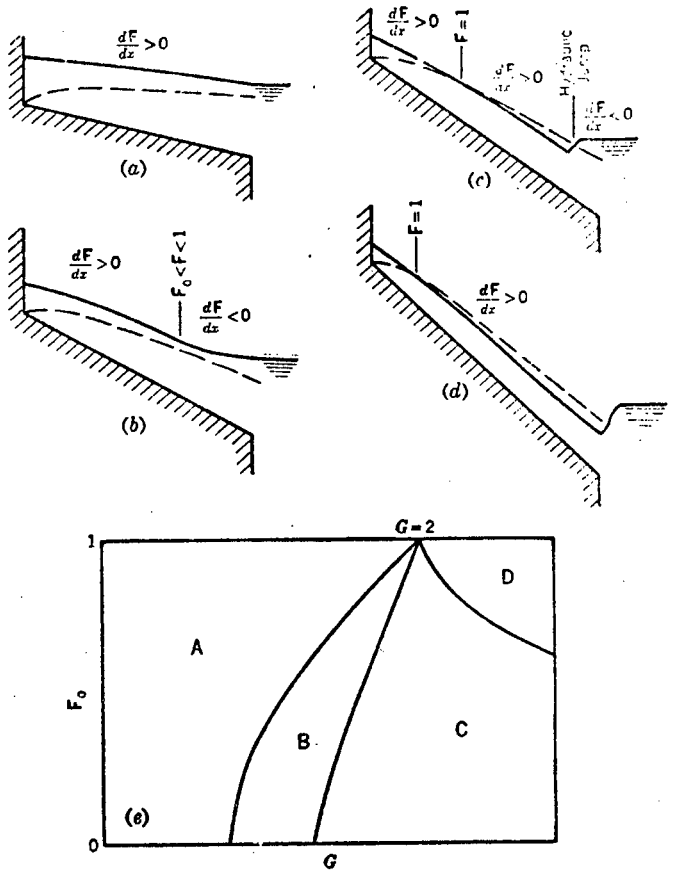

Figure 12 : Types of flow according to Li.[10]

the channel so that F_o is less than unity. The boundary between sections B and C is given as $G = 1 + F_o$ for rectangular channels and the vertical line, $G = 2$, for triangular channels.

Section D represents steep channels which are submerged to a lesser extent, so that the hydraulic jump forms at the end of the channel. The flow is thus supercritical at the downstream end so one would not expect this case to be represented by this section where $F_o < 1$. However, if the depth downstream of the jump is used to calculate F_o and G, then the resulting point will fall into this region, and the correct value for Y_u will be obtained. However, it is possible to obtain a value of F_o greater than unity so it is obvious that Li's chart in figure 6 is incomplete and should be extended upwards. This has been done and is shown in figure 13.

Section E is similar to section D but represents the case where the downstream end of the channel is drowned to a level less than the critical depth at that point. The upper boundary of this section is the line representing the case where the outlet is not drowned at all and can be shown empirically to be represented approximately by the lines $G = \frac{3}{2} F_o + 1{,}65$ for rectangular channels and $G = 4F_o - 2$ for triangular channels.

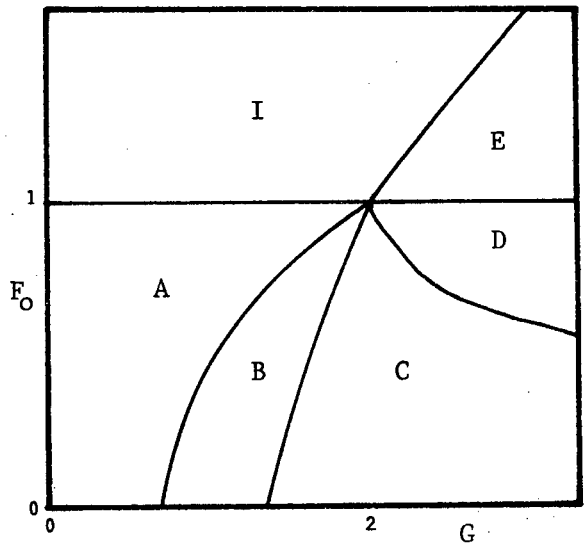

Figure 13

Section I represents the case where, at the end of the channel, the depth suddenly decreases in a sort of negative jump where F_o, already greater than one, suddenly increases. As this phenomenon cannot occur in practice, section I does not represent a real solution to the problem.

The boundary lines all intersect at the point $F_o = 1$, $G = 2$. It is interesting to note that this point represents the case in which the natural and artificial control points coincide.

Moving around this point through the different sections, a number of interesting observations can be made. The boundary between sections I and E represents free outflow from a steep channel. Moving downwards represents an increasing level of submergence of the downstream end of the channel. At the $F_o = 1$ line, the submergence is to the critical depth, while at the boundary between sections C and D,

the level of submergence is such that the downstream reaches of the channel start being flooded. Moving across section C represents increasing the level of submergence still further, causing the hydraulic jump to move upstream until at the boundary between B and C, the supercritical flow has been completely flooded. Moving into section B represents submerging to an even higher level so that the whole channel is flooded. The level of submergence now affects the entire water surface profile, even at the extreme upstream end. Looking at figure 12b it is not immediately obvious that this is in fact a steep slope. However, if the downstream flooding was removed, supercritical flow would indeed develop in any channel falling into section B.

It is impossible to move into section A by increasing the level of submergence. Indeed, the boundary between sections A and B represents infinite submergence. Moving from this line into section B represents decreasing submergence for steep slopes, and moving from this line into section A represents decreasing submergence for mild slopes. This continues as one moves up through section A to the line $F_o = 1$ which represents free outfall.

The two boundaries of section I (i.e. with sections A and E) thus both represent zero flooding and free outflow from the channel. Moving into section F from either of these boundaries, represents an increasing degree of negative submergence, for mild slopes on the one side and steep slopes on the other. It therefore seems reasonable to postulate that section I is divided by some line which, similar to the boundary between sections A and B, represents infinite negative submergence and the boundary between mild and steep slopes. This large negative submergence would involve negative water depths, and the Froude number would involve the square root of a negative number. The line is therefore imaginery and of no practical interest to engineers. Finding its exact equation will therefore be left to any mathematician who might find interest in such an exercise.

In order that this chart be of any use, it must be drawn in detail for a particular case. Li presented charts drawn for rectangular and triangular channels and these are reproduced in figures 14 and 15. It is unfortunate that these charts are drawn only for sections A and B as a clearer understanding is often obtained when a picture can be seen as

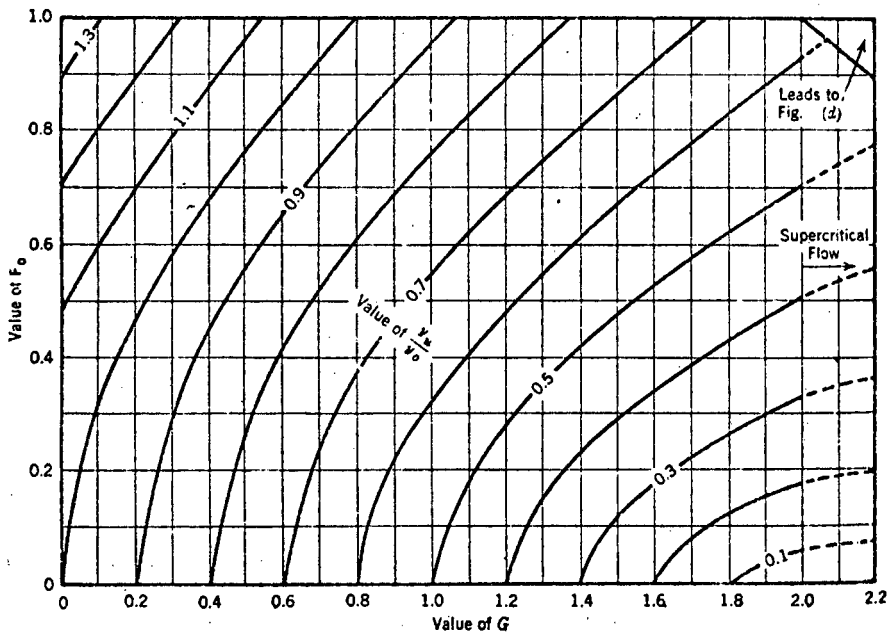

FIGURE 14 : Li's chart for triangular channels

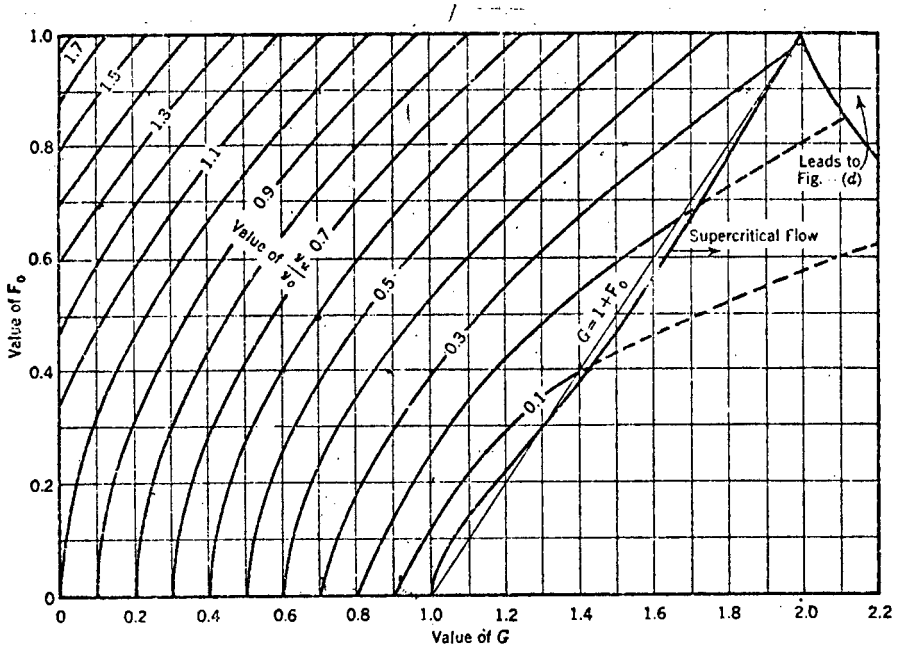

FIGURE 15 : Li's chart for rectangular channels

a whole. However, the charts presented are perfectly satisfactory in practice as the curves in sections C, D and E can be approximated closely by straight lines. These lines were given by Li only for section C but can easily be shown to be equally valid for sections D and E. They are

for rectangular channels

$$\frac{Y_u}{Y_o} = 1{,}24 \quad \frac{F_o^2}{G^2} \qquad \ldots\ldots \quad (47)$$

and for triangular channels

$$\frac{Y_u}{Y_o} = \frac{F_o^{\frac{2}{3}}}{G^{\frac{2}{3}}} \qquad \ldots\ldots \quad (48)$$

For trapezoidal channel, results from figures 14 and 15 (or equations 47 and 48) can be combined by the empirical equation:

$$\frac{Y_u}{Y_o} = \left[\frac{Y_u}{Y_o}\right]_r - \left[\frac{1}{3}\right]^E \left[\left(\frac{Y_u}{Y_o}\right)_r - \left(\frac{Y_u}{Y_o}\right)_t\right] \qquad \ldots\ldots \quad (49)$$

where $E = \frac{a_2}{a_o}$

a_2 is the area removed from the bottom of a triangular channel to make the required trapezoidal channel.

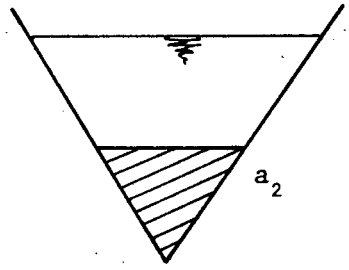

Figure 16

$\left(\frac{Y_u}{Y_o}\right)_r$ and $\left(\frac{Y_u}{Y_o}\right)_t$ are those values obtained from the charts for rectangular and triangular charts respectively, using the values of F_o as calculated for a trapezoidal channel.

The methods discussed above give the water depth at the upstream end of the channel. The downstream depth is also known in many cases, but not in the case of a freely discharging steep channel. To find that depth Li produced a chart which is reproduced in figure 17. This chart is self-explanatory and gives not only the downstream depth, but the complete surface profile in the supercritical region. The curve is not completely accurate as it does not show the variation with E (see equation 49). However, this difference is small and has not been included here.

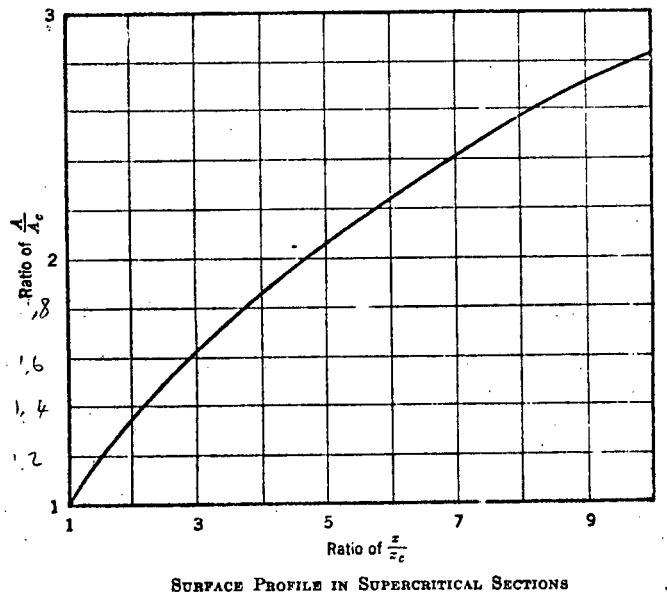

SURFACE PROFILE IN SUPERCRITICAL SECTIONS

Figure 17

This curve is represented in figure 13 by the boundary line between sections E and I, but is not easily used in that form. With supercritical flow, the downstream depth is not known so a trial and error process must be used till a depth is found which gives a point exactly on the curve. This is very tedious and for practical purposes, figure 17 is far more useful.

3.5 Solution by Computer

The hand methods of analysis discussed in this thesis are useful if a small amount of work is to be done on this problem, but would be extremely slow and tedious if a large number of water surface profiles were to be calculated. In this case, it would be far more sensible to solve the problem by computer.

The necessary program is relatively simple and can again be divided into two distinct problems, namely finding the control point and numerically integrating the differential equation from this point.

Finding the control point has been discussed in a number of papers, including one by K. Smith[15] but the whole problem is discussed and made very clear by Humpidge and Moss.[19]

To find the control point one simply equates the numerator and denominator of equation (25) to zero as before. This is usually done by the Newton-Raphson method. Care must be taken with the choice of the initial estimate as too small an estimate could lead to the alternative solution at the upstream end where $x = 0$ and $d = 0$ and the equations also hold. However, if a reasonable initial estimate is made, no problems should be encountered.

Humpidge and Moss also considered the possibility of a number of control points existing and showed how to find which is dominant. However, this is not a likely problem in practical side channel spillways and the only complication which normally needs to be accounted for, is that the natural control point found above is usually beyond the end of the receiving channel. The starting point for the calculation is then at the downstream end of the channel where the depth depends on downstream conditions. When the control point has been found, the full profile is calculated by numerical integration, usually using a Runge-Kutta method.

A problem arises in calculating dd/dx at the control point. At a natural control point, $dd/dx = 0/0$ and can not be easily calculated, while at an artificial control point, dd/dx is infinite and the integration is not possible. This was overcome by Humpidge and Moss by using a starting value of d of 1,05 times d_c when working upstream and 0,95 times

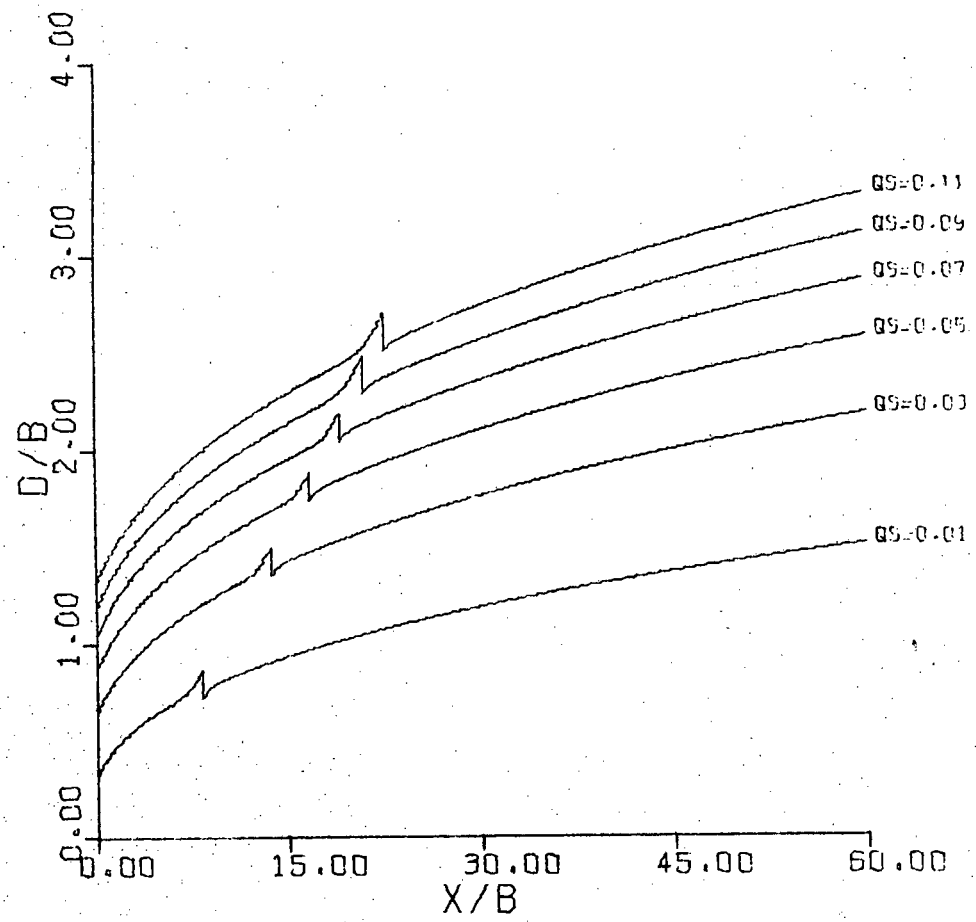
4.00
3.00
2.00
1.00
0.00
D/B
0.00
15.00
30.00
45.00
60.00
X/B
QS=0.11
QS=0.09
QS=0.07
QS=0.05
QS=0.03
QS=0.01

Figure 18

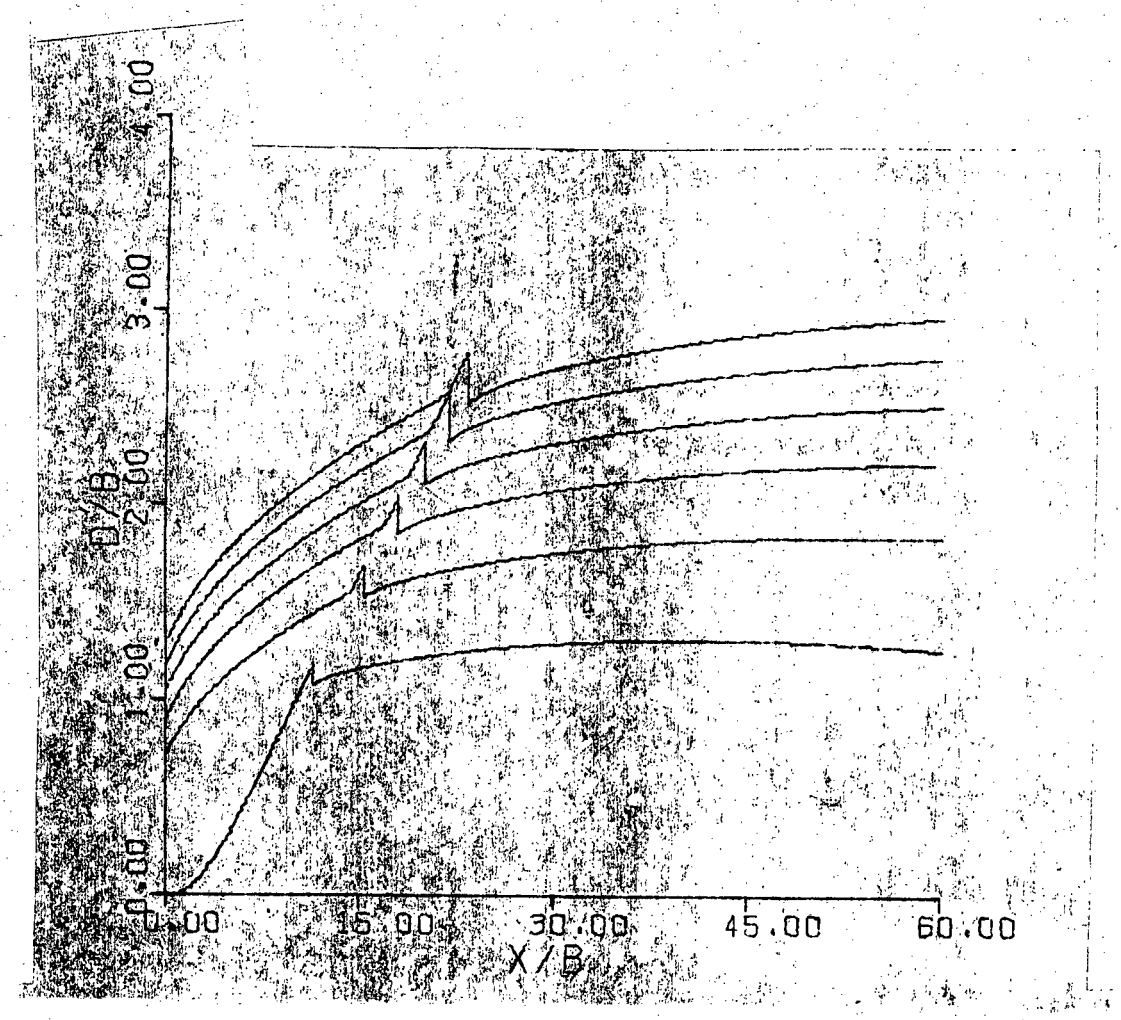

Figure 19

d_c when working downstream and it was claimed that this strategem had little effect on the profile since the specific energy, E, varies little with d for values near d_c.

The effect was indeed found to be small and it can be seen in figure 19 that a smooth curve can be drawn through the discontinuity at the control point. It was found, however, that the figure of 1,05 used by Humpidge was not universally applicable and that in some cases, the curve diverged from the correct solution as seen in the lowest curve of figure 18.

These curves were calculated in dimensionless form using equation (68) rather than equation (25) and are therefore applicable to all channels of the same geometric shape. The different curves represent different values of the dimensionless lateral inflow $QS = q^2/gb^3$. For low flows (i.e. for small values of d_c) it was found that the value of 1,05 was not suitable. Figure 19 was therefore drawn starting with a value of $d_c^* + 0,1$ when d_c^* was smaller than 2 and $d_c^* + 0,15$ when it was larger than 2. This worked satisfactorily in this case but other cases were found where it did not work. Although no universally applicable value has been found it is a simple matter to adjust the factor if a particular value does not work in a particular case.

It should be noted that this problem arises only in the case of a natural control point. With an artificial control, the value of $d = 1,05\ d_c$ was found to be satisfactory in all cases.

Although the above method appears to have been used by all previous investigators, some doubt existed as to the accuracy of the results obtained by making such a large approximation at the control point. It was therefore necessary to solve accurately for dd/dx at a natural control point.

Equation (25) can be written as

$$\frac{dd}{dx}\left[1 - \frac{q^2x^2B}{gA^3}\right] = S_o - \frac{2q^2x}{gA^2} - \frac{q^2x^2n^2p^{\frac{4}{3}}}{A^{\frac{10}{3}}} \quad \ldots\ldots \quad (50)$$

which can be differentiated with respect to x to give

$$\frac{d^2d}{dx^2}\left[1 - \frac{q^2x^2B}{gA^3}\right] - \frac{dd}{dx}\left[\frac{2q^2xB + q^2x^2\frac{dB}{dx}}{gA^3} - \frac{3q^2x^2B\,\frac{dA}{dx}}{gA^4}\right] + \frac{2q^2}{gA^2}$$

$$- \frac{4q^2x}{gA^3}\frac{dA}{dx} + q^2n^2\frac{2xp^{\frac{4}{3}}}{A^{\frac{10}{3}}} + \frac{4x^2p^{\frac{1}{3}}\frac{dp}{dx}}{3A^{\frac{10}{3}}} - \frac{10x^2p^{\frac{4}{3}}\frac{dp}{dx}}{3A^{\frac{10}{3}}} = 0 \quad \ldots\ldots (51)$$

At the control point the Froude number is equal to unity so the term including the second derivative of the depth disappears, and the above equation can be solved if the dimensions of the channel are known.

For trapezoidal channels,

$$A = bd + d^2\tan\theta$$

$$\frac{dA}{dx} = (b + 2d\tan\theta)\frac{dd}{dx}$$

$$B = b + 2d\tan\theta$$

$$\frac{dB}{dx} = 2\tan\theta\frac{dd}{dx}$$

$$p = b + 2d\sec\theta$$

$$\frac{dp}{dx} = 2\sec\theta\frac{dd}{dx}$$

These can be substituted into the equation at the control point to give:

$$\left[\frac{dd}{dx}\right]_c^2\left[\frac{3(b + 2d\tan\theta)^2}{bd + d^2\tan\theta} - 2\tan\theta\right]$$

$$- \left[\frac{dd}{dx}\right]_c\left[\frac{6(b + 2d\tan\theta)}{x} - \frac{n^2g\sec\theta}{(bd + d^2\tan\theta)^{\frac{1}{3}}}\left[\frac{8(b + 2d\sec\theta)^{\frac{1}{3}}}{3} - \frac{20(b + 2d\sec\theta)^{\frac{4}{3}}}{3(bd + d^2\tan\theta)}\right]\right]$$

$$+ \frac{2(bd + d^2\tan\theta)}{x^2} + \frac{2n^2(b + 2d\sec\theta)^{\frac{4}{3}}}{x(bd + d^2\tan\theta)^{\frac{1}{3}}} = 0 \quad \ldots\ldots (52)$$

This equation is a quadratic in dd/dx and could be solved but the resulting equation would be very complicated and it is simpler to first substitute in the values for a particular channel and then to solve.

Equation (52) can be considerably simplified by neglecting the effect of friction to give

$$\left[\frac{dd}{dx}\right]_c^2 \left[\frac{3(b + 2d\ \tan\theta)^2}{bd + d^2\tan\theta} - 2\ \tan\theta\right] - \left[\frac{dd}{dx}\right]_c \left[\frac{6(b + 2d\ \tan\theta)}{x}\right]$$

$$+ \frac{2(bd + d^2\tan\theta)}{x^2} = 0 \qquad \ldots\ldots \quad (53)$$

For rectangular channels, again neglecting friction, this can be greatly simplified to give

$$\left[\frac{dd}{dx}\right]_c^2 - \left[\frac{dd}{dx}\right]_c \cdot \frac{2d}{x} + \frac{2d^2}{3x^2} = 0 \qquad \ldots\ldots \quad (54)$$

which can be solved to give

$$\left[\frac{dd}{dx}\right]_c = \frac{d}{x} \pm \frac{d}{x\sqrt{3}} \qquad \ldots\ldots \quad (55)$$

It can be seen that both solutions are positive but it would appear from studies of practical examples, that it is always the smaller which is applicable.

Therefore, for rectangular channels, neglecting friction

$$\left[\frac{dd}{dx}\right]_c = \frac{0,42d}{x} \qquad \ldots\ldots \quad (56)$$

If for Hind's example given on page 18, $\left[\frac{dd}{dx}\right]_c$ is calculated from equation (52), a value of 0,0300 is obtained. Equation (53) gives a value of 0,0296. The effect of friction is thus only 1,33% in this case.

Any of equations (52) to (56) can thus be used to calculate dd/dx at the control point, after which the equation can be solved numerically in the usual way.

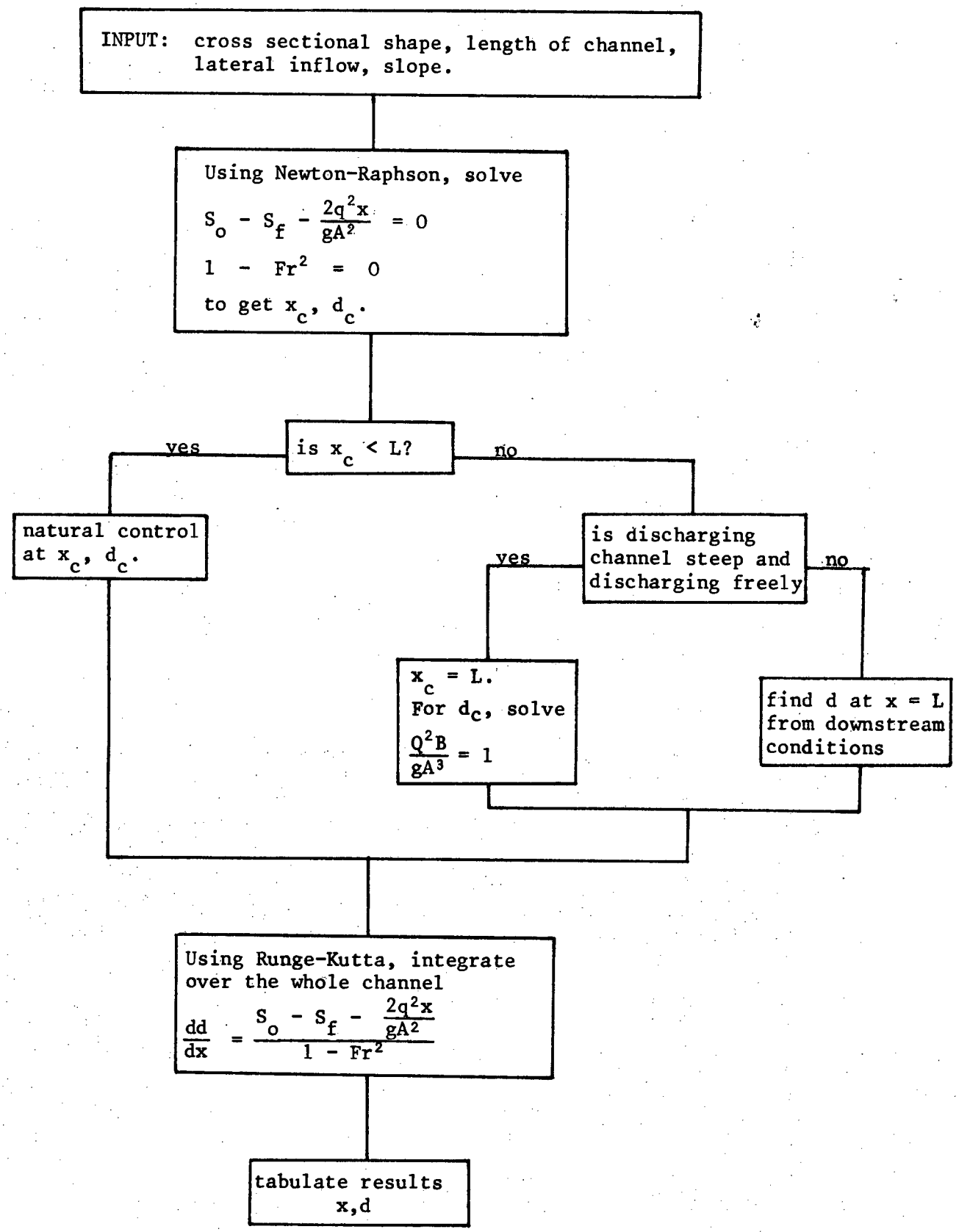

Figure 20 : Simplified flow diagram for the calculation of the water surface profile in a prismatic side channel spillway of uniform slope.

3.6 The Effect of Friction

Although there has not been much work done on this subject, it has been noticed that the law of resistance for spatially varied flow is at variance with laws ordinarily ascribed to constant flow in open channels. This has been discussed in papers by Keulegan,[9] and Fox and Goodwill.[18] Their results, however, are not very conclusive, and constants used in the formulae have been evaluated only for special cases. Their work is therefore of little practical use. The total effect of friction in side channel spillways is not large, so small differences in its method of calculation are not important. For the purposes of this thesis, the effect of friction has therefore been calculated according to the laws for constant flow in open channels, e.g. Manning's equation.

In much of the work previously discussed, the effect of friction has been completely neglected, and Li[10] attempted to quantify the effect of this simplification. In sloping canals, the effect of friction is usually considered to be cancelled by the momentum of the incoming water, which, entering downwards, has a small component along the channel. In horizontal channels however, this is not so, and for this case, Li drew a graph which is reproduced here as figure 21. For the purpose of this graph, h_f is the friction head lost as calculated by the Chezy or Manning formulae, using the total discharge and the depth as at the downstream end. If this is done with practical examples of side channel spillways this graph shows that the increase in the depth at the upstream end is very small, usually less than 1%. However, for effluent channels around sewage-treatment tanks, this value can become as high as 10%.

It should not be thought that these figures are applicable along the whole channel. Friction has a cumulative effect and the error introduced by ignoring it decreases from this maximum at the upstream end, to a minimum at the control point.

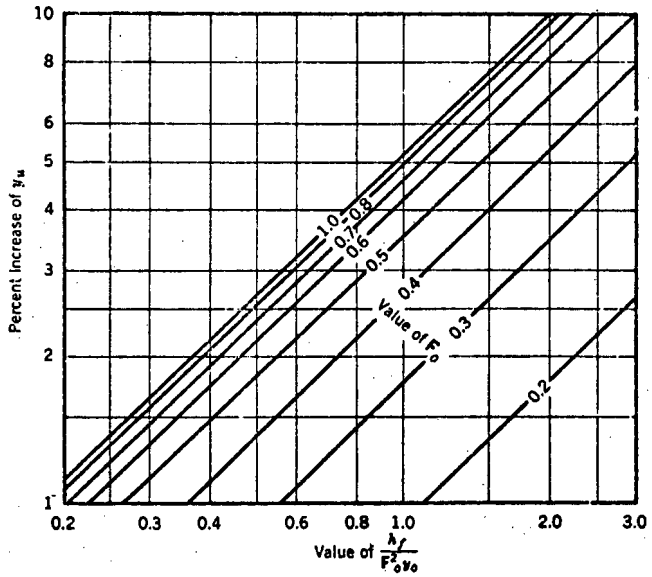

INCREASE OF y_u AS A RESULT OF FRICTION IN LEVEL CHANNELS

Figure 21

3.7 Inflow over the Upstream End

When the spillway crest is L or U shaped so that water enters over the upstream end, two complications are introduced.

The first is that equations (25) and (26) are no longer directly applicable as these are derived from equation (17) using the assumption that Q, the flow at any point, is equal to qx. However, the flow in this case is equal to $Q_o + qx$ where Q_o is the flow over the upstream end. This can be substituted into the relevant equation if this is to be solved directly. However, if any of the design charts are to be used, this cannot be done and a different stratagem must be used. If the receiving channel is extended in the upstream direction by a fictitious length of

$x' = Q/q$ and the lateral inflow, q, is considered to enter along the whole of this new extended length, then the conditions in the lower section of this channel will be equivalent to conditions in the original channel with flow over the upstream end. Equations (25) and (26) are therefore applicable if x is measured from a point x' above the upstream end.

This method was used to calculate the water surface profile for the side channel spillway studied by Farney and Markus[11] and the results are compared in figure 22. It can be seen that Hind's method gives a very bad result. The authors did not show exactly how they obtained this curve but it is presumed that equation (37) was used and that the inaccuracy was caused by the theoretically infite slope at the control point. This shows that this equation should be used only with great caution.

infinite

The computer solution was obtained from equation (25) by the methods described in the previous chapter. As the curves in figure 31 are obtained from the same computer program, they would have resulted in exactly the same curve. It can be seen that this result compares well with observed depths near the downstream end but at the upstream end, the observed depths are much lower.

This is due to the second complication, which is the fact that the water entering over the upstream end has considerable momentum in the direction of flow. Farney and Markus calculated values of β, the momentum correction coefficient, which could be used to bring the calculated values down to the observed depths. However, as these apply only to that particular channel they are not presented here. There is at present, no known method of calculating this factor and model tests must be used if it is to be found.

Designers can use the method described above with confidence, knowing that it is conservative at the upstream end. However, if in large channels, this depth reduction could result in appreciable economic savings, then model tests must be used to be able to achieve optimum design.

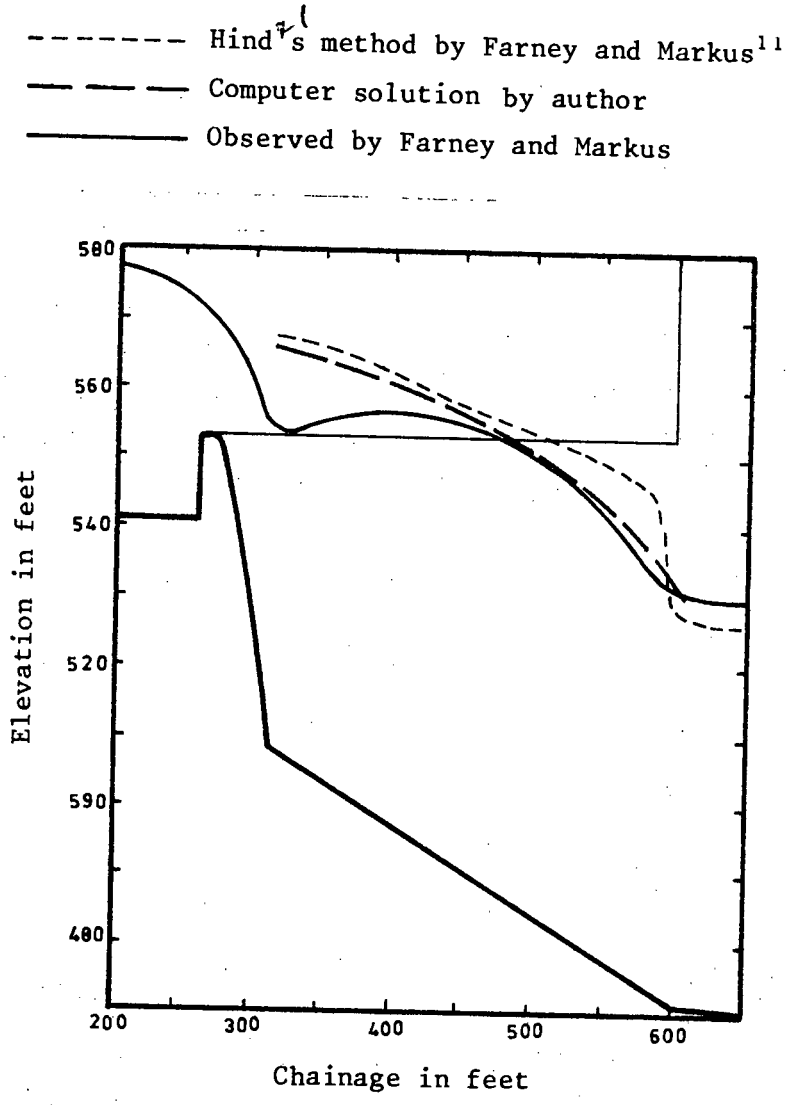
Hind's method by Farney and Markus[11]
Computer solution by author
Observed by Farney and Markus
580
560
540
520
590
480
200
300
400
500
600
Elevation in feet
Chainage in feet

Figure 22

4. THE DEVELOPMENT OF NEW DESIGN CHARTS

4.1 The Control Point

The water surface profile in a side channel spillway cannot be found by any method unless the control point is known. As discussed earlier, this is calculated by equating the numerator and the denominator of equation (25) to zero.

If friction is neglected, it is possible to draw a simple chart from which the control point can be easily found. Equations (30) and (31) are put in terms of the dimensions of a trapezoidal channel to give

$$S_o g(bd + d^2\tan\theta)^3 - 2q^2x(bd + d^2\tan\theta) = 0 \quad \ldots\ldots (57)$$

$$g(bd + d^2\tan\theta)^3 - q^2x^2(b + 2d\tan\theta) = 0 \quad \ldots\ldots (58)$$

From equation (58)

$$x^2 = \frac{g(bd + d^2\tan\theta)^3}{q^2(b + 2d\tan\theta)} \quad \ldots\ldots (59)$$

This can be substituted in equation (57) to give

$$\frac{4q^2}{S_o^2 g} = (bd + d^2\tan\theta)(b + 2d\tan\theta) \quad \ldots\ldots (60)$$

if $d^* = d/b$

then
$$\frac{4q^2}{S_o^2 g b^3} = (d^* + d^{*2}\tan\theta)(1 + 2d^*\tan\theta) \quad \ldots\ldots (61)$$

From this equation, d^* can be plotted, for particular values of θ, against

$$\frac{4q^2}{S_o^2 g b^3}$$

Similarly, from equation (59)

$$\frac{x^2q^2}{gb^5} = \frac{(d^* + d^{*2}\tan\theta)}{1 + 2d^*\tan\theta} \quad \ldots\ldots (62)$$

and from this equation, d^* can be plotted against $\frac{x^2q^2}{gb^5}$ for particular values of θ.

Equations (57) and (58) represent conditions at the control point where $d = d_c$ and $x = x_c$. With these substitutions, these equations can be plotted as follows:

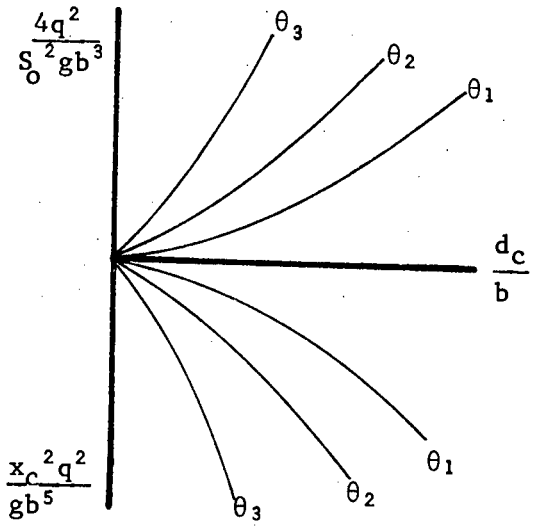

Figure 23

For any trapizoidal channel, one can calculate $4q^2/S_o^2gb^3$ all of which terms will be known. d_c/b and thus d_c can thus be read off. From the lower chart one can then read off the value of $x_c^2q^2/gb^5$, from which x_c can be calculated as the other factors are known.

In the case of a channel with mild slope and known critical depth at the end (due to free outfall or a steep discharging channel), one can put $x_c = L$ and thus calculate $x_c^2q^2/gb^5$ from which one can read off the value of d_c. In this case the answer is exact as this relationship is not affected by the neglected friction.

Alternatively, $4q^2/S_o^2gb^3$ can be plotted against $x_c^2q^2/gb^5$ with d_c/b as parameter. As this gives a much neater chart, this method has been preferred in the drawing of figure 32 at the end of this chapter.

For rectangular channels, a much simpler analysis can be done. Once again neglecting friction, equation (25) reduces to

$$\frac{dd}{dx} = \frac{S_o - \frac{2q^2x}{gb^2d^2}}{1 - \frac{q^2x^2}{gb^2d^3}} \quad \ldots\ldots \quad (63)$$

Putting the denominator equal to zero gives

$$d_c^3 = \frac{q^2x_c^2}{gb^2} \quad \ldots\ldots \quad (64)$$

Putting the numerator equal to zero and substituting for d gives

$$x_c = \frac{8q^2}{gb^2S_o^3} \quad \ldots\ldots \quad (65)$$

This can be substituted back into equation (64) to give

$$d_c = \frac{4q^2}{gb^2S_o^2} \quad \ldots\ldots \quad (66)$$

If friction is ignored, the control point in rectangular channels can thus be calculated directly.

4.2 The Water Surface Profile

When the control point has been found, the next step is to find the water surface profile itself.

Equation (26) can be written in terms of the dimensions of a trapezoidal channel as

$$\frac{dd}{dx} = \frac{S_o - \frac{2q^2x}{g(bd + d^2\tan\theta)^2} - \frac{q^2x^2n^2(b + 2d\sec\theta)^{\frac{4}{3}}}{g(bd + d^2\tan\theta)^{\frac{10}{3}}}}{1 - \frac{q^2x^2(b + 2d\tan\theta)}{g(bd + d^2\tan\theta)^3}} \quad \ldots\ldots \quad (67)$$

It is required to find a quick method of finding the depth at various points along a proposed new side-channel spillway. This is not easy, as, for the one dependent variable, d, there are seven completely independent variables which must be considered.

$$d = f(q, S_o, b, \theta, n, x, x_c)$$

Obviously, these cannot all be included independently on a simple graph with only two axes, but must somehow be combined together into dimensionless groups.

$$\text{let} \quad d^* = d/b$$
$$x^* = x/b$$
$$q^* = q^2/gb^3$$
$$n^* = n^2g/b^{\frac{1}{3}}$$

Substituting these into equation (67) gives

$$\frac{dd}{dx} = \frac{S_o - \frac{2q^*x^*}{(d^* + d^{*2}\tan\theta)^2} - \frac{q^*x^{*2}n^*(1 + 2d^*\sec\theta)^{\frac{4}{3}}}{(d^* + d^{*2}\tan\theta)^{\frac{10}{3}}}}{1 - \frac{q^*x^{*2}(1 + 2d^*\tan\theta)}{d^* + d^{*2}\tan\theta)^3}} \quad \ldots\ldots \quad (68)$$

There is now one variable fewer, b having been absorbed into the others.

$$d^* = f(q^*, S_o, \tan\theta, n^*, x^*, x_c^*)$$

It is also obvious that the variable x_c is only necessary in the case of mild slopes. When a natural control forms within the channel, its position is a function of the other variables already included in the analysis. For steep slopes,

$$\therefore \quad d^* = f\{x^*, q^*, n^*, S_o, \tan\theta\}$$

If charts are drawn for particular values of S_o and θ, and friction is neglected only three variables are left and curves can be plotted as follows:

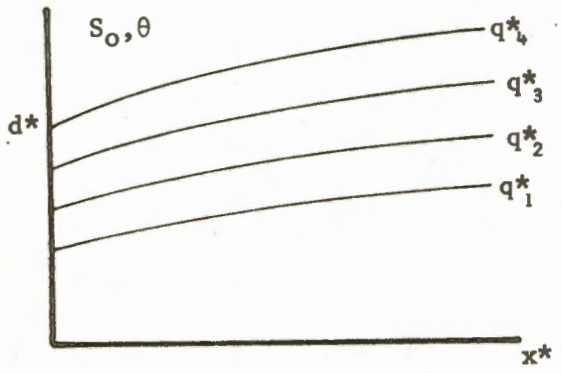

Although this allows very quick and direct reading of water depths, it is very cumbersome, because of the large number of such sets of curves which would have to be drawn to account for all values of θ and S_o.

For the case of mild slopes and critical depth at the downstream end, this is not possible because of the extra variable, i.e. spillway length, L. Graphs could, however, be drawn to give the depths at particular values of x, e.g. at the upstream end (x = 0) or at the mid-point (x = L/2). The depth at the outlet end is known from figure 32.

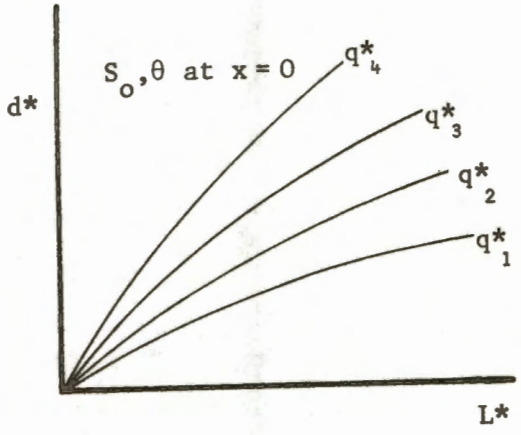

Figure 25

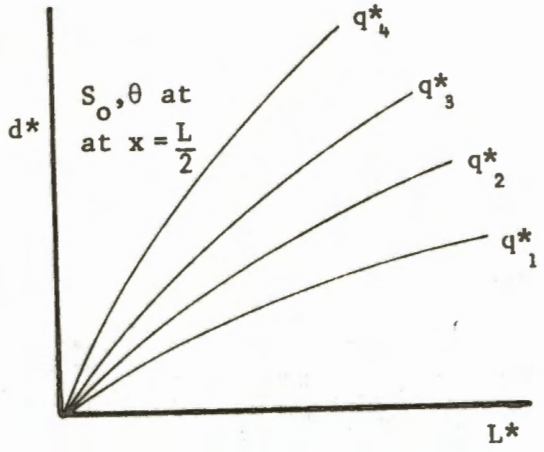

Figure 26

This means that for every type of channel cross section, three sets of curves (figures 24, 25 and 26) would have to be drawn for each different invert slope S_o. This would entail a whole booklet of curves and is obviously impractical.

The only solution appeared to be to find combinations of the above dimensionless groups which act together. Now the water surface profile depends on two things; its slope along the channel and its control point. From equation (26) it is immediately obvious what dimensionless groups govern the rate of change of depth along the channel. The denominator depends only on the Froude number, while the numerator depends on S_o, S_f, and $2q^2x/gA^2$. The effect of the control point,

however, is not immediately apparent, but it is obvious that it could depend on a number of variables such as q, S_o, and L which could be grouped together in some dimensionless form. It was decided that this form should be found empirically.

With conditions otherwise as in Hind's example, the water surface profiles were calculated with various values of q, S_o and L and for each, Fr^2 was plotted against $S_o - S_f - 2q^2x/gA^2 = C$.

When the flow was varied, it was found that for mild slopes, a family of curves was obtained, (figure 27), but for steep slopes a single curve was obtained passing through the point C = 0, Fr = 1, but which became longer for increasing q. These curves were, however, different for different values of S_o, all passing through the point $C = -S_o$ at Fr = 0 as shown in figure 28.

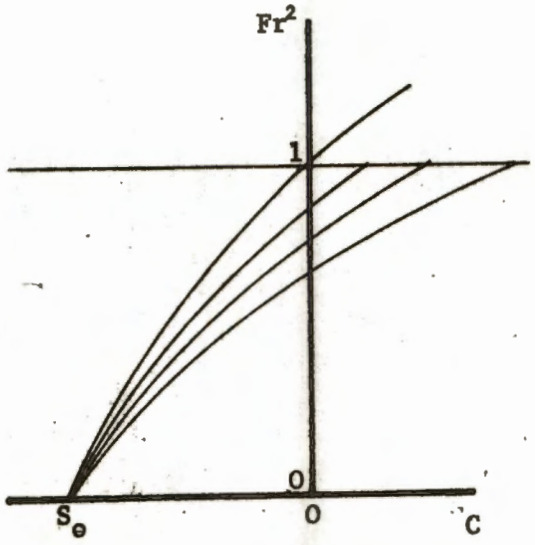

Figure 27

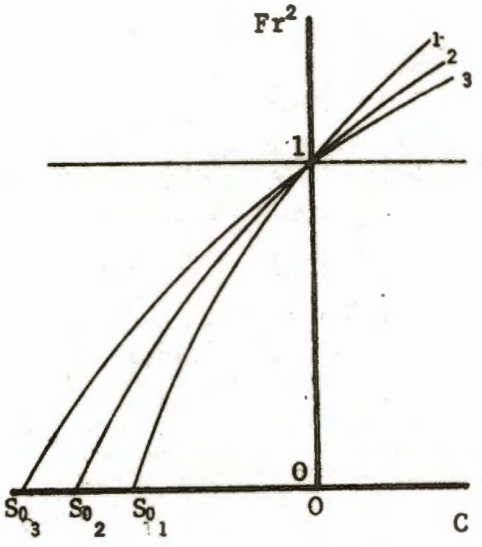

Figure 28

It was immediately obvious that it was not practical to plot Fr against C for all S_o on a single graph as the overlapping of the curves in the case of mild slopes would make it illegible. It is therefore necessary to plot a different set of curves for each S_o. The curves for mild and steep slopes could, however, be plotted together as they are part of the same family of curves.

It was also decided to plot the curves against $CC = S_f + 2q^2x/gA^2$ instead of against C. This had the effect of moving the entire family of curves to the right by a value of S_o. All curves then tend to CC = 0 at $Fr^2 = 0$ and for steep slopes, the curve passes through $CC = S_o$ at $Fr^2 = 1$ as shown.

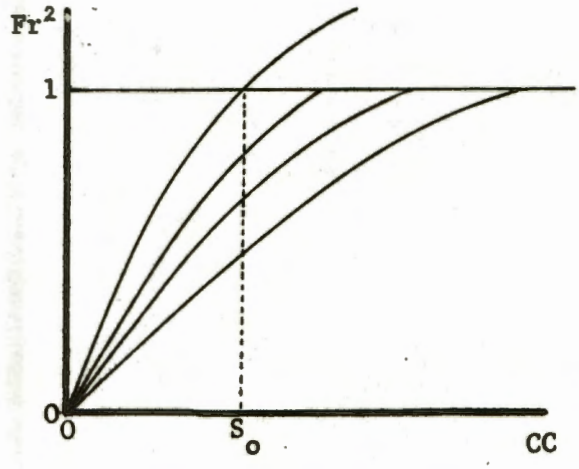

Figure 29

The next step was to plot Fr^2 against CC for constant S_o and q but for varying L. The effect appeared to be exactly the same as for q, the curves being of the same family. Once again, for steep slopes (i.e. $L > x_c$) the shape of the curve was not changed by changing L. For each S_o, a family of curves can thus be drawn which is applicable to all side-channels of that invert slope. For very small S_o, there is obviously no supercritical flow and the curve does not extend above $Fr^2 = 1$. In this case, the family of curves looks as follows:

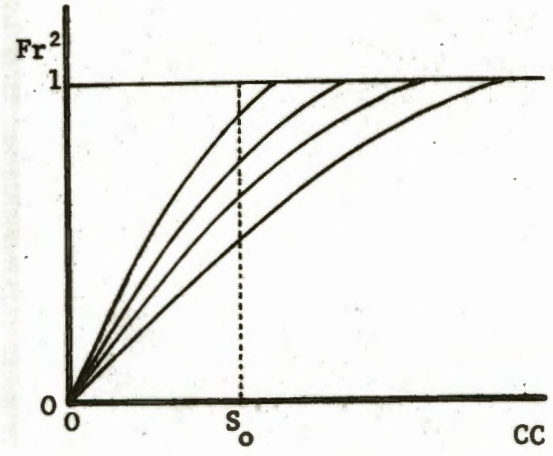

Figure 30

Although no dimensionless group has been analytically found to include the effect of the control point, it is now obvious that the missing terms are merely Fr^2 and CC at some known point. To find which curve of the family is relevant in a particular case, it is necessary to know the depth at some point for which Fr and CC can be calculated. The point defined by these two values will indicate the relevant curve.

In most cases, this known point will be an artificial control point where the depth is critical and $Fr^2 = 1$ so it will only be necessary to calculate CC_c. In the case of a natural control point, the relevant curve will be the one passing through the point $Fr^2 = 1$, $CC = S_o$.

These curves are also valid for the case where the control point lies some distance beyond the end of the spillway. The depth at the end of the overflow section must then be calculated by some other method (e.g. the backwater function) and Fr^2 and CC for this point will establish the relevant curve.

It was felt that these curves could be simplified further, and after much trial and error, it was noticed that the curves for each invert slope were similar if their horizontal scales were given linear adjustments. The values of CC for each curve were divided by their respective values of CC at $Fr^2 = 1$, to give $CS = CC/CC_c$. A family of curves was obtained all of which passed through the points (0,0) and 1,1). The relevant parameter for these curves was found to be L/x_c where x_c is the distance to the point where the control point would have formed in an infinitely long channel with all other factors the same.

For horizontal channels, x_c is infinitely large so L/x_c is zero. For steep slopes a single curve is obtained which applies to all values of L/x_c greater than unity. Because the subcritical range ($Fr < 1$) is considered to be more important than the supercritical range ($Fr > 1$), it was decided to emphasise the former by using a log scale.

The set of curves is presented in figure 31 and is applicable to prismatic channels of any cross-sectional shape and of any uniform slope. Before the curves can be used, however, it is still necessary to find the control point and this can be done, as described earlier by means of figure 32.

Figure 31

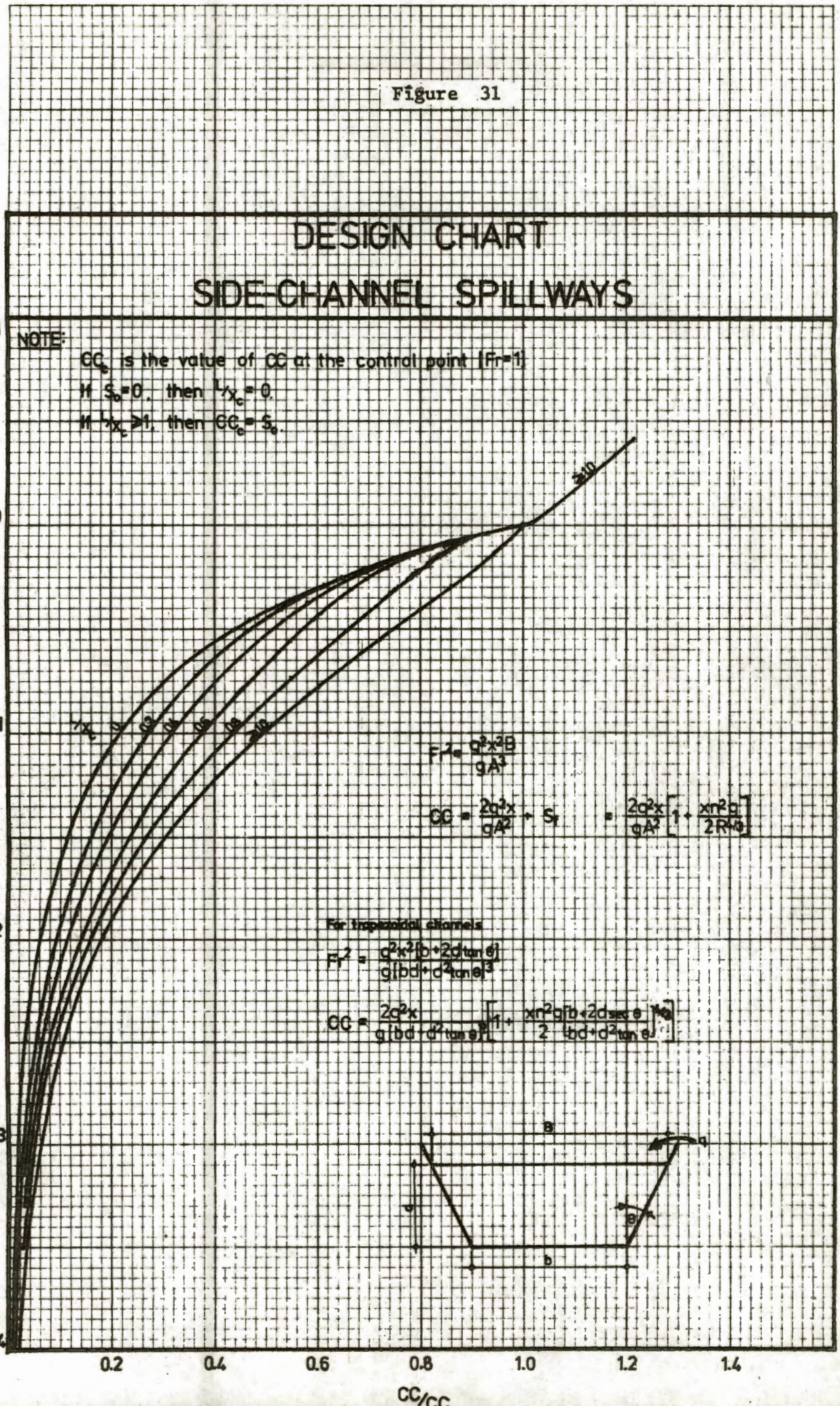
DESIGN CHART
SIDE-CHANNEL SPILLWAYS
NOTE:
CC_c is the value of CC at the control point (Fr=1)
If $S_o=0$, then $L/X_c=0$
If $L/X_c \geq 1$, then $CC_c = S_o$
L/X_c
Log Fr^2
CC/CC_c
$Fr^2 = \frac{q^2x^2B}{gA^3}$
$CC = \frac{2q^2x}{gA^2} + S_f = \frac{2q^2x}{gA^3}\left[1 + \frac{xn^2g}{2R^{4/3}}\right]$
For trapezoidal channels
$Fr^2 = \frac{q^2x^2[b+2d\tan\theta]}{g[bd+d^2\tan\theta]^3}$
$CC = \frac{2q^2x}{g[bd+d^2\tan\theta]^3}\left[1 + \frac{xn^2g[b+2d\sec\theta]^{4/3}}{2[bd+d^2\tan\theta]^{1/3}}\right]$
B
d
b
q
θ

Figure 32

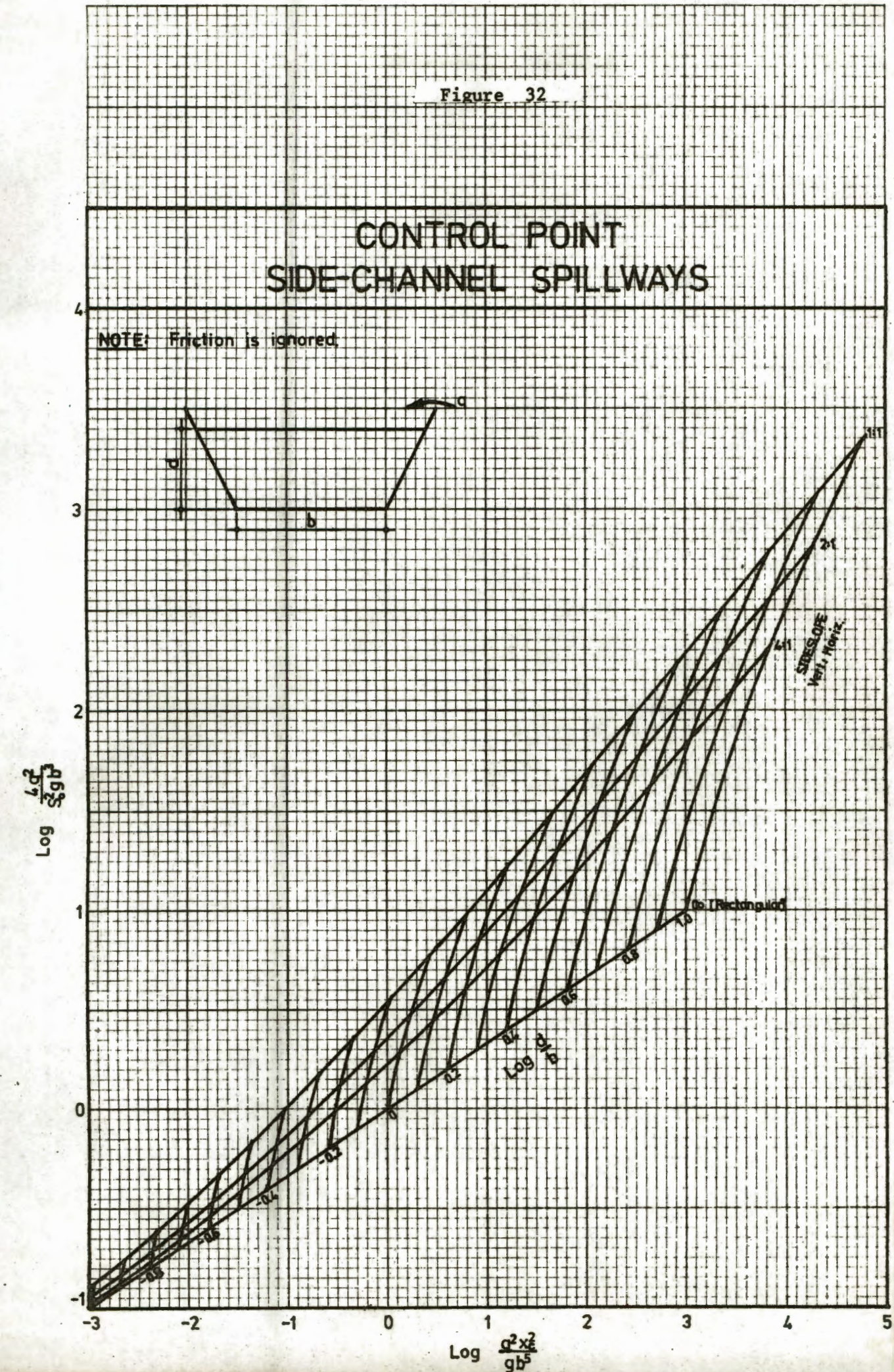
CONTROL POINT
SIDE-CHANNEL SPILLWAYS
NOTE: Friction is ignored.
q
d
b
1:1
2:1
4:1
SIDESLOPE Vert.: Horiz.
(∞ Rectangular)
1.0
0.8
0.6
0.4
0.2
0
-0.2
-0.4
-0.6
-0.8
Log d/b
Log $\frac{4Q^2}{S_c^2 g b^3}$
Log $\frac{Q^2 x_c^2}{g b^5}$
-3
-2
-1
0
1
2
3
4
5
-1
0
1
2
3
4

5. MODEL TESTS

5.1 Description of Model

In order to check the accuracy of the preceding theoretical analysis, a model was built of a side-channel spillway, and the water surface profile was studied under various conditions.

The model was built in an existing basin, of dimensions 9,74m x 6,09m x 1,0m, which represented the dam for which the spillway was to be built. Water was supplied to the basin from an overhead tank at flows of up to 0,09m^3/s. Water flowing over the spillway was pumped back to the tank which was kept overflowing to ensure a constant head.

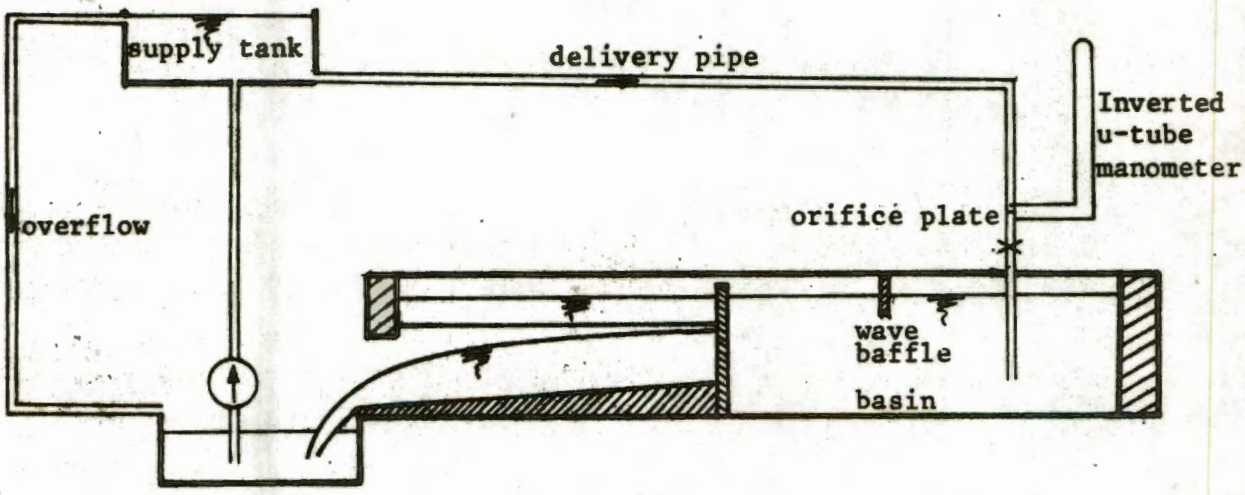

Figure 33 : Diagramatic sketch of water supply system

To avoid unnecessary disturbances of the water in the basin, the delivery pipe was extended to discharge below the water surface. However, small surface waves were still evident so a board was positioned on the surface as a wave baffle between the delivery pipe and the model and this had the effect of stilling the water in the vicinity of the model.

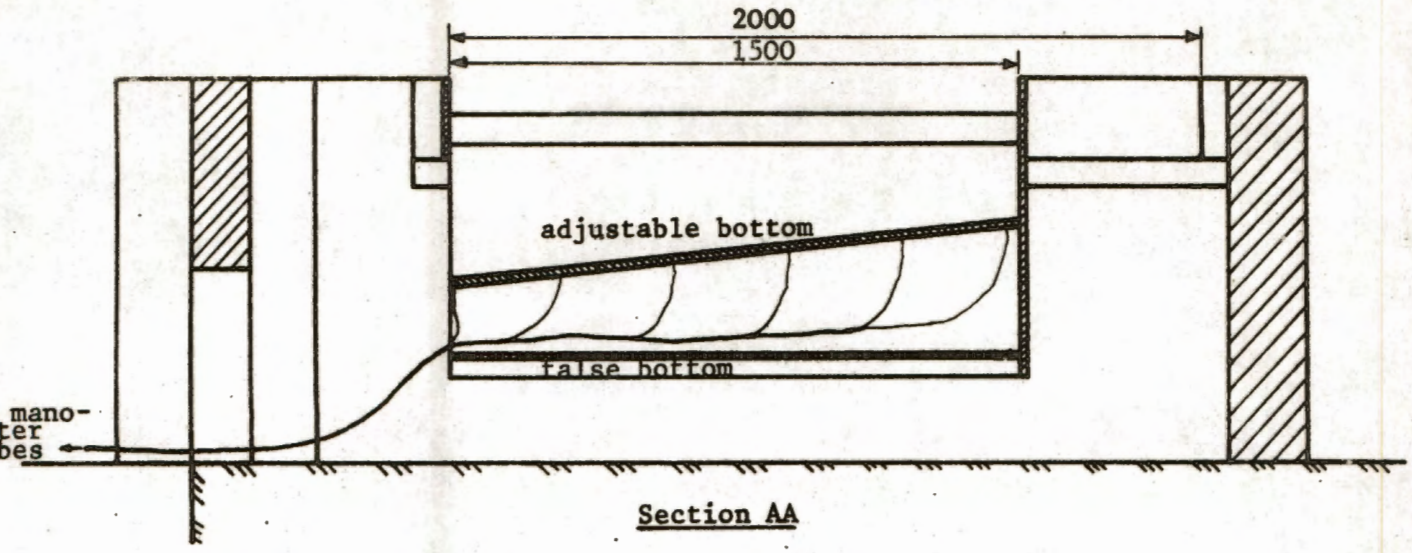

Section AA

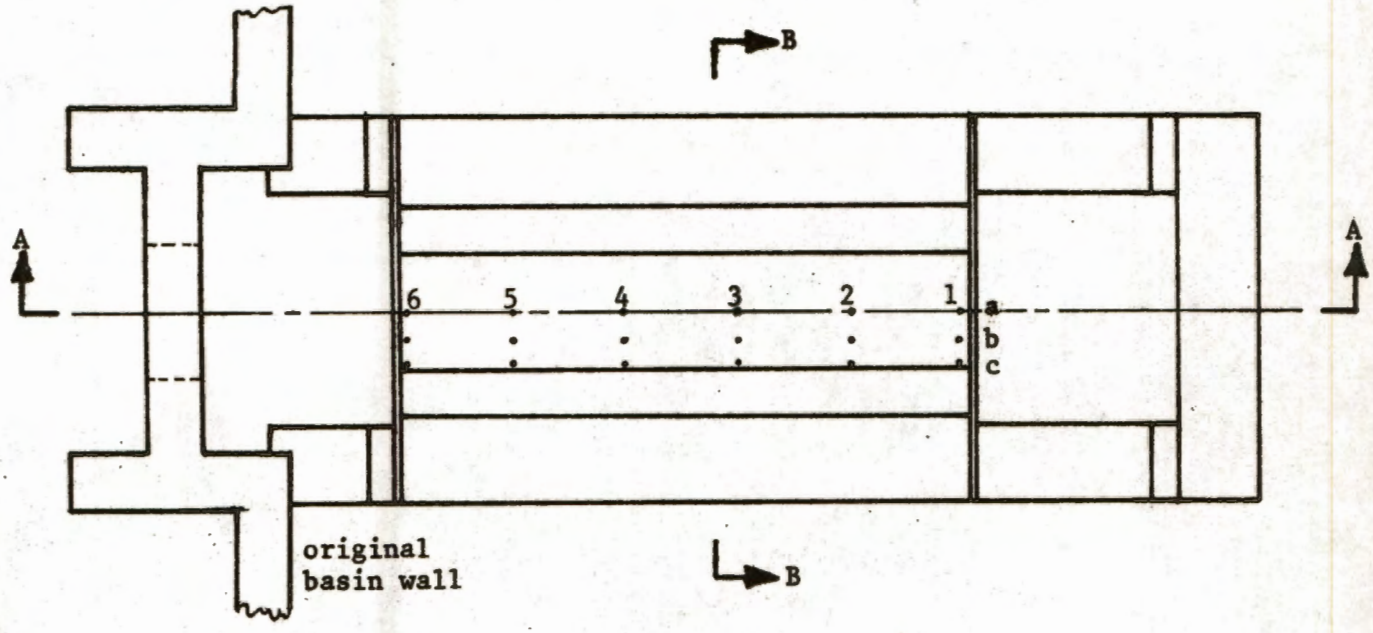

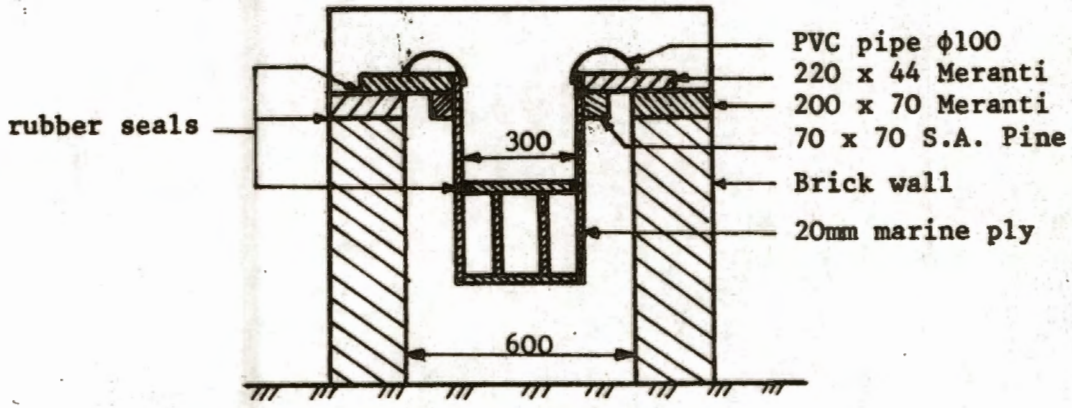

Section BB

FIGURE 34 : Details of model

Details of the model are shown in figure 34. A double sided spillway was used to obtain a symmetrical cross-sectional water surface in the receiving channel. The length of each crest was 1,5m but provision was made for an extension to 2,0m. The crests were made of semicircular PVC pipe of diameter 100mm. The sides and bottom of the receiving channel were of 20mm marine ply and this unit, consisting of spillway crests and receiving channel was bolted down onto a plastered brick outer wall which was topped with 70 x 200mm meranti beams.

The first model was different from that finally used in that it did not have the false bottom shown in the sketch. This meant that to alter the invert slope, it was necessary to remove the whole unit, crests and all. Because of the difficulty experienced in accurately levelling the crests, this was a very time consuming method. To overcome this difficulty, a false bottom was placed permanently in a horizontal position at a position lower than would be required for any invert slope or flow. The real invert was then placed above this resting on wedges which could be of different heights and slopes. The invert was sealed by means of sponge rubber strips along its sides and its upstream edge and could thus be lifted out of position to change the supporting wedges and thus change its slope and height.

It was also decided to change the width of the channel from the 0,4m used initially to 0,3m to obtain greater water depth in the channel.

5.2 Measurements

The flow was measured by means of an orifice plate in the delivery pipe. When the water depth in the basin is constant, this inflow is equal to the total flow over the spillway. The head drop across the orifice plate was measured by means of an air over water inverted u-tube manometer.

A Linford[26] gives the equation for flow through an orifice plate in accordance with BS 1042 (1951) as

$$Q = \frac{C_d A_2}{\sqrt{1 - n^2}} \sqrt{2gh} \qquad \ldots\ldots \quad (69)$$

where $n = \frac{A_2}{A_1}$

A_2 is area of orifice
A_1 is area of pipe
C_d is discharge coefficient
h is the head difference across the u-tube manometer.

The diameter of the orifice was 0,1196m (4,71 inches) and the diameter of the pipe was 0,1524m (6 inches). From the appropriate graph presented by Linford, C_d can be found to be 0,62. These figures can be put into equation (69) to give

$$Q = 0{,}0391 \sqrt{h} \qquad \ldots\ldots \quad (70)$$

At maximum flow, the head difference across the manometer was 5,3m. This great height, together with the fact that the water levels fluctuated considerably, made it difficult to obtain accurate readings of the head difference. Best results were obtained if two people read the two levels simultaneously. This was repeated a number of times and the average value was used in equation (70).

The accuracy of the flow measurement was tested by comparing the results obtained with a direct measurement where the volume of water entering the tank in a certain time interval was measured. The two flows agreed to within 0,6% so equation (70) was used with confidence.

The extreme turbulence in the receiving channel made accurate water depth measurement meaningless, and an attempt was made to obtain some sort of average depth. Initially the depths were measured directly, using a thin steel rule. With depth variations of up to 30 and 40 mm at a point where the depth was only about 200mm, this was an accurate enough method, but was extremely tedious.

To make measuring easier, pressure tappings were used. Holes were drilled through the bottom and plastic tubes were inserted, their other end being clamped vertically on a calibrated board where the water levels could be easily read.

To obtain the cross-sectional, as well as the longitudinal water surface profile, three longitudinal rows of tappings were used. One row was positioned along the centre line, another was placed as close to the corner as possible and the third was between the two, i.e. at the quarter point. The cross-section being symmetrical, it was hoped that the full cross-sectional profile could thus be obtained along the length of the channel. For easy reference, each hole was numbered from 1 to 6 starting at the upstream end, and the three rows were labelled a, b and c from the centre outwards.

5.3 Observations

The water in the receiving channel was extremely turbulent, making accurate measurement impossible. However, the manometer tubes did dampen this effect to a certain extent, and it is felt that the readings obtained gave a reasonable average water depth.

In the first model, the receiving channel was relatively deep so that the water entering over the spillway crests had a considerable distance to fall before reaching the water surface in the channel. It was hoped that the turbulence could be appreciably reduced by making the channel shallower so that the water surface was closer to crest level. However, this was not found to be the case. Even when the spillway was drowned, no lessening of the turbulence could be observed.

It would therefore appear that this extreme turbulence is a feature of all structures of this kind. Indeed the turbulence is necessary, being the mechanism of momentum interchange required to accelerate the incoming water in the direction of the flow in the channel.

Despite the turbulence, certain characteristics of the water surface profile were very obvious. In cross-section, the profile was humped, i.e. the water was deeper along the centre line than along the sides. This was apparantly due to the effect of the water entering vertically downwards against the two sides, flowing perpendicularly across the bottom, meeting in the middle and swirling upwards. With low flows and steep invert slopes, this was particularly noticeable as the water at the upstream end was extremely shallow. The water could be clearly seen flowing perpendicularly across the bottom from either end and bubbling up into a narrow, well defined ridge along the centre line.

Another observation was that at the extreme upstream end of the channel, with larger flows, the water surface first rose for a short distance before falling in a downstream direction. This is not accounted for by equation (26), but can be accounted for by the inclusion of the momentum correction factor as in equation (27). However, the effect is small in the case of no flow over the upstream end, and for design purposes, can be neglected.

On comparing the depths obtained from the manometer tubes with observed results, two discrepancies became apparent.

(i) The manometers showed the water to be much deeper at the sides than was actually the case. This was apparently due to the velocity head of the water entering the channel vertically downwards against the sides. All readings from manometers in row (c) were therefore ignored. The results obtained from the other rows were considered sufficient as row (a) gave the maximum depth along the centre, while row (b) gave a value which could be considered as a reasonable average across the cross-section.

(ii) The manometers at the downstream end showed the depth to be much less than was actually the case. This was due to the

extreme curvature of the water surface as it passed over the free overfall. These values were therefore also ignored. In tests 2 and 3, the water depth was therefore also measured directly at the downstream end.

The actual readings taken during testing are tabulated in appendix A but the results are shown graphically on the following pages.

5.4 Conclusions

It can be seen from these results that the theoretical curves agree closely with the results obtained in the experiments. It is regretted that the effect of the size of the model on factors such as the amount of turbulence could not be investigated as this could possibly lead to variations in depth. However, it is felt that any such effects would be small and it is therefore concluded that the forgoing theory can be used with confidence to design side channel spillways.

$b = 0{,}3$ m $n = 0{,}015$?

$L = 1{,}5$ m $S_c = S_o$?

$S_o = 0$

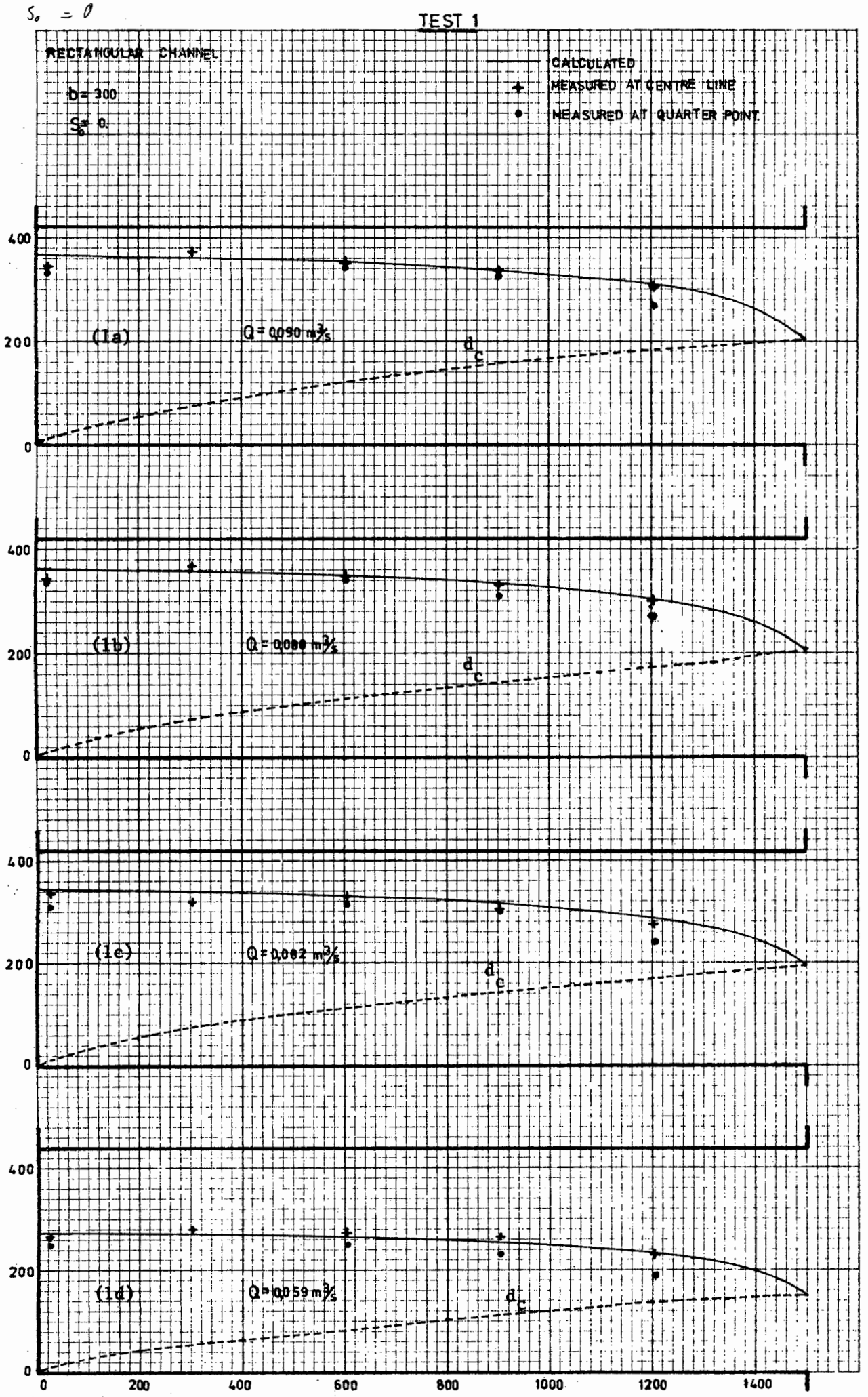

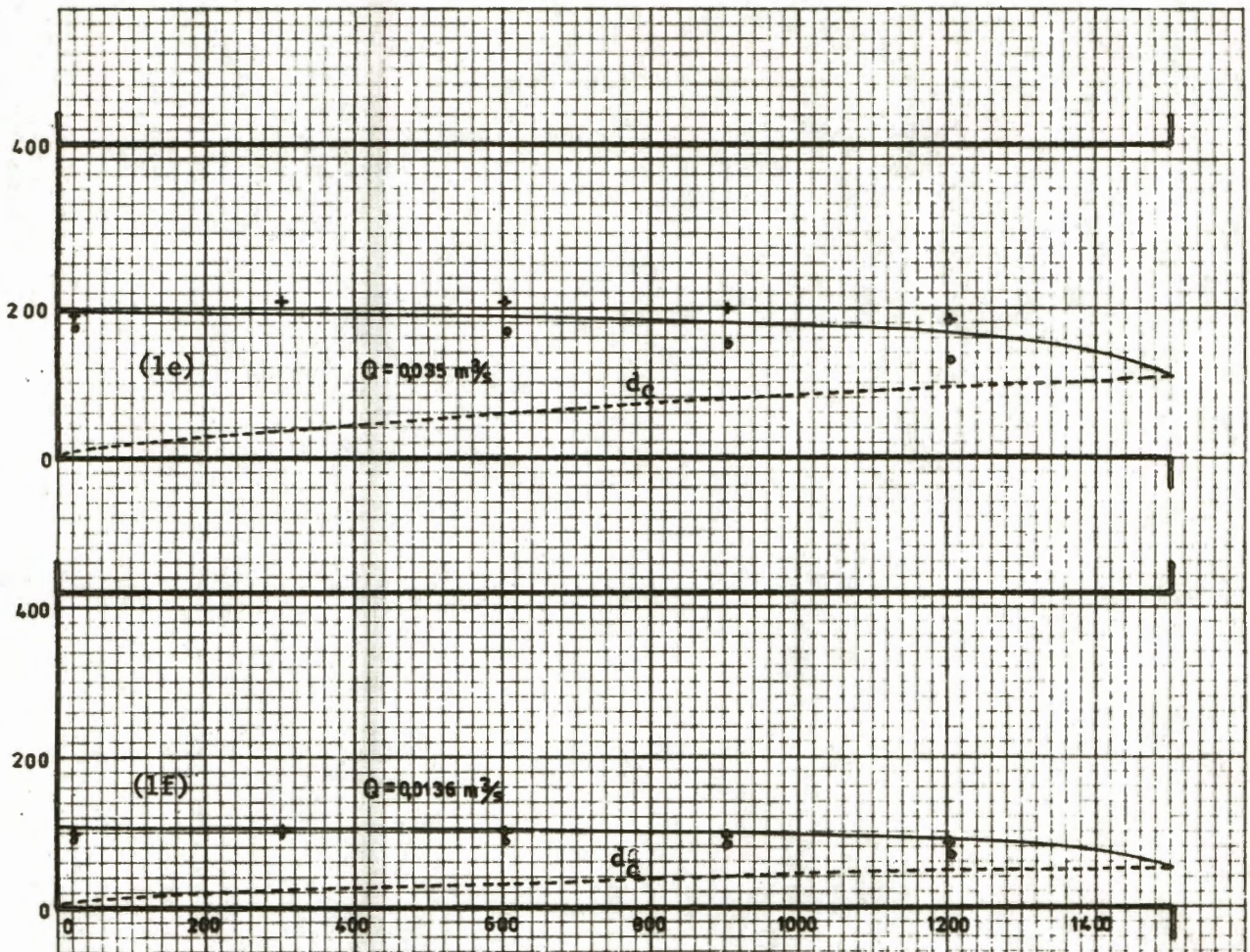
400
200
0
(1e)
Q = 0,035 m³/s
dc
400
200
0
(1f)
Q = 0,0136 m³/s
dc
0
200
400
600
800
1000
1200
1400

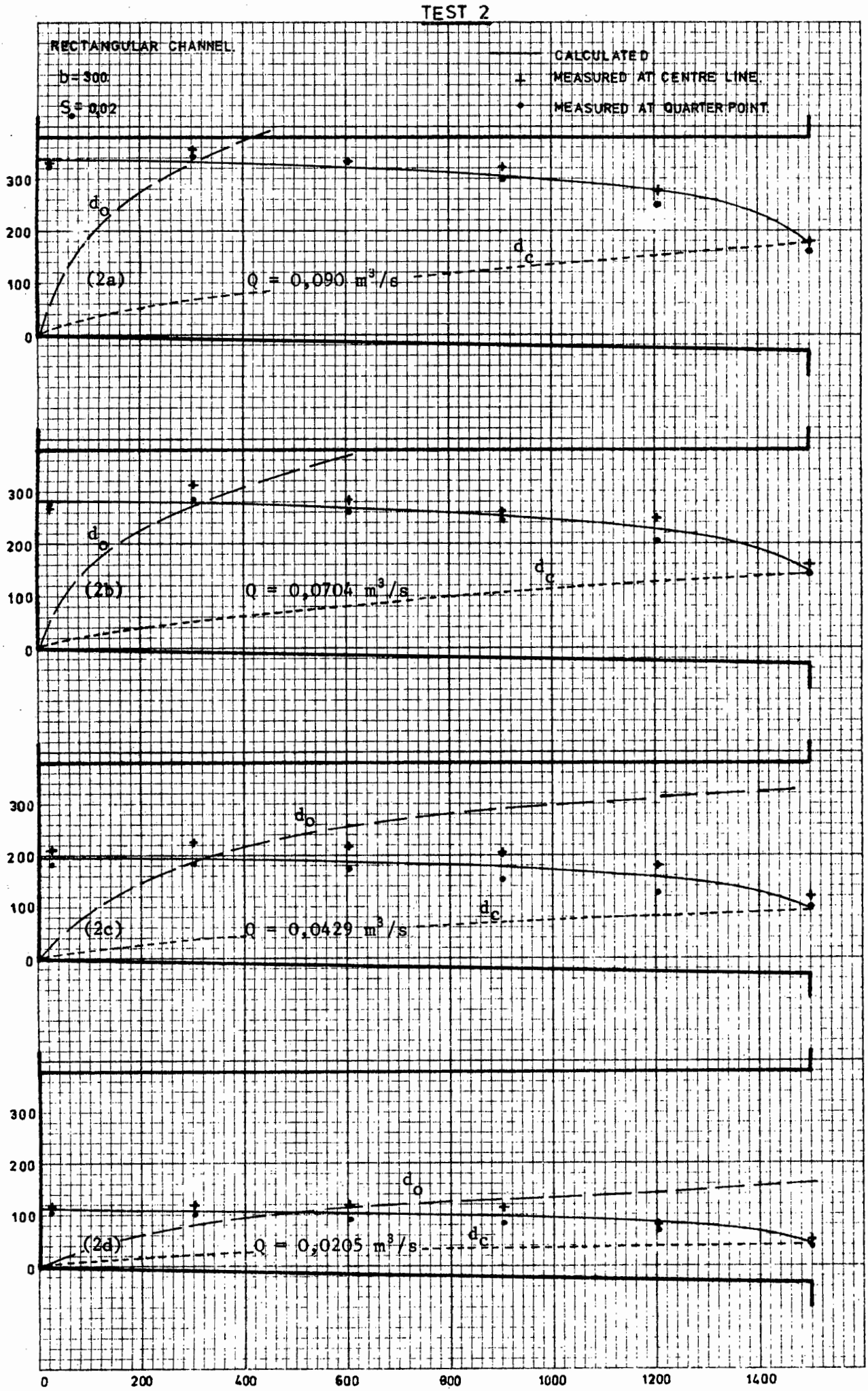
TEST 2
RECTANGULAR CHANNEL
b = 300
S = 0,02
CALCULATED
MEASURED AT CENTRE LINE
MEASURED AT QUARTER POINT
(2a)
Q = 0,090 m³/s
(2b)
Q = 0,0704 m³/s
(2c)
Q = 0,0429 m³/s
(2d)
Q = 0,0205 m³/s
d_o
d_c
0
100
200
300
400
600
800
1000
1200
1400

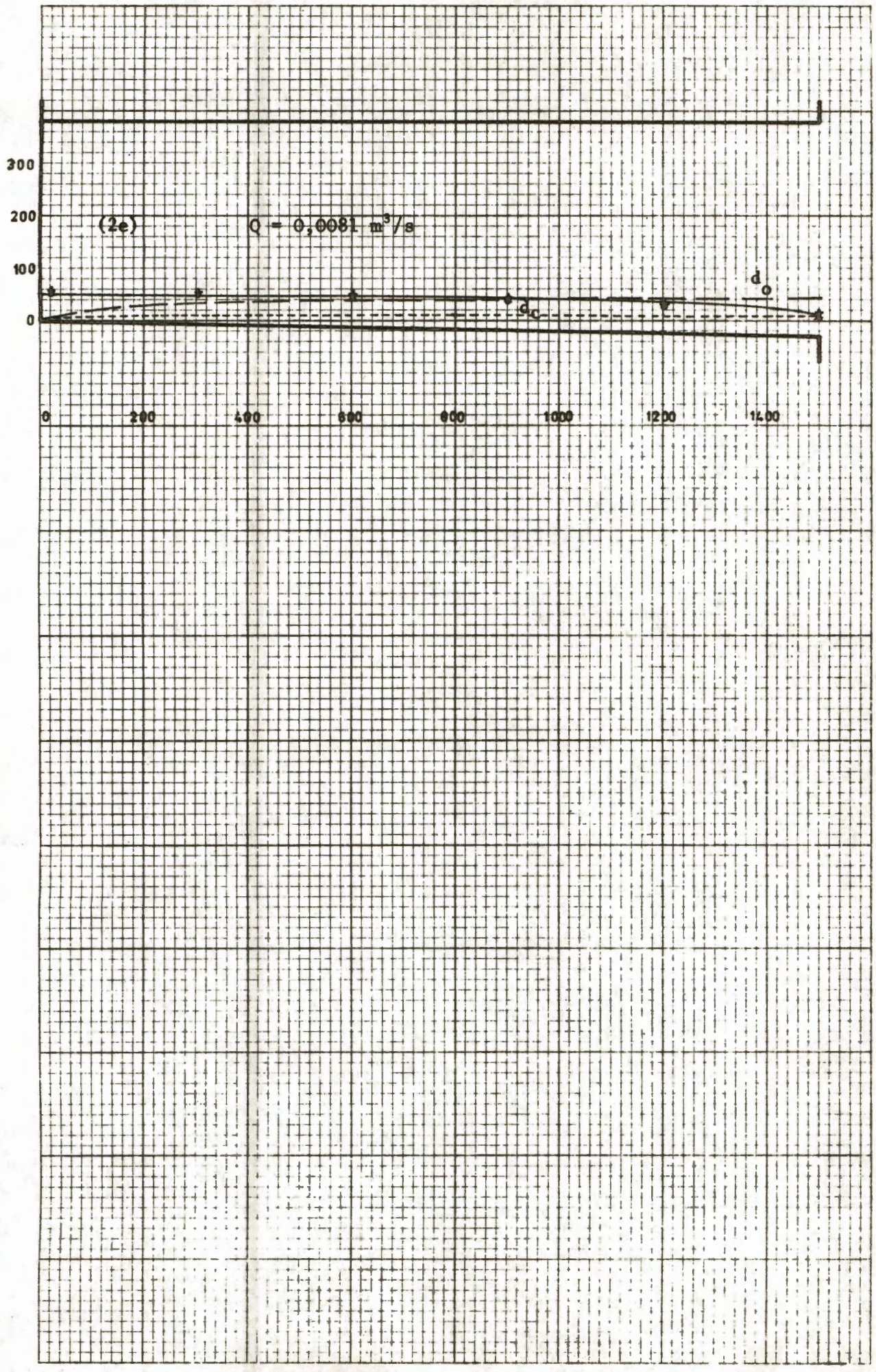
300
200
100
0
(2e)
Q = 0,0081 m³/s
d
o
d
c
0
200
400
600
800
1000
1200
1400

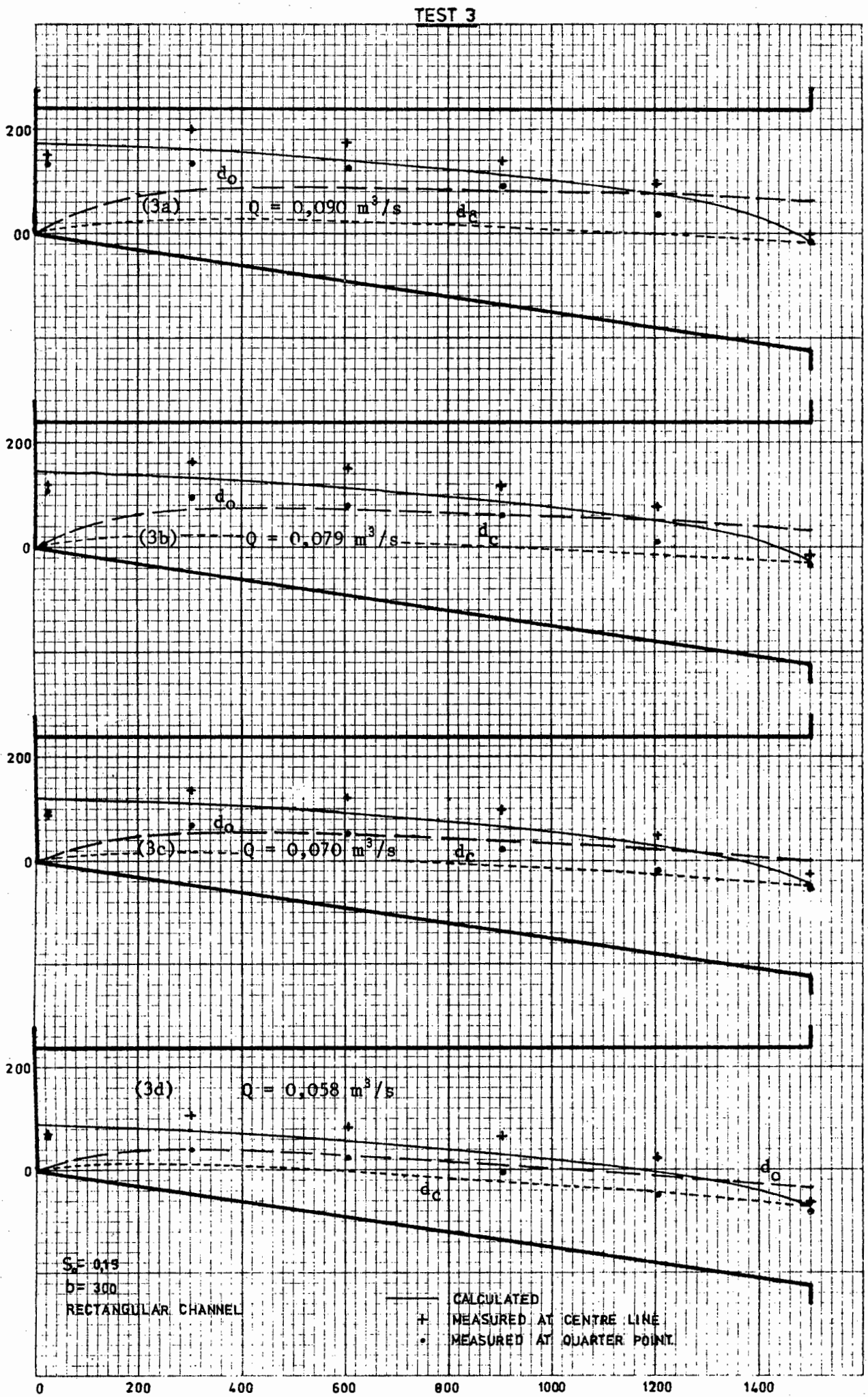
TEST 3
200
00
d_o
(3a) Q = 0,090 m³/s
d_c
200
0
d_o
(3b) Q = 0,079 m³/s
d_c
200
0
d_o
(3c) Q = 0,070 m³/s
d_c
200
0
(3d) Q = 0,058 m³/s
d_o
d_c
S_o = 0,15
b = 300
RECTANGULAR CHANNEL
CALCULATED
MEASURED AT CENTRE LINE
MEASURED AT QUARTER POINT
0
200
400
600
800
1000
1200
1400

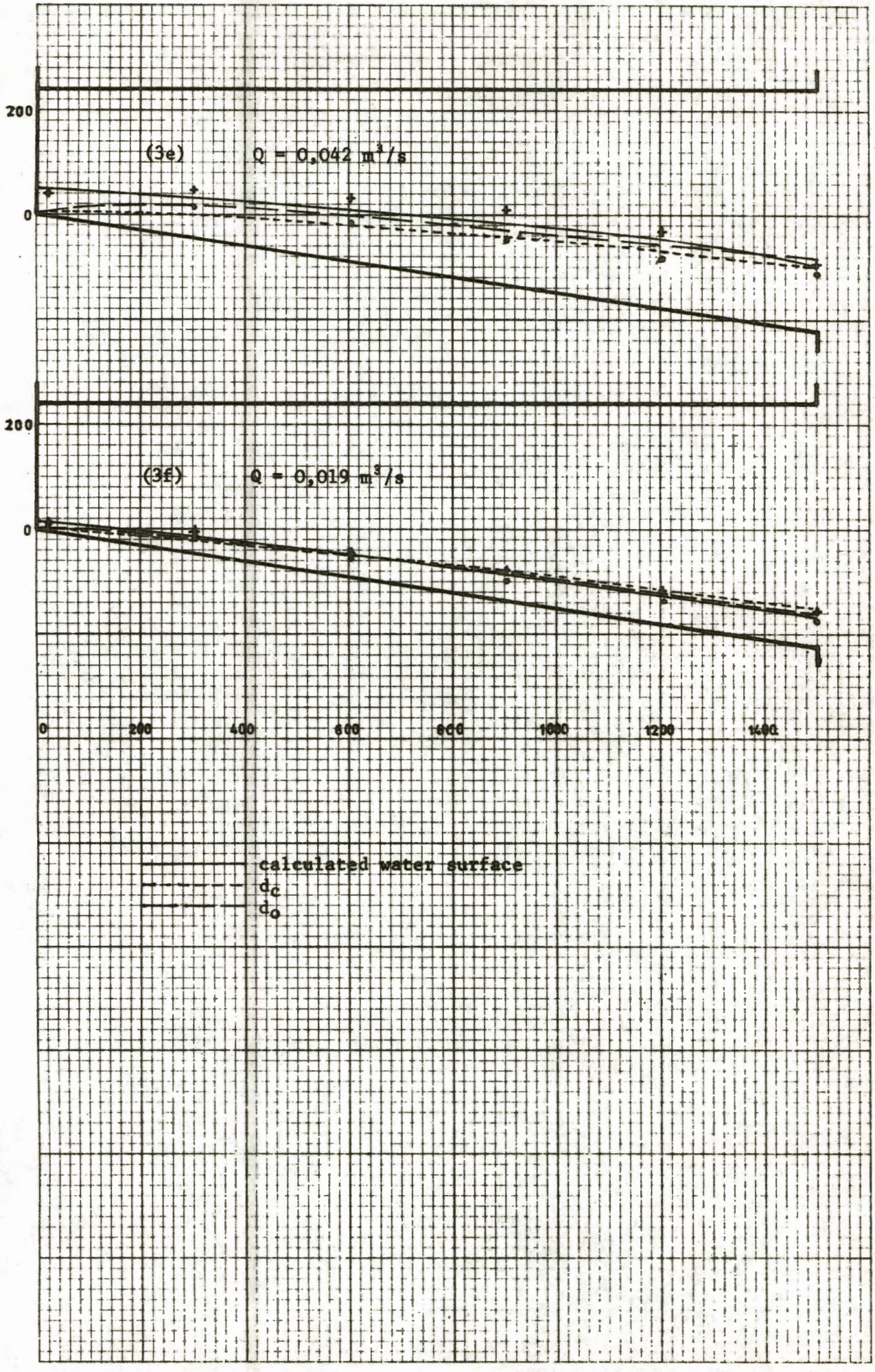
200
0
(3e) Q = 0,042 m³/s
200
0
(3f) Q = 0,019 m³/s
0
200
400
600
800
1000
1200
1400
calculated water surface
d_c
d_o

6. THE MTATA DAM SPILLWAY

6.1 General Description

An opportunity arose to test a u-shaped side-channel spillway when the department was approached by a firm of consulting engineers with a request to test their hydraulic design of the side channel spillway proposed for the new Mtata dam.

A rockfill wall was to be built with a length of over 600m and a maximum height of 36m. At one end of the wall, a double-sided side channel spillway was proposed with a semi-circular section at the upstream end, giving the spillway crest a horse-shoe shape. The straight sections of the crest were 45m long and 38,32m apart with a ogee profile. From the receiving channel, the water flowed down a 317m curved discharging channel, back to the Mtata river. This channel was trapezoidal with a base width of 10m and a sideslope of 4:1. Both the receiving and discharging channels had a uniform slope of 1:200. The design flow was 2430m^3/s. The general layout can be seen in figure 35.

A head-discharge curve was to be drawn for the spillway and the flow condition in the receiving and discharging channels was to be investigated.

6.2 The Model

It was decided to build a scale model of the spillway in the basin used previously and to use as much as possible of the previous spillway. The maximum flow available in the laboratory was 0,09m^3/s or 1/27000 of the prototype design flow. This gave a maximum permissable linear scale of 1:59. A scale of 1:64 was finally chosen.

Before deciding exactly how much of the prototype to model, some calculations were done to isolate any problem areas.

A depth of 4,5m was allowed between the top of the dam and the spillway crest level. Using this head and the nett spillway length of 134,69m, the design flow gave a discharge coefficient of $C_d = 1,89$ in the equation

$$Q = C_d L h^{\frac{3}{2}} \qquad (71)$$

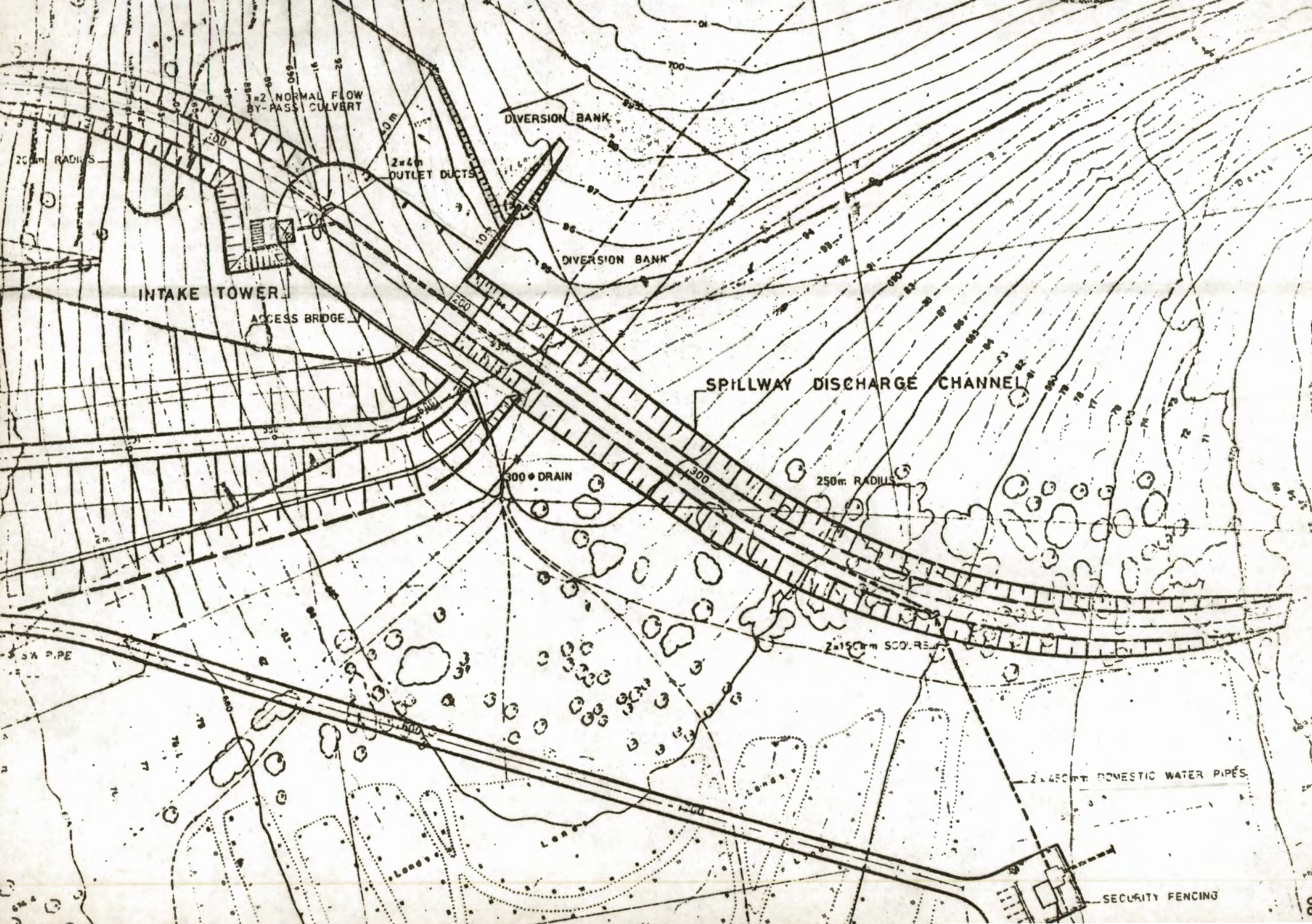
3×2 NORMAL FLOW
BY-PASS CULVERT
DIVERSION BANK
2×4m
OUTLET DUCTS
DIVERSION BANK
INTAKE TOWER
ACCESS BRIDGE
SPILLWAY DISCHARGE CHANNEL
300ø DRAIN
250m. RADIUS
2×150mm SCOURS
2×450mm DOMESTIC WATER PIPES
SECURITY FENCING

The coefficient for an ogee spillway under design head is 2,25 so this appeared to be very conservative. However, the approaches to the spillway were, in this case, very shallow while ogee profiles and their corresponding coefficients are obtained for deep water approaches. It was therefore decided to model accurately the approaches to the spillway. Indeed, this was a requirement of the client.

The next step was to calculate the water depths in the receiving and discharging channels. Considering the discharging channel as concrete lined, with a Manning's n of 0,017, gave a normal depth of 14,66m. The critical depth for this channel is 15,82m. The discharging channel is therefore hydraulically steep. The receiving channel is of extremely mild slope so the depth at its downstream end will be critical, i.e. 15,82m. As this channel is 23m deep, it would appear to be extremely conservatively designed. However, if the discharging channel is not concrete lined and a Manning's n of 0,033 is assumed, then the normal depth is 21,865m and the slope is mild. The depth at the downstream end would be this value of 21,8m, which would result in slight drowning of the spillway crests at the upstream end. This would then be a reasonable economic design. It would appear however, that with a concrete lined discharging channel, the receiving channel could be made shallower.

As mentioned above, the depth at the downstream end of the receiving channel should be critical, i.e. 15,82m. The water surface in the discharging channel should then tend to the normal depth of 14,66m by means of an S2 profile. The depth of the channel decreased in a downstream direction and at approximately chainage 360m, becomes less than the normal depth. The channel would therefore overflow beyond this point. The channel becomes very shallow towards the downstream end and a considerable amount of water would overspill the banks and could be expected to spread over a wide area. It was therefore necessary to model a wide section of land on either side of the channel in the region where overflow was expected.

Before construction could begin it was necessary to first dismantle the existing model. The unit consisting of receiving channel and spillway crests was unbolted and lifted out, leaving the supporting brick structure topped with the 70mm thick meranti beams along the two sides.

The raised brickwork at the upstream end was then knocked down to the same level as the sides and also topped with a 70mm beam. A watertight joint was obtained by means of a thin sheet of rubber and contact adhesive. A 1,22 x 2,44m (4 x 8 ft) sheet of 20mm marine ply was placed over this structure and tightly screwed down. To obtain a tight seal thin strips of "German sponge" rubber were placed between the ply and the underlying beams. A u-shaped piece was then cut from the ply to take the receiving channel.

The receiving channel and spillway crests were constructed as a unit and then fitted in position. The semicircular upstream end was turned on a lathe as a full circle and then cut in half. One half was then joined to the straight section. Yellowtung beams 220 x 70mm were glued and dowelled together to make up pieces of the required size. This unit was then placed in position, accurately levelled, and fixed by means of brackets, to the marine ply board. The control tower and splitters were fixed in position by means of thin metal pins which could easily be withdrawn to test the spillway behaviour with different splitter configurations.

The upper stretch of the discharging channel, chainage 200 to 300, was straight. This was therefore made from varnished 9mm marine ply and was supported at intervals of 390mm (25m prototype size). For the lower section, because of the curve, a completely different method of construction was used. Radial cross-sections were cut out of 6mm plywood and accurately fixed in position every 312 mm (20m prototype size) along the centre line. The spaces between were filled with sand and the final finish was obtained by covering the sand with a sand-cement plaster of about 10mm thick.

To model accurately the roughness of the prototype was impossible. However, it was felt that the smooth plaster would be a reasonable model of the prototype's concrete lined channel. The varnished timber in the upstream section would probably be too smooth, but it was felt that any error introduced, would be small.

The area surrounding the spillway was modelled in the same way, with templates being cut to the shape of the ground contours and placed perpendicular to the spillway at intervals of 156mm (10m prototype size). Here, however, the model was not built up from the ground but was built on boards which were supported on brick pillars at their outside edges and on the marine ply board at the centre.

Scales:
Drawing to prototype 1:2000
Drawing to model 1:31,25

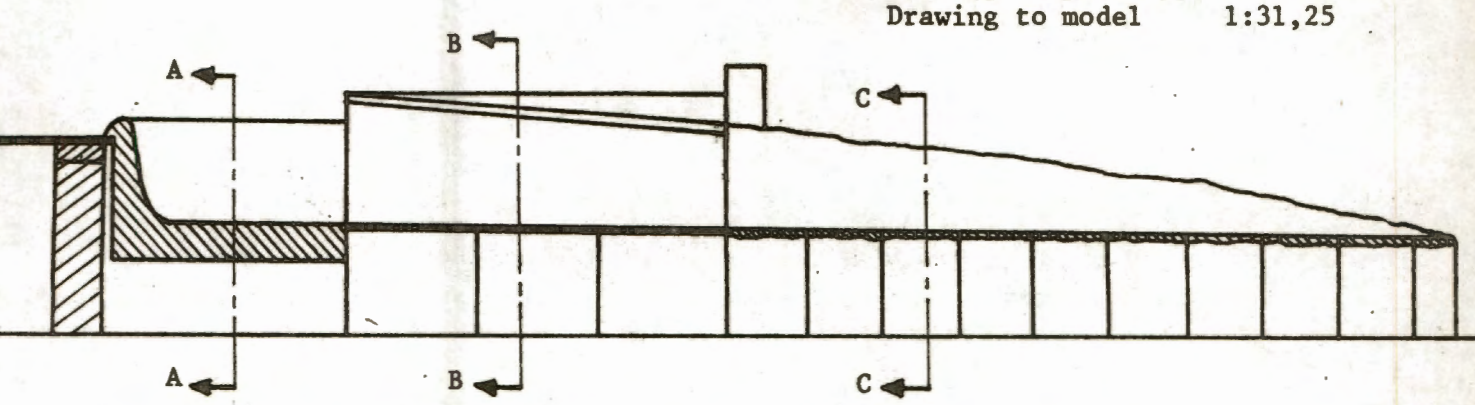

Longitudinal section along receiving and discharging channels

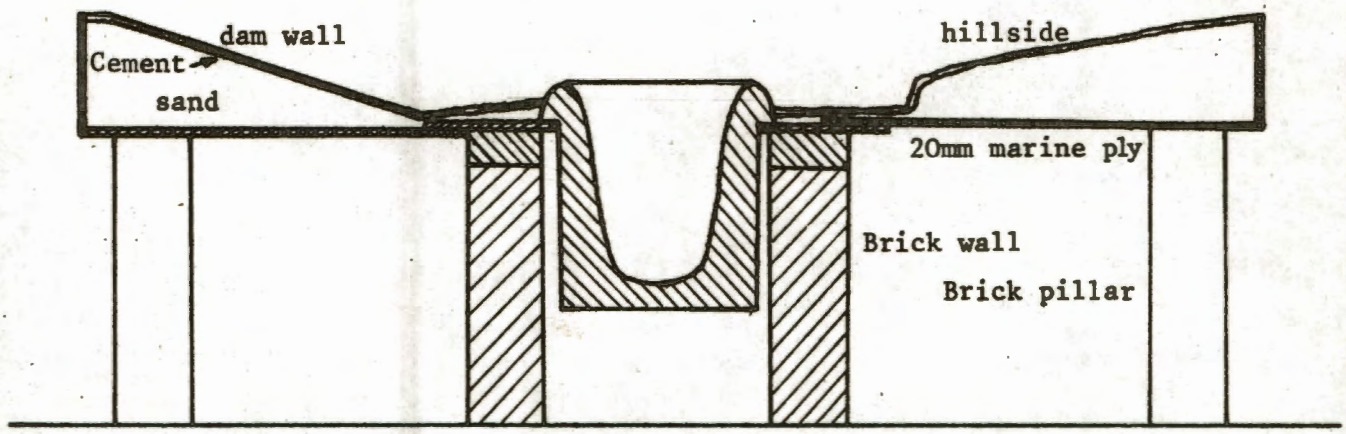

Section AA

Scales:
Drawing to model 1:20
Model to prototype 1:64

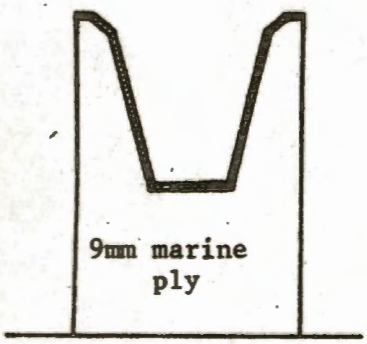

Section BB

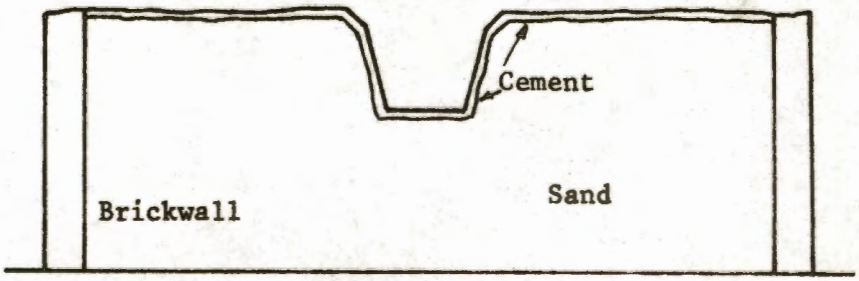

Section CC

FIGURE 36 : Mtata dam model

6.3 Measurements

The flow was measured by means of an orifice plate in the supply pipe as before.

The depth of water in the basin, and thus the head on the spillway crest was measured by means of a point gauge situated in the corner of the basin where the water surface was least disturbed. This gave the deep pool level. Because of the shallow approaches to the spillway, the water velocities in that region were high and considerable drawdown occurred. Some depth measurements were therefore required in this region. These were made by means of a second point gauge which was mounted on a steel angle spanning the receiving channel perpendicularly, as can be seen in the photographs.

Water depths in the receiving and discharging channels were measured directly by means of a thin steel rule held upright in the water. With the exceedingly turbulent flow, more accurate measurement was not possible, and the effect of the rule on the flow was neglible.

6.4 Results

The actual readings taken during testing are tabulated in appendix B, but are shown here, scaled up to prototype size, in figures ~~37~~ 38 and ~~38~~ 39.

Depth measurements in the receiving and discharging channels were made at the design flow of 2430 m^3/s and at one tenth of this flow, the latter being considered the average annual flood.

As can be seen from figure ~~37~~ 38, both channels operated satisfactorily under both conditions although considerable flooding did occur along the lower reaches. A large amount of scouring is likely under these conditions but as no information was available about the vegetation or about the depth and nature of the topsoil, no attempt was made to determine the extent of scour. Indeed, scouring could drastically change the ground contours and the whole flow pattern in the area. Although excessive scouring is not desirable, it is preferable to the great expense

which would be necessary to eliminate it. The design of the receiving and discharging channels is therefore considered satisfactory.

To test the behaviour of the spillway, head-discharge curves were drawn under three conditions:

(i) The first condition was with all the splitters and the control tower in position according to the plans. The results show that the dam would be overtopped at a flow of 2225 m^3/s which is only 92% of the design flow. Under these conditions, the discharge coefficient in equation (71) is only 1,72.

(ii) The control tower and splitters were then removed and the test was repeated. Under these conditions, the dam was only overtopped at a flow of 2475 m^3/s which is 102% of the design flow. The discharge coefficient in this case was 1,74. This indicates that the increased discharge was due almost entirely to the increased spillway length and the splitters appear to have resulted in a lowering of the discharge coefficient instead of improving conditions.

(iii) For the third test, therefore, all unnecessary splitters were removed, leaving only three which was considered the minimum number required to support the footbridge to the control tower, which was also left in position. In this case the dam overtopped at a flow of 2300 m^3/s which is 95% of the design flow. The discharge coefficient under these conditions was 1,66, which was markedly lower than in previous cases. This was surprising as the conditions were a compromise between those in conditions 1 and 2 and it had been expected that the coefficient would likewise be an average of the two. It was therefore concluded that the control tower had an adverse effect on the flow conditions and that in condition (i), this had been countered by the splitters.

It was therefore decided to include one more splitter to reduce the effect of the tower. This was placed at chainage 155, i.e. where the straight section of the crest met the curved section. A single test was done under this condition. At the design flow, the head was found to be 4,614m. The dam wall was therefore once again submerged

but this time only very slightly. The discharge coefficient was 1,71 this time, which is much closer to those in the first two conditions. Using this value and the maximum allowable head of 4,5m, equation (71) gives the flow as 2340 m^3/s or 96% of the design flow.

It was therefore recommended to the client that this configuration of splitters be adopted. Any further increase in discharge would have to be achieved by either lengthening the spillway or improving the approach conditions by excavation.

The client in fact decided that for structural reasons all the splitters on the right-hand side were necessary for supporting the foot-bridge and furthermore that the single splitter on the opposite side should be moved closer to the tower and was finally positioned at the extreme upstream end, i.e. on the centre line. It was also decided that because the design flow had been fairly arbitrarily fixed upon, a small reduction in capacity was acceptable. Unfortunately, no tests were done with the final splitter configuration.

Figure 38 : MTATA DAM

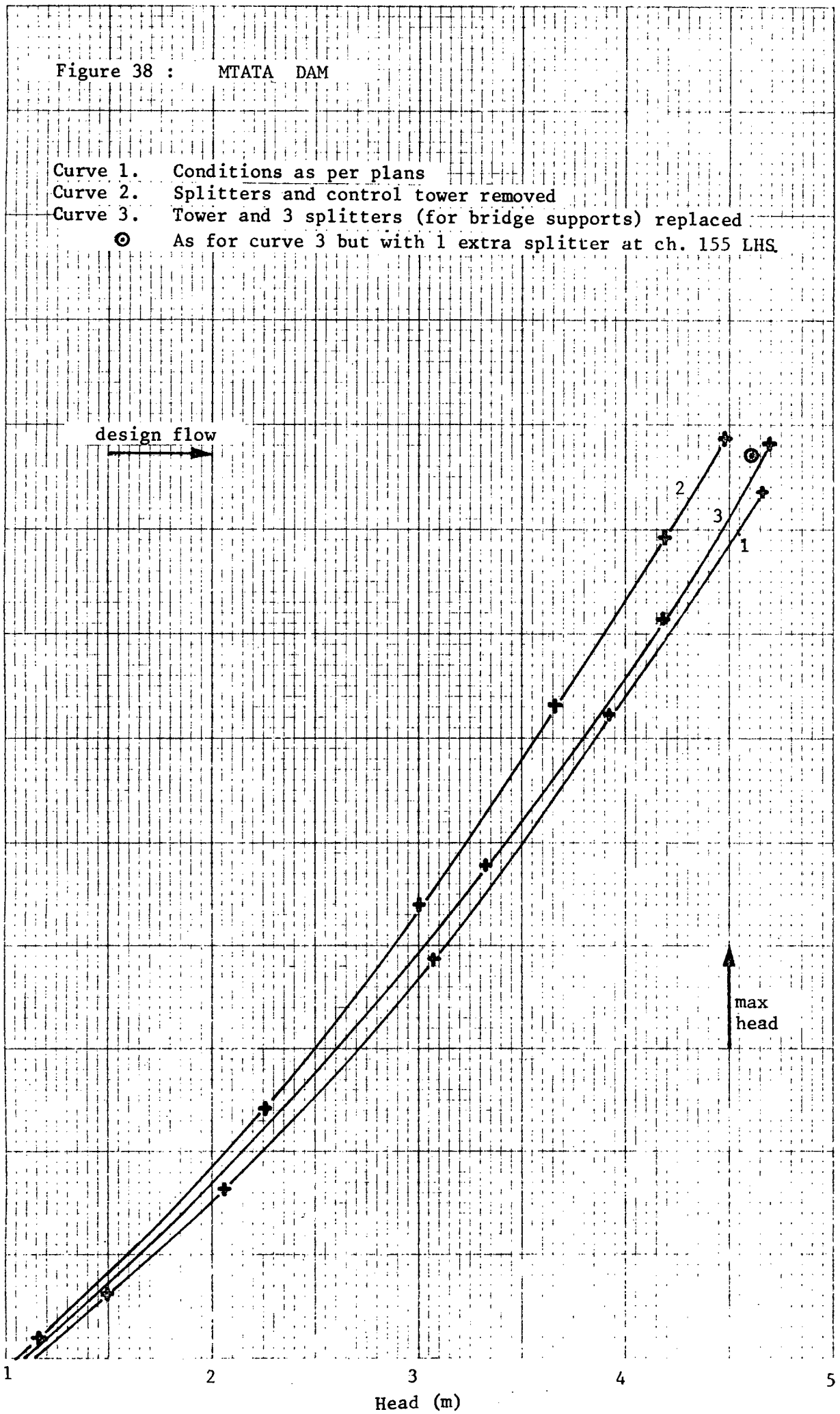

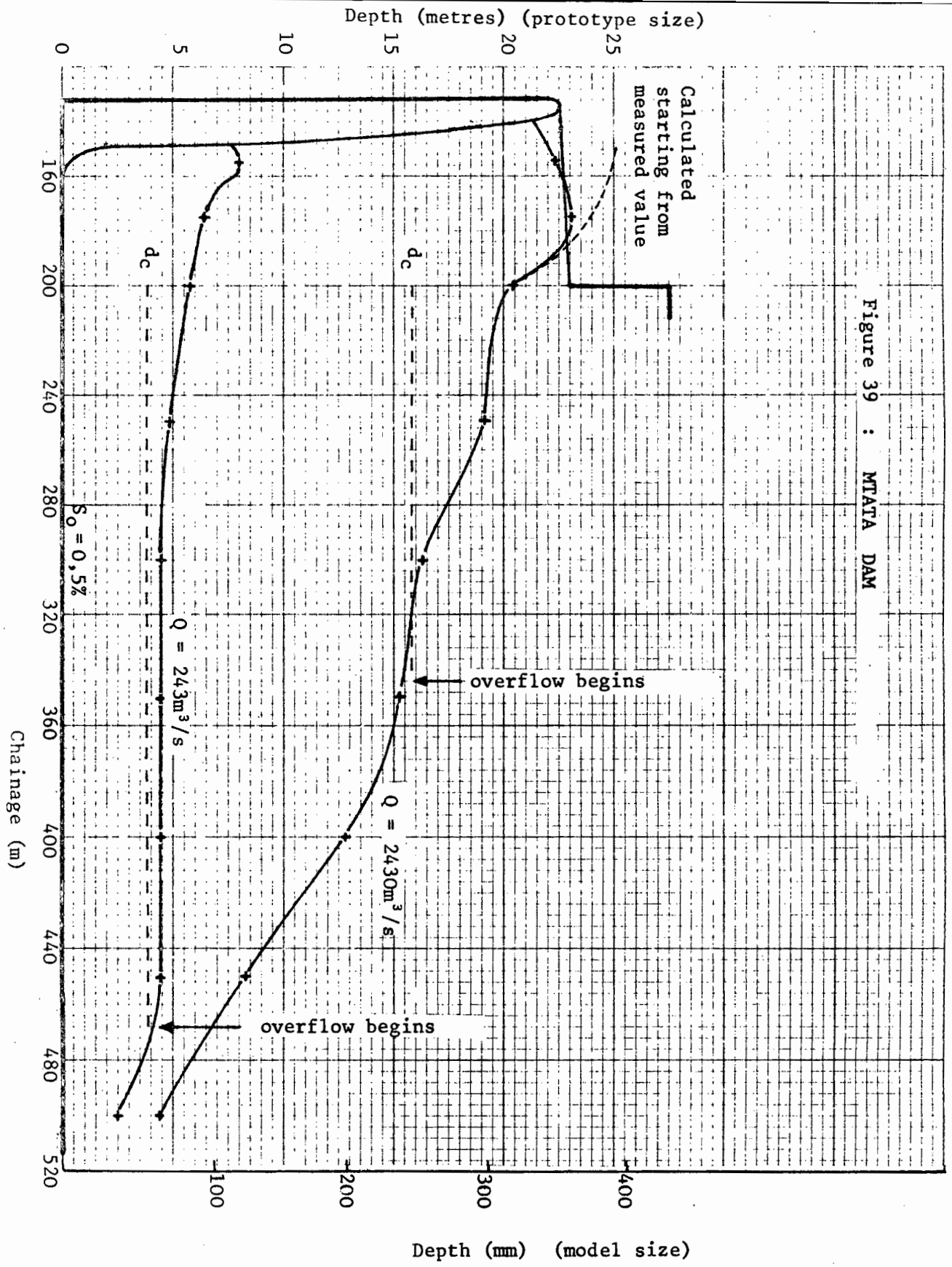

Figure 39 : MTATA DAM

6.5 Observations and Discussion

Looking at the model in operation led to a number of interesting observations being made. These can also be clearly seen in the photographs.

As in the previous model, the flow was extremely turbulent, and the water surface was distinctly humped in cross section. This was again apparently due to the incoming water entering vertically downwards against the sides and swirling upwards at the centre.

The humped effect was also very noticeable longitudinally. This was apparently due to the effect of the water entering over the upstream end. This phenomenon was also noticed by Farney and Markus[11] who adjusted the basic equation to account for this by including an emperical "momentum correction factor".

At low flows an interesting phenomenon occurred in the receiving channel at the centre of the curved section. The water entering over the curved section of spillway flowed down the sides and then radially inwards towards the centre of the semicircle where it was forced upwards in a type of fountain. This can be clearly seen in photograph 4. As the flow was increased, the fountain itself did not appear to change but was slowly drowned as the area surrounding it filled with water. It would appear that the same type of behaviour occurs at the bottom of the channel even when it is full and this could be responsible for the shape of the surface profile.

From figure 37, it can be seen that at both flows tested, the depth was greater than the critical depth. This is contrary to expectations and indicates that the roughness of the model channel had been underestimated.

For a mild slope, the depth in the discharging channel should be equal to the uniform depth along the whole channel. For the smaller flow, it would therefore appear from the graph that the normal depth was 70mm (4,5m prototype size) which occurred between chainage 300 and chainage 450. From this depth, and the flow of 0,00742 m^3/s (2430 m^3/s prototype size), it can be calculated that the corresponding value of Manning's n is 0,0137 which seems a reasonable value to expect. If this figure is applied to the larger flow, a normal depth of 306 mm is

calculated. This is indeed the depth measured just downstream of the spillway in the region between chainage 200 and chainage 240. The decrease in depth downstream of this point could possibly be attributed to drawdown caused by the water overflowing the banks lower down.

Looking at the curve for the lower flow, it can be seen that the water depth increases upstream of chainage 300. The model is, in fact, smoother in this region than further downstream so the water would be expected to become shallower. It was noticed, however, that the extremely turbulent, swirling flow in the receiving channel seemed to be carried downstream into the discharging channel and was noticeable up to about chainage 300. This then, is a possible cause of the increase in depth.

However, this effect should be even more noticeable with the larger flow. Looking at the curve for the design flow, it therefore seems possible that the depth of approximately 0,25m at chainage 300 is the normal depth and that the deeper water upstream of this point is due to the effect mentioned above. This normal depth would then indicate a value of Manning's n of 0,0098 in this case.

This figure is considerably lower than for the small flow. It should be realised, however, that Manning's n is dependent on size so varies for different flows and between model and prototype.

As friction is the dominating factor determining the normal depth, the Reynolds number in the different cases is worth investigating.

The model scale value of the design flow of 2430 m^3/s was 0,0742 m^3/s and the measured depth at chainage 300 was 0,25m. From the formula $R_e = 4Q/\nu R$, the Reynolds number is found to be $3,65 \times 10^6$ and from the formula $f = 2gn^2/R^{\frac{1}{3}}$, the friction factor is found to be 0,0043. From the standard friction factor versus Reynolds number chart, this condition is represented by a point in the completely turbulent zone, where the friction factor is independent of the Reynolds number. From the chart the value of K/4R can be seen to be 0,0005 which gives a value of K of 0,2mm. This appears to be reasonable although no measurements were made of roughness.

If for the prototype, with the flow of 2430 m^3/s, the depth is taken as 16m, then the Reynolds number is $1,87 \times 10^9$ which is again in the region

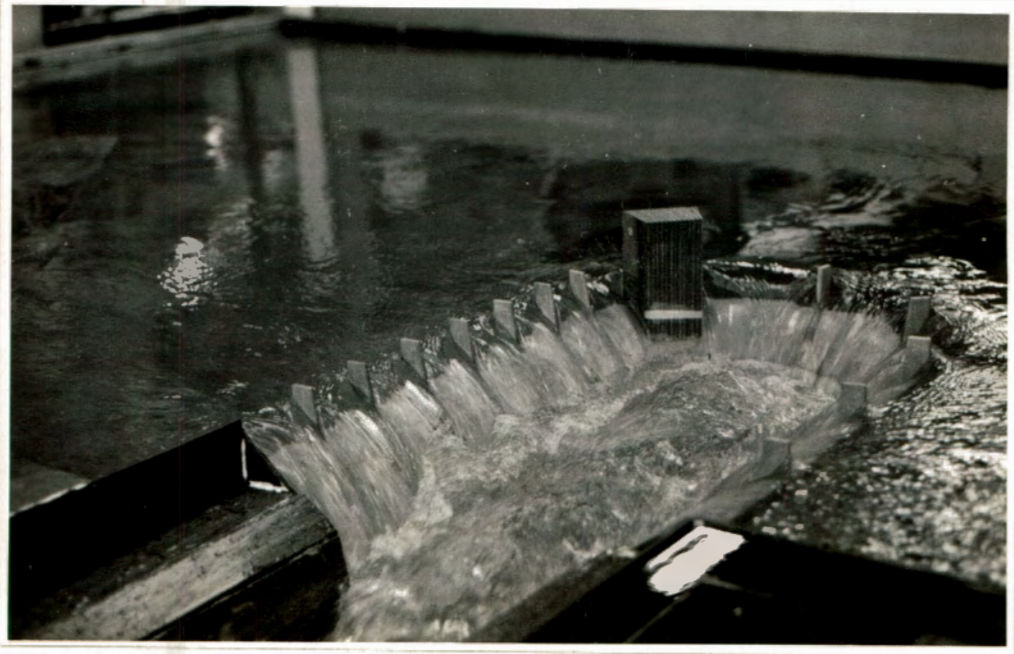

1

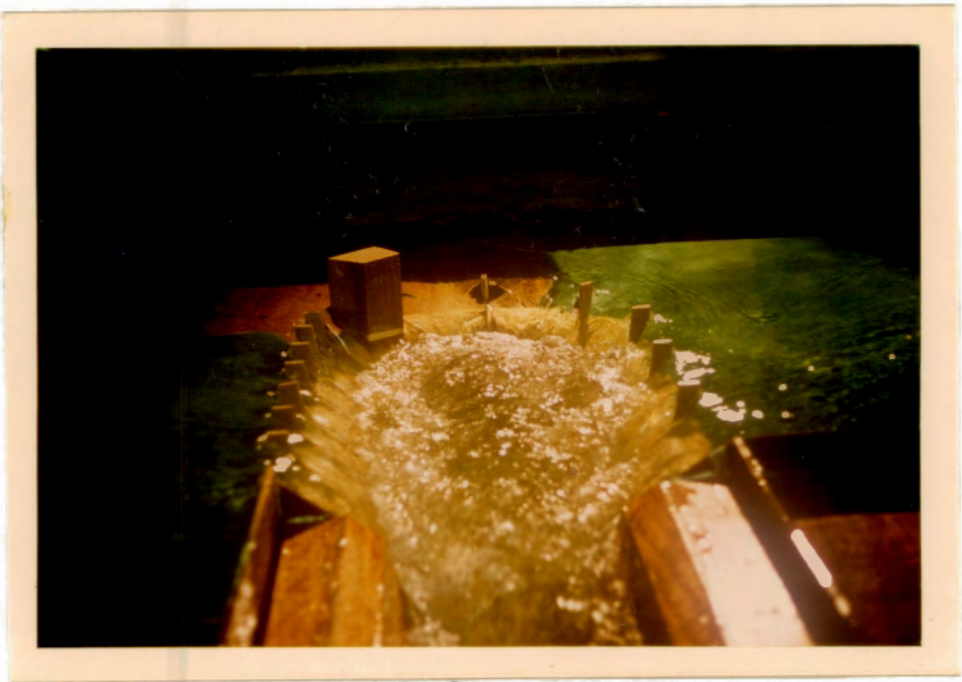

2

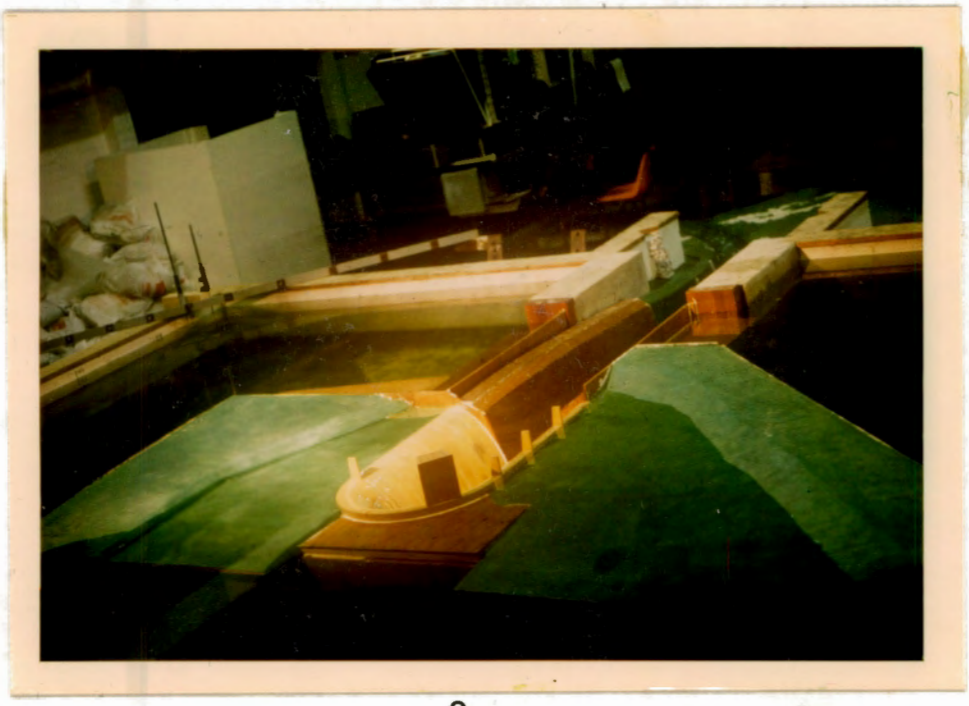

3

4

1 & 2 Receiving channel flowing full. Note the extreme turbulence and the hump shaped surface profile.

3 General view of model at a fairly high flow. Note very shallow approaches to the spillway.

4 The receiving channel at a low flow. Note the 'fountain' which develops at the centre of the curved section.

where the friction factor is independent of Reynolds number. To be able to scale up directly the depths measured in the model, the friction factor must be the same in the model and prototype. For this to be the case K/4R must be the same in the two cases which means that K for the prototype must be 64 times greater than in the model which means it should be 12,8mm.

This is unrealistically high and means that the model was made too rough. It can therefore be expected that in the prototype, depths will be shallower than predicted by the model. The clients design is therefore safe and can be constructed with confidence.

1 & 2 Receiving channel flowing full. Note the extreme turbulence and the hump shaped surface profile.

3 General view of model at a fairly high flow. Note very shallow approaches to the spillway.

7. DESIGN PROCEDURE

This thesis is concerned with the calculation of the water surface profile in the receiving channel of a side-channel spillway. However, before this can be done, it is necessary to know the dimensions of the structure. The aim of the designer is to choose these dimensions so that the cost of the structure is as low as possible, while ensuring that it has the required capacity. The required procedure can be summarised in the following steps.

1. From the design flow and maximum allowable head, choose the shape of the spillway crest and the length of the spillway.
2. Choose reasonable dimensions for the receiving channel, i.e. general configuration with respect to spillway, cross-section, invert slope, etc.
3. Decide on the configuration of the discharging channel.
4. Find the position of the control point (e.g. from Figure 32).
5. Calculate the water surface profile to ensure that the channel is running at capacity. It is usually considered acceptable that the spillway be drowned to a depth of half the head. An initial check can be done by using figures 14 or 15 to find the upstream depth. If this gives a satisfactory value, the complete profile should be calculated from figure 31 or by computer.
6. Make a rough estimation of quantities and cost.
7. Return to step 2 above and using different dimensions repeat steps 2 to 6.
8. Having found the most economical side channel spillway, compare its cost with that of other types of structures.
9. Complete the detailed design of the chosen structure.

APPENDIX A

TABULATED RESULTS OF MODEL TESTS

TEST NO. 1a

Flow Measurement:

top	5,85	5,84	5,86	5,85	
bottom	0,55	0,59	0,54	0,56	$\bar{h}$
difference	5,30	5,25	5,32	5,29	5,29

$Q = 0{,}0391\sqrt{\bar{h}} = 0{,}0899$ cumecs.

Water Depths:

			Readings			Water Depths		
No	x	base level	a	b	c	a	b	c
1	22,5	280	625	615	-	345	335	-
2	305	280	655	-	650	375	-	370
3	605	280	630	625	640	350	345	360
4	905	280	615	605	630	335	325	350
5	1205	280	585	550	606	305	270	325
6	1495	280	375	330	450	95	50	170

TEST NO. 1b

Flow Measurement:

top bottom	5,89 77	5,90 76	5,90 75	5,91 76	$\bar{h}$
difference	5,12	5,14	5,15	5,15	5,14

$Q = 0{,}0391\sqrt{\bar{h}} = 0{,}0886$ cumecs.

Water Depths:

			Readings			Water Depths		
No	x	base level	a	b	c	a	b	c
1	22,5	280	625	615	-	345	335	-
2	305	280	650	-	655	370	-	375
3	605	280	630	620	640	350	340	360
4	905	280	615	590	625	335	310	345
5	1205	280	580	550	600	300	270	320
6	1495	280	385	335	460	105	55	180

TEST NO. 1c

Flow Measurement:

top	6,04	6,06	6,03	6,04	$\bar{h}$
bottom	1,74	1,70	1,72	1,73	
difference	4,30	4,36	4,31	4,71	4,42

$Q = 0{,}0391\sqrt{\bar{h}} = 0{,}0822$ cumecs.

Water Depths:

			Readings			Water Depths		
No	x	base level	a	b	c	a	b	c
1	22,5	280	615	590	-	335	310	-
2	305	280	600	-	635	320	-	355
3	605	280	615	595	625	335	315	345
4	905	280	585	580	615	305	300	335
5	1205	280	555	520	600	275	240	320
6	1495	280	370	335	455	90	55	175

TEST NO. 1d

Flow Measurement:

top	5,88	5,89	5,85	5,89	
bottom	3,63	3,62	3,64	3,62	$\bar{h}$
difference	2,25	2,27	2,21	2,27	2,25

$Q = 0{,}0391\sqrt{\bar{h}} = 0{,}0587$ cumecs.

Water Depths:

			Readings			Water Depths		
No	x	base level	a	b	c	a	b	c
1	22,5	280	545	530	-	265	250	-
2	305	280	560	-	600	280	-	320
3	605	280	555	530	580	275	250	300
4	905	280	545	510	565	265	230	285
5	1205	280	510	470	555	230	190	275
6	1495	280	365	335	425	85	55	145

TEST NO. 1e

Flow Measurement:

top	5,580	5,590	5,586	5,585	
bottom	4,795	4,782	4,786	4,783	$\bar{h}$
difference	0,785	0,808	0,800	0,802	0,799

$Q = 0{,}0391\sqrt{\bar{h}} = 0{,}0350$ cumecs.

Water Depths:

			Readings			Water Depth		
No	x	base level	a	b	c	a	b	c
1	22,5	280	470	455	-	190	175	-
2	305	280	490	-	515	210	-	235
3	605	280	490	450	520	210	170	240
4	905	280	480	435	505	200	155	225
5	1205	280	465	410	495	185	130	215
6	1495	280	355	320	370	75	40	90

TEST NO. 1f

Flow Measurement:

top	4,14	4,13	4,13	4,12	
bottom	2,92	2,91	2,92	2,91	$\bar{h}$
difference	1,22	1,22	1,21	1,21	1,215

$Q = 0{,}0391\sqrt{\bar{h}} = 0{,}0136$ cumecs.

Water Depths

			Readings			Water Depths		
No	x	base level	a	b	c	a	b	c
1	22,5	280	380	376	-	100	96	-
2	305	280	385	-	398	105	-	118
3	605	280	381	367	391	101	87	111
4	905	280	376	362	387	96	82	107
5	1205	280	365	350	373	85	70	93
6	1495	280	308	303	311	28	23	31

TEST NO. 2a

Flow Measurement:

top	6,120	6,115	6,121	6,103	$\bar{h}$
bottom	0,770	0,840	0,815	0,810	
difference	5,350	5,275	5,306	5,293	5,306

$Q = 0{,}0391\sqrt{\bar{h}} = 0{,}090$ cumecs.

Water Depths:

			Readings			Water Depths		
No	x	base level	a	b	c	a	b	c
1	22,5	300	633	626	624	333	326	324
2	305	294	650	645	665	366	351	371
3	605	288	635	635	650	347	347	360
4	905	282	620	600	640	340	318	360
5	1205	276	580	545	610	300	270	330
6	1495	270	375	335	455	105	65	185
7	1500	-	-	-	-	210	190	160

TEST NO. 2b

Flow Measurement:

top	6,200	6,200	6,230	6,200	
bottom	2,980	2,968	2,975	2,955	$\bar{h}$
difference	3,220	3,232	3,255	3,245	3,238

$Q = 0{,}0391\sqrt{\bar{h}} = 0{,}0704$ cumecs.

Water Depths:

			Readings			Water Depths		
No	x	base level	a	b	c	a	b	c
1	22,5	300	568	573	570	268	273	270
2	305	294	615	585	630	321	291	336
3	605	288	586	565	620	298	277	332
4	905	282	560	545	605	278	263	323
5	1205	276	550	505	675	274	229	399
6	1495	270	365	330	440	95	60	170
7	1500	-	-	-	-	190	170	140

TEST NO. 2c

Flow Measurement:

top	5,827	5,825	5,825	5,826	
bottom	4,615	4,626	4,618	4,620	$\bar{h}$
difference	1,212	1,199	1,207	1,206	1,206

$Q = 0{,}0391\sqrt{\bar{h}} = 0{,}0429$ cumecs.

Water Depths:

			Readings			Water Depths		
No	x	base level	a	b	c	a	b	c
1	22,5	300	515	483	502	215	183	202
2	305	294	528	484	550	234	190	256
3	605	288	521	477	542	233	189	254
4	905	282	510	456	533	228	174	251
5	1205	276	483	427	515	207	151	239
6	1495	270	350	316	490	80	46	220
7	1500	-	-	-	-	150	130	100

TEST NO. 2d

Flow Measurement:

top	6,586	6,587	6,586	6,586	
bottom	6,310	6,311	6,310	6,310	$\bar{h}$
difference	0,276	0,276	0,276	0,276	0,276

$Q = 0{,}0391\sqrt{\bar{h}} = 0{,}0205$ cumecs.

Water Depths:

			Readings			Water Depths		
No	x	base level	a	b	c	a	b	c
1	22,5	300	417	407	424	117	107	124
2	305	294	424	402	450	130	108	156
3	605	288	424	394	446	136	106	158
4	905	282	416	384	435	134	102	153
5	1205	276	395	368	425	119	92	149
6	1495	270	314	311	326	44	41	56
7	1500	-	-	-	-	80	65	60

TEST NO. 2e

Flow Measurement:

top	6,518	6,518	6,518	
bottom	6,475	6,475	6,475	$\bar{h}$
difference	0,043	0,043	0,043	0,043

$$Q = 0{,}0391\sqrt{h} = 0{,}0081 \text{ cumecs.}$$

Water Depths:

			Readings			Water Depths		
No	x	base level	a	b	c	a	b	c
1	22,5	300	358	354	338	58	54	38
2	305	294	357	351	348	63	57	54
3	605	288	351	346	349	63	58	61
4	905	282	344	337	336	62	55	54
5	1205	276	331	328	334	55	52	58
6	1495	270	296	292	294	26	22	24
7	1500	-	-	-	-	44	33	36

TEST NO. 3a

Flow Measurement:

top	5,610	5,600	5,615	5,590	
bottom	0,339	0,3400	0,375	0,362	$\bar{h}$
difference	5,271	5,260	5,230	5,228	5,247

$Q = 0{,}0391\sqrt{\bar{h}} = 0{,}090$ cumecs.

Water Depths:

			Readings			Water Depths		
No	x	base level	a	b	c	a	b	c
1	22	447	600	585	-	153	138	-
2	301	405	650	585	660	245	180	255
3	597	361	630	575	635	269	214	274
4	894	316	590	545	605	274	229	289
5	1191	272	545	485	580	273	213	308
6	1477	229	335	290	420	106	61	191
7	1500	-	-	-	-	220	210	160

TEST NO. 3b

Flow Measurement:

top	5,855	5,830	5,850	5,840	
bottom	1,765	1,779	1,772	1,795	$\bar{h}$
difference	4,090	4,051	4,078	4,045	4,066

$Q = 0{,}0391\sqrt{\bar{h}} = 0{,}079$ cumecs.

Water Depths:

			Readings			Water Depths		
No	x	base level	a	b	c	a	b	c
1	22	447	570	560	-	123	114	-
2	301	405	615	544	655	210	139	250
3	597	361	602	530	630	241	169	269
4	894	316	570	510	605	254	194	259
5	1191	272	530	460	550	258	188	278
6	1477	229	335	285	400	106	560	171
7	1500	-	-	-	-	210	190	150

TEST NO. 3c

Flow Measurement:

top	5,820	5,810	5,820	5,826	
bottom	2,629	2,635	2,652	2,605	$\bar{h}$
difference	3,191	3,175	3,168	3,221	3,189

$Q = 0{,}0391\sqrt{\bar{h}} = 0{,}070$ cumecs.

Water Depths:

			Readings			Water Depths		
No	x	base level	a	b	c	a	b	c
1	22	447	540	542	-	93	95	-
2	301	405	585	518	640	180	113	235
3	597	361	575	505	610	214	144	249
4	894	316	550	475	570	234	159	254
5	1191	272	500	435	550	228	163	278
6	1477	229	330	280	390	101	51	161
7	1500	-	-	-	-	200	170	120

TEST NO. 3d

Flow Measurement:

top	6,290	6,295	6,300	6,290	
bottom	4,075	4,068	4,070	4,082	$\bar{h}$
difference	2,215	2,227	2,230	2,208	2,220

$Q = 0{,}0391\sqrt{\bar{h}} = 0{,}058$ cumecs.

Water Depths:

			Readings			Water Depths		
No	x	base level	a	b	c	a	b	c
1	22	447	518	516	-	71	69	-
2	301	405	558	490	610	153	85	205
3	597	361	538	475	590	177	114	229
4	894	316	520	442	555	204	126	239
5	1191	272	475	400	535	203	128	263
6	1477	229	318	270	380	89	41	151
7	1500	-	-	-	-	160	140	120

TEST NO. 3e

Flow Measurement:

top	6,040	6,030	6,030	6,025	
bottom	4,875	4,880	4,886	4,894	$\bar{h}$
difference	1,165	1,150	1,144	1,131	1,148

$Q = 0{,}0391\sqrt{h} = 0{,}042$ cumecs.

Water Depths:

			Readings			Water Depths		
No	x	base level	a	b	c	a	b	c
1	22	447	488	487	-	41	40	-
2	301	405	500	463	550	95	58	145
3	597	361	482	435	520	121	74	159
4	894	316	460	402	505	144	86	189
5	1191	272	422	365	473	150	93	201
6	1477	229	303	265	325	74	36	96
7	1500	-	-	-	-	130	110	80

TEST NO. 3f

Flow Measurement:

top	5,765	5,765	5,765	
bottom	5,525	5,525	5,525	$\bar{h}$
difference	0,240	0,240	0,240	0,240

$Q = 0{,}0391\sqrt{\bar{h}} = 0{,}019$ cumecs.

Water Depths:

			Readings			Water Depths		
No	x	base level	a	b	c	a	b	c
1	22	447	464	460	-	17	13	-
2	301	405	448	437	431	43	32	26
3	597	361	410	395	394	49	34	33
4	894	316	376	355	358	60	39	42
5	1191	272	338	317	336	66	45	64
6	1477	229	267	260	265	38	31	36
7	1500	-	-	-	-	70	50	60

APPENDIX B

TABULATED RESULTS OF MTATA DAM TESTS

TEST 1 : All Splitters in position as in original plans

Flow Measurement (m, m^3/s)					Deep pool (mm)		Prototype values	
h_1	h_2	Δh	$\bar{h}$	Q	gauge	head	h(m)	$Q(m^3/s)$
6,459	6,559	0,100	0,100	0,0124	250,6	23,1	1,478	405
6,336	6,597	0,261						
6,340	6,610	0,270	0,266	0,0202	259,7	32,2	2,061	661
4,862	5,770	0,908						
4,860	5,770	0,910	0,909	0,0373	275,5	48,0	3,072	1222
4,050	6,019	1,969						
4,045	6,050	2,005						
4,046	6,051	2,005	1,993	0,0552	288,8	61,3	3,923	1809
2,931	6,260	3,229						
2,938	6,275	3,337						
2,926	6,277	3,351	3,339	0,0714	300,3	72,8	4,659	2341

TEST 2 : Control Tower and all splitters removed

Flow Measurement (m, m^3/s)					Deep pool (mm)		Prototype values	
h_1	h_2	Δh	$\bar{h}$	Q	gauge	head	h(m)	$Q(m^3/s)$
5,308	5,363	0,055	0,055	0,0092	245,6	18,1	1,158	300
5,020	5,472	0,452						
5,018	5,468	0,450	0,451	0,0263	562,7	35,2	2,253	860
4,528	5,630	1,102						
4,529	5,626	1,117	1,109	0,0412	274,4	46,9	3,002	1349
3,790	5,830	2,040						
3,812	5,810	2,008						
3,785	5,830	2,045	2,031	0,0557	284,6	57,1	3,654	1826
2,900	5,973	3,073						
2,895	5,980	3,085						
2,999	5,950	2,951	3,036	0,0681	292,8	65,3	4,179	2232
2,305	6,000	3,695						
2,289	6,010	3,721						
2,315	6,000	3,685	3,700	0,0752	297,4	69,9	4,474	2464

TEST 3 : With tower and 3 splitters for bridge supports

Flow Measurement (m, m^3/s)					Deep pool (mm)		Prototype values	
h_1	h_2	Δh	h	Q	gauge	head	h(m)	$Q(m^3/s)$
5,436	5,260	0,176	0,176	0,0164	250,9	23,4	1,498	538
5,715	4,433	1,282						
5,708	4,435	1,273						
5,708	4,440	1,268	1,274	0,0440	279,4	51,9	3,322	1446
5,945	3,460	2,485						
5,960	3,425	2,535						
5,950	3,400	2,550	2,523	0,0621	292,7	65,2	4,173	2035
6,070	2,399	3,671						
6,080	2,405	3,675						
6,065	2,425	3,640	3,662	0,0748	300,9	73,4	4,698	2451

TEST 4 : With Tower, 3 bridge supports, and a splitter on the opposite side at chainage 155.

Flow Measurement (m, m /s)					Deep pool (mm)		Prototype values	
h_1	h_2	Δh	$\bar{h}$	Q	gauge	head	h(m)	$Q(m^3/s)$
6,150	2,539	3,611			300,2			
6,142	2,520	3,622			299,5			
6,120	2,555	3,565			299,6			
6,120	2,549	3,571	3,592	0,0741	299,0	72,1	4,614	2428

TEST 5 : Depths measured along centre line of receiving and discharging channels

	Chainage	155	175	200	250	300	350	400	450	500	
Flow (m^3/s)	Q_m = 0,0074	125	100	90	75	70	70	70	70	39	Depth in model (mm)
	Q_p = 243	8,00	6,40	5,76	4,80	4,48	4,48	4,48	4,48	2,50	Prototype equivalent (m)
	Q_m = 0,0742	350	360	320	300	255	240	200	130	70	Depth in model (mm)
	Q_p = 2430	22,40	23,04	20,48	19,20	16,32	15,36	12,80	8,32	4,48	Prototype equivalent (m)

SUPPLEMENTARY TESTS : The splitter configuration in test 1a was as in test 1, in 2a as in 2 and in 3a as in test 3.

No	Flow Measurement (m, m^3/s)				Deep pool (mm)		L.H.S. (mm)		R.H.S. (mm)	
	h_1	h_2	Δh	Q	gauge	head	gauge	head	gauge	head
1a	6,035	2,483	3,552							
	6,055	2,450	3,605							
	6,070	2,435	3,635	0,0742	300,6	73,1	425,2	62,9	434,5	69,5
2a	6,040	2,430	3,610							
	6,050	2,415	3,635							
	6,050	2,423	3,627	0,0744	296,7	69,2	420,5	58,2	428,2	63,2
3a	6,035	2,483	3,552							
	6,055	2,450	3,605							
	6,070	2,435	3,635	0,0742	300,6	73,1	424,0	61,7	433,3	68,3

APPENDIX C

BIBLIOGRAPHY

1. 1926 : Hinds, J., "Side channel spillways", Transactions, American Society of Civil Engineers, Vol. 89, 1926, pages 881-927, discussion pages 928-939.

2. 1933 : Lane, E.W., "Hydraulic model tests for boulder dam spillways", Engineering News-Record, Vol. 111, No. 6, August 10th, 1933, pages 155-159.

3. 1934 : Meyer-Peter, E. and Favre, H., "Analysis of boulder dam spillways made by Swiss Laboratory", Engineering News-Record, Vol. 113, No. 17, October 25th, 1934, pages 520-522.

4. 1934 : Beij, K.H., "Flow in roof gutters", Journal of Research, U.S. National Bureau of Standards, Vol. 12, No. 2, February 1934, pages 193-213.

5. 1940 : Camp, T.R., "Lateral spillway channels", Transactions, American Society of Civil Engineers, Vol. 105, 1940, pages 606-617, discussion pages 618-637.

6. 1941 : Jordaan, J.M., "A note on trough spillways", Minutes of Proceedings of the South African Society of Civil Engineers, Vol. 39, 1941, pages 89-106, discussion pages 161-165.

7. 1944 : Keulegan, G.H., "Spatially variable discharge over a sloping plane", Transactions, American Geophysical Union, Pt. VI, 1944, pages 956-959.

8. 1944 : Izzard, C.F., "The surface profile of overland flow", Transactions, American Geophysical Union, Pt. VI, 1944, pages 959-968.

9. 1952 : Keulegan, G.H., "Determination of critical depth in spatially variable flow", Proceedings of the Second Midwestern Conference of Fluid Mechanics, The Ohio State University, Engineering Experiment Station, Bulletin 149, September 1952, pages 67-80.

10. 1955 : Li, W.H., "Open channels with nonuniform discharge", Transactions, American Society of Civil Engineers, Vol. 120, 1955, pages 255-274, discussion pages 275-280.

11. 1962 : Farney, H.S. and Markus, A., "Side channel spillway design", Proceedings of the American Society of Civil Engineers, Hydraulic Division, May 1962, pages 131-154. Discussion, November 1962, pages 225-231, January 1963, pages 227-229, July 1963, pages 209-215, and November 1963, pages 223-228

12. 1962 : Woo, D.C. and Brater, E.F., "Spatially varied flow from controlled rainfall", Proceedings of the American Society of Civil Engineers, Hydraulics Division, November 1962, pages 31-56. Discussion July 1963, pages 233-240 and November 1963, pages 249-250.

13. 1962 : Sharp, B.B. and James, J.P., "Spatially varied flow at the toe of a rock-fill slope". Proceedings of the 1st Australasian Conference on Hydraulics and Fluid Mechanics. December 1962.

14. 1963 : Myburgh, R.I.D.M., "Nooitgedacht earth dam central trough spillway". Transactions of the South African Institution of Civil Engineers, Vol. 5, No. 7, July 1963, pages 193-208. Discussion Vol. 6, No. 1, January 1964, pages 9-11.

15. 1967 : Smith, K.V.H., "Control point in a lateral spillway channel". Proceedings of the American Society of Civil Engineers, Hydraulics Division, May 1967, pages 27-34. Discussion January 1968, pages 317-321, July 1968, pages 1130-1134 and January 1969, pages 447-448.

16. 1967 : Hu, W.W., "Hydraulics of spatially varied pipe flow". Proceedings of the American Society of Civil Engineers, Hydraulics Division, November 1967, pages 281-296. Discussion July 1968, pages 1168-1171, November 1968, pages 1568-1569.

17. 1970 : Yen, B.C. and Wenzel, H.G., "Dynamic equations for steady spatially varied flow", Journal of the Hydraulics Division, Proceedings of the American Society of Civil Engineers, Vol. 96, No. HY3, March 1970, pages 801-814, Discussion, No. HY12, pages 2661-2665, No. HY7, pages 1137-1138.

18. 1970 : Fox, J.A. and Goodwill, I.M., "Spatially varied flow in open channels", Proceedings of the Institute of Civil Engineers, July 1970, pages 311-325, Discussion pages 579-588.

19. 1971 : Humpidge, H.B. and Moss, W.D., "The development of a comprehensive computer program for the calculation of flow profiles in open channels". Proceedings of the Institute of Civil Engineers, September 1971, pages 49-64.

20. 1971 : Moss, W.D., "Hydraulic design of side-channel spillways", Water and Water Engineering, August 1971, pages 302-307.

21. 1972 : Yen, B.C., Wenzel, H.G. and Yarn, Y.N., "Resistance coefficients for steady spatially varied flow". Journal of the Hydraulics Division, Proceedings of the American Society of Civil Engineers, Vol. 98, HY8, August 1972, pages 1395-1410.

22. 1972 : Smith, K.V.H., "Computer determination of the critical depth control points in open channel flow", Journal of the Hydraulics Division, Proceedings of the American Society of Civil Engineers, 1972, pages 461-470.

23. 1973 : Kinori, B.Z., "Channels with spatially increasing discharge, Water Power, May, 1973, pages 184-188.

24. 1973 : Shen, H.W. and Li, R., "Rainfall effect on sheet flow over a smooth surface", Journal of the Hydraulics Division, Proceedings of the American Society of Civil Engineers, May 1973, pages 771-792.

25. 1974 : Wilkinson, D.L., "Free surface slopes at controls in channel flow", Journal of the Hydraulics Division, Proceedings of the American Society of Civil Engineers, August 1974, pages 1107-1117.

26. Linford, A., "Flow measurement and meters", E and FN Spon Ltd., 22 Henrietta Street, London.

APPENDIX D

EXAMINATIONS WRITTEN TO COMPLETE THE REQUIREMENTS OF THE DEGREE

Examination		Year Passed	Credit Rating	Mark Obtained
	Management Accounting	June 1975	5	2+
	Probability and Statistics for Engineers	June 1975	4	2+
CE 516	Prestressed Concrete	Nov. 1975	5	2-
CE 525	Coastal Engineering	Feb. 1976	5	1
CE 519	Steel Structures	Nov. 1976	3	2+
CE 511	Hydraulic Transport of Solids in Pipelines	Feb. 1977	5	
Thesis	"Side Channel Spillways"	Feb. 1977	20	
		TOTAL.....	47	
	No of Credits required		40	

UNIVERSITY OF CAPE TOWN

DEPARTMENT OF ACCOUNTING

JUNE 1975 EXAMINATION

INTRODUCTION TO MANAGEMENT ACCOUNTING

SCORE: ◯ OUT OF 15 MARKS

INVENTORY COSTING

In a 'perpetual inventory' system of accounting for inventory the debit balance on the 'finished goods inventory' account should represent the cost of inventory on hand. There are various methods of determining cost.

YOU ARE REQUIRED TO
Name and explain briefly an alternative to each of the methods given below.

1.0 With regard to the cost of goods manufactured (debits to the inventory account):

1.1 DIRECT COSTING
An alternative is [ ] which means that :

1.2 'ACTUAL' COSTING
An alternative is [ ] which means that :

1.3 JOB COSTING
An alternative is [ ] which means that :

1.4 JOINT COSTS SPLIT ACCORDING TO SOME MEASURE OF SALES REVENUE
An alternative is [ ] which means that :

2.0 With regard to the cost of goods sold (credits to the inventory account):

2.1 WEIGHTED AVERAGE COST
An alternative is [ ] which means that :

ITMA 1975/FINAL/2

SCORE: ◯ OUT OF 5 MARKS

INVENTORY VALUATION

In placing a valuation on inventory for the purpose of the annual financial statements one has to consider not only the cost of the inventory.

YOU ARE REQUIRED TO

1. State what basis of valuation other than cost might be appropriate.

2. State with which statute and/or convention one would be complying.

PROCESS COSTING

Accounting A and Accountant B have been asked to cost a month's production of the same process. Part of their respective calculations are given below.

YOU ARE REQUIRED TO

Answer the questions on the following page.
(You may assume that there are no arithmetical errors)

ACCOUNTANT A'S SCHEDULE

		UNITS	MATERIALS	CONVERSION
	INPUTS		COSTS	
a	Beginning w i p (½ converted)	2 000	R 1 800	R 4 325
b	Started	18 000	18 000	34 600
c		20 000	R19 800	R38 925
	OUTPUTS		EQUIVALENT UNITS	
d	Completed			
	– from beginning w i p	2 000	–	1 000
	– started and finished	13 000	13 000	13 000
e	Normal loss	1 500	1 500	500
f	Ending w i p (4/5 converted)	3 500	3 500	2 800
g		20 000	18 000	17 300

ACCOUNTANTS B'S SCHEDULE

		UNITS	MATERIALS	CONVERSION
	INPUTS		COSTS	
a	Beginning w i p (⅓ converted)	2 000	R 1 800	R 4 325
b	Started	18 000	18 000	34 600
c		20 000	19 800	38 925
	OUTPUTS		EQUIVALENT UNITS	
d	Completed	15 000	15 000	15 000
e	Normal loss	1 500	1 500	500
f	Ending w i p (4/5 converted	3 500	3 500	2 800
g		20 000	20 000	18 300

Please refer to the previous page and answer the following questions:

1. Explain why they have arrived at different equivalent units.
   Which is correct and why ? 2

2. Explain why they have both used the same costs. 2

3. Give a probable explanation for the computation of equivalent units in respect of normal loss. 2

4. Using Accountant A's schedule, show (as far as the information allows) for all ledger accounts involved, the balances and the entries required to record the month's production.

CAPITAL INVESTMENT APPRAISAL AND BREAKEVEN

A small company manufactures a single product with one machine (Model A) which was purchased exactly two years ago for R40 000. The economic life of model A was (and is) estimated to be 10 years, after which it will have a scrap value of Rnil. Model A can be sold now for R12 000.

At present there is a fully automatic model B on offer for R50 000 delivered and installed. Model B has an estimated economic life of 8 years after which its estimated scrap value will be R3 000. Both machines qualify for an annual income tax depreciation allowance at the rate of 10% per annum on cost. Assume: that the company has a large taxable income; that the tax rate is 40%; that tax for any year is paid at the end of that year; that all cash flows occur at the end of the year.

The company's required earnings rate is 10% after tax. The present values of R1 at 10% are as follows:

Year 1	0,9
2	0,8
3	0,7
4	0,7
5	0,6
6	0,6
7	0,5
8	0,5
9	0,4
10	0,4

The following data apply to each machine respectively.

(All figures in thousands)	Model A	Model B
Production and sales	30 units	30 units
Sales Revenue	R210	R210
Variable cost	R135	R120
Fixed costs excluding depreciation	60	60
	195	180
Net income before depreciation	15	30

YOU ARE REQUIRED TO

1. Advise whether model A should be replaced by Model B, giving reasons.

2. If model A were to be replaced by model B show how the break even units and revenue would be affected.

Please use the worksheet on the following page.

UNIVERSITY OF CAPE TOWN

UNIVERSITY EXAMINATION OCTOBER 1975

PROBABILITY AND STATISTICS FOR ENGINEERS

EXTERNAL EXAMINER : PROFESSOR D.M. SCHULTZ
INTERNAL EXAMINER : MR. A.M. HURWITZ

TIME : 3 HOURS

ANSWER ANY SIX OF THE FOLLOWING NINE QUESTIONS.

---

1. (a) Briefly explain the meaning of each of the following terms (and give an example in each case):

"sample space"; "element of a sample space"; "event"; "null event".

(b) Prove: $P(E_1 \cup E_2) = P(E_1) + P(E_2) - P(E_1 \cap E_2)$ where P denotes "Probability", and E_1, E_2 are arbitrary events defined on a sample space S.

(c) 8 short stories are to be arranged in a book. If the arrangement is to be done in a random fashion, what is the probability that (i) neither the longest nor the shortest story will be placed first, (ii) the longest is placed last but the shortest is not placed first?

2. (a) Write down the probability functions of the hypergeometric, binomial and Poisson distributions, and in each case briefly describe the situation(s) in which they are used (i.e. the conditions under which they are valid and applicable).

(b) Suppose that 5% of the asprin tablets pressed by a certain type of machine are chipped. The tablets are boxed 12 per box. What percent of the boxes would you estimate:

(i) to be free of chipped tablets
(ii) to have exactly x chipped tablets.

(c) A bag of grass seeds is known to contain 1% weed seeds. A sample of 100 seeds is drawn randomly from the bag. Find the probabilities of 0,1,2,3 weed seeds being in the sample.

3. (a) What is an "operating characteristic curve" - how is it derived? What is the "Average Outgoing Quality"? Briefly explain its significance.

2/.....

continued .....

(b) In a quality control scheme, suppose that it is desired to reject with certainty all lots with more than 7% defectives, and to accept all lots with exactly 7% or less defectives.

What would the sample scheme and operating characteristic curve be in this case?

(c) Under the sampling scheme $n = 2$ and $c = 1$ (c = allowable number of defectives), and given the probabilities:

$P(x = 0|\theta = 0,1) = 0,81$
$P(x = 0|\theta = 0,2) = 0,64$
$P(x = 0|\theta = 0,3) = 0,49$
$P(x = 0|\theta = 0,4) = 0,36$
$P(x = 0|\theta = 0,5) = 0,25$
$P(x = 1|\theta = 0,1) = 0,18$
$P(x = 1|\theta = 0,2) = 0,32$
$P(x = 1|\theta = 0,3) = 0,42$
$P(x = 1|\theta = 0,4) = 0,48$
$P(x = 1|\theta = 0,5) = 0,50$

sketch the operating characteristic curve with respect to the scheme.

(a) Find the mean and variance of the binomial distribution using the moment generating function.

(b) Suppose that a point, e, is picked at random inside the unit circle in the (x,y)-plane.

What is the sample space in this situation?

Let r be the distance from the point e to the centre of the circle. What is the cumulative distribution function of r? What is the probability density function and the sample space of r?

(c) Let x_1 be a number taken at random on the interval (0,1) and x_2 a number taken at random on the interval $(x_1,1)$. Show that the distribution of x_2 has probability density function

$$f(x_2) = -\log(1-x_2)$$
$$0 < x_2 < 1$$
$$= 0 \quad \text{elsewhere}$$

(Hint: Use conditional distributions.)

University Examination October 1975
Probability and Statistics for Engineers

(a) A random variable is said to have the Normal Distribution $N(\mu,\sigma^2)$ if its probability density function is

$$f(x) = \frac{1}{\sigma\sqrt{2\pi}} \; e^{-\frac{1}{2}\left(\frac{x-\mu}{\sigma}\right)^2} \qquad -\infty < x < \infty$$

Show that μ is the mean of the distribution.

(b) What is the "Standard Normal Distribution", and what is its use? How do we approximate a binomial distribution to a normal?

(c) It is known that the probability of dealing a bridge hand with at least one ace is approximately 0,7. If a person plays 100 hands of bridge, what is the approximate probability that the number of hands he will receive containing at least one ace will be between 60 and 80 inclusive?

(a) What is a "statistic"? a "parameter"? If we are considering a population whose distribution has a parameter θ, what do we mean by an "unbiased estimator" for θ?

(b) Show how to construct a $100(1-\alpha)\%$ confidence interval for the difference of means from two normal populations with equal but unknown variances.

(c) Suppose that random samples of 25 are taken from two large lots of bulbs, and the standard deviations of the bulb lives were found to be: $S_A = \sqrt{10}$

$$S_B = \sqrt{12}$$

Find 95% confidence limits for $\frac{\sigma_A^2}{\sigma_B^2}$, the ratio of the population variances.

(Note: $F(n_1,n_2;\ 1-\frac{\alpha}{2}) = \frac{1}{F(n_1,n_2;\ \frac{\alpha}{2})}$)

(a) What do we mean by the "Power" of a statistical test?

(b) If, in a left-sided statistical test of $H_0 : \mu = \mu_o$ against $H_1 : \mu = \mu_1 < \mu_o$, we let

α = Probability of a type I error
β = probability of a type II error

Show, with the aid of a sketch, what the power function value is at μ_o.

4/.....

continued .....

(c) The standard deviation of muzzle velocities of a random sample of nine rounds of ammunition was found to be $s = 93,2$ ft. per second. If the "standard" value of σ for the muzzle velocity of this type of ammunition is 70 ft. per second is the value of s significantly large at the 5% level of significance?

(a) In "Goodness of Fit" tests the Chi-squared statistic

$$\chi^2 = \sum_{i=1}^{K} \frac{(f_i - n\theta_i)^2}{n\theta_i}$$ is used. Explain the theory underlying this statistical test.

(b) How is the χ^2 statistic of part (a) used to test independence of factors in a 2×2 "contingency table" when the probabilities of the two factors are unknown?

(c) Pieces of Vulcanite were examined according to porosity and dimensional defects, and the results are shown in the following table:

	Porous	Non-Porous
With Defective Dimensions	142	331
Without Defective Dimensions	1233	5099

Test the hypothesis that the two criteria of classification are independent at the 5% level.

(a) Breifly explain, with the aid of a sketch, the concept of fitting a straight line to a set of data points, (x_i, y_i) $i = 1...n$, by the method of least squares. If we assume that the straight line has an equation of the form $E(y|x) = \alpha+\beta x$, write down the least squares formulae for estimating α and β.

(b) Write down the formula giving the sample correlation coefficient r.

If the population correlation coefficient is ρ, how would you test the hypothesis $H_0 : \rho = 0$ against the alternative hypothesis $H_1 : \rho \neq 0$?

(c) The data shown below was obtained in an experiment to study the relationship between the amount of beta-enthyroidine x (in milligrams) in an aqueous solution and colorimeter reading of turbidity y of the solution.

5/.....

9. (c) continued .....

y	x
89	40
175	50
272	60
335	70
390	80
415	90

(i) Determine the regression line of y on x.
(ii) Estimate the variance, σ^2, of y.

UNIVERSITY OF CAPE TOWN

DEPARTMENT OF CIVIL ENGINEERING

UNIVERSITY EXAMINATION: DECEMBER, 1975

M.Sc. IN CIVIL ENGINEERING

COURSE CE 516: PRESTRESSED CONCRETE

Time allowed: 3 hours

Attempt ALL questions

Any books and notes may be used

1. (a) State as concisely as possible the reason why it is essential in prestressed concrete design to check both the serviceability and and ultimate limit states.

[3 marks]

(b) In a partially prestressed member a certain amount of untensioned reinforcement is normally required. Show, with the aid of appropriate diagrams, how you would determine, in the design of a particular member according to CP 110, the relative costs of using prestressing steel, high yield reinforcing steel or mild steel to provide the additional reinforcement required. Assume that unit rates for the three types of steel are available.

[12 marks]

2. Write brief notes (about half a page) on each of the following:-

(a) The main factors affecting creep in prestressed concrete listed in order of importance with respect to a typical structure such as a highway bridge.

(b) The reasons for avoiding either too small or too large a percentage of steel in a prestressed concrete member.

(c) Compare and contrast flexural cracking and shear cracking.

(d) Linear transformation of a cable profile.

(e) The mechanism of failure of a concrete beam in torsion, with comments on the effect of shear and bending moment in combination with torsion.

[25 marks]

/3. .....

3.

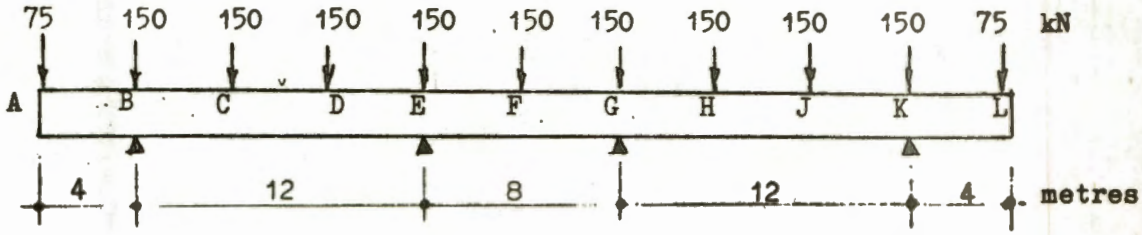

The rectangular, post-tensioned concrete beam shown above is simply supported at B, E, G and K. The beam carries eleven equally spaced columns supporting an upper floor. The sustained loads transmitted by these columns to the beam are as shown (viz. 75 kN at A and L; 150 kN at all the other points). In addition to its self-weight, the beam has to carry a sustained load of 20 kN/m throughout its length.

Use the load balancing method, balancing all sustained loads, to give a suitable preliminary design (i.e. beam size, cable profile and prestress force).

The design should comply with the following constraints:-

(a) Minimum width of beam : 250 mm

(b) Maximum depth of beam : 1200 mm

(c) Minimum cover distance to centroid of tendons: 100 mm

(d) Maximum average concrete stress : 6 MPa.

Assume furthermore that prestressing losses are negligible so that the prestressing force is constant throughout.

Assume Weight of Concrete = 25 kN/m^3

[20 marks]

4.

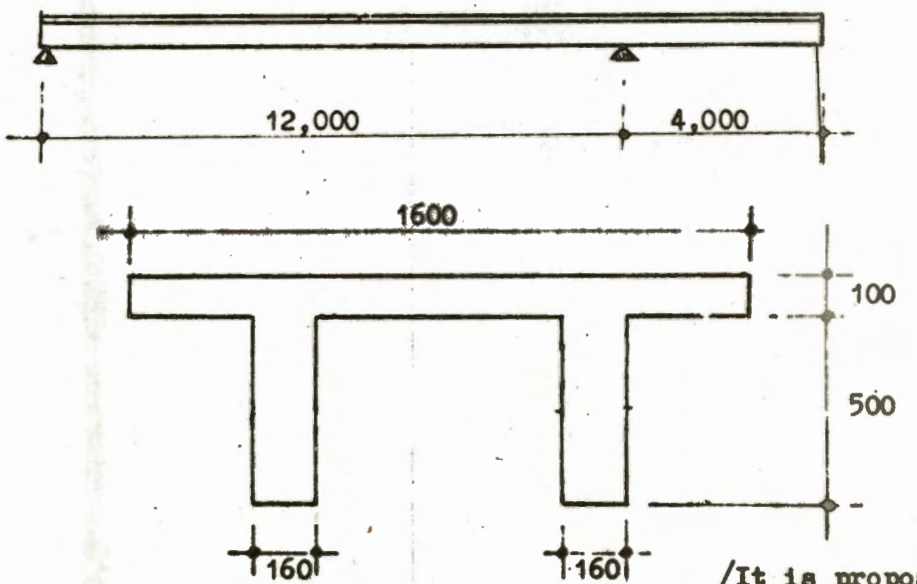

/It is proposed ...

4. (Continued)

It is proposed to build a prestressed concrete floor spanning 12 metres with an additional 4 metre cantilever. Pretensioned double-T units of the uniform cross-section shown above are to be used. These are to be designed according to CP 110 as Class 3 members, using the minimum prestressing force and providing additional untensioned reinforcement where necessary.

The floor is required to carry an imposed loading of 10 kN/m^2 over any part.

Prestressing is to be accomplished using straight horizontal tendons only.

Determine the following:-

(a) The minimum prestressing force required and its eccentricity. (Consider only the support points and midspan. neglecting the slightly higher moments just to the left of midspan).

(b) The area of additional untensioned reinforcement required at midspan using either prestressing wire or high yield reinforcing steel.

Comment on the merits and demerits of the resulting design.

Necessary data:

Use Concrete Grade 50 (i.e. f_{cu} = 50 MPa)

Permissible compressive stress for serviceability limit state: 16,7 MPa
Permissible hypothetical tensile stress for serviceability limit state (including depth factor): 5,8 MPa.

Weight of concrete = 25 kN/m^3

Minimum cover distance to centroid of prestressing tendons: 80 mm

Factors of Safety for Ultimate Limit State: Dead Load: 1,4
Imposed Load: 1,6

Characteristic strength of prestressing wire: f_{pu} = 1550 MPa

Residual prestress (after losses): 0,6 f_{pu}

Characteristic strength of high yield steel: f_y = 460 MPa

Cost of untensioned prestressing wire: R700/ton

Cost of high yield reinforcing steel: R350/ton

Modulus of Elasticity for steel: 200 GPa

Design curves for prestressing wire and high yield steel are attached.

[40 marks]

UNIVERSITY OF CAPE TOWN

DEPARTMENT OF CIVIL ENGINEERING

M.Sc IN CIVIL ENGINEERING

UNIVERSITY EXAMINATION : FEBRUARY 1976

CE 525 : Coastal Engineering

All Questions may be attempted — Time : 3 hours

Constants

Sea water density = 1025 kg/m^3

Sea water weight = 10 kN/m^3

1. A swell of 10 second period with a deep water wave height of 3 m approaches a beach with the wave crests parallel to the shore. Trace the progress of this wave in shoaling water through to the breaker point including the following calculations :-
   (a) the wave length and wave celerity in deep water
   (b) the water depth at which the wave begins to be affected by the presence of the sea bed.
   (c) the wave length and wave celerity for water depths at 10 m intervals between d=80 m and d=10 m, and at 1 m intervals between d=10 m and d=1 m.
   (d) the depth of water in which the wave breaks, the type of breaker and the wave height at breaking. Ignore the effect of wave set up or down.
   (e) sketch the effect of wave set up and down including an estimate of depths.
   (f) estimate the wave heights in the surf zone.
   (g) calculate the energy flow in W/m in water depths of 10 m, 5 m, and 2 m.

slope
50

2. A cylindrical pipe is laid on the sea bed across a harbour entrance in 10 m of water, the pipe diameter being 1 m and the axis of the pipe is parallel to the local wave crests. If the local wave length is 50 m, estimate the wave period, and find the peak magnitudes of the velocity and acceleration force components per metre length of pipe. Estimate the peak resultant force in the inshore direction, and the

.Sc. examination CE 525
eb.1976

3.(a). A storm at sea generates waves with a period range of 6 to 12 seconds. The resulting swell travels towards a harbour 400 km away. Estimate the time required for the longest waves to cover the intervening distance, assuming deep water throughout. Also estimate how much later the shortest waves will begin to arrive.

(b). A refraction diagram is constructed for a bay and the spacing between a particular pair of adjacent orthogonals doubles in travelling from deep water to the 10 m depth, the wave period being 7 seconds. Estimate the percentage change in wave height ocurring between these zones on the assumption that no breaking waves are present between the zones.

(c).Suggest some of the requirements you would incorporate into a specification for armour blocks.

4. The overleaf page shows the plan views of three separate coastal structures on which oblique waves impinge. In each case indicate areas where you consider deposition or erosion will occur, and also estimate the shape of the breaker line once stable conditions are established

5. There is a continuous dissipation of energy due to tidal movements of water over the earths surface, and in some instances useful power is abstracted from the sea in tidal power schemes. Suggest what effect this may have on the dynamics of the earth-moon system over very long periods of time.

UNIVERSITY OF CAPE TOWN

DEPARTMENT OF CIVIL ENGINEERING

UNIVERSITY EXAMINATION: 13th NOVEMBER, 1976

CE 519 - STEEL STRUCTURES

Time allowed: 3 hours

1.

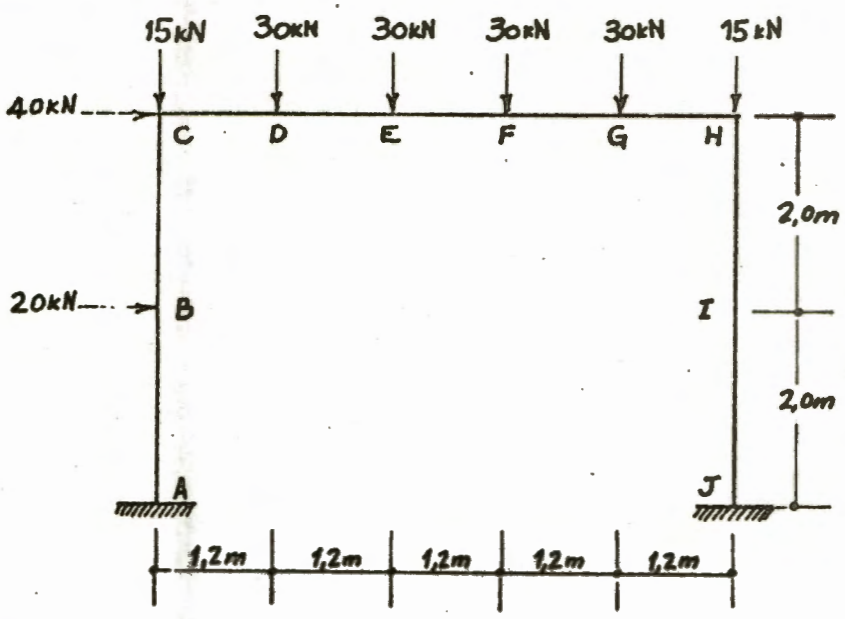

The rectangular frame shown above is to be designed by plastic methods. The loads shown are working loads: the vertical loads represent dead plus superimposed loads and the horizontal loads represent wind loads. The wind loads may act from left to right (at B and C as shown) or from right to left (at H and I).

1. Use limit analysis to determine the least value of M_p for which the frame can equilibrate all factored load combinations using the following assumptions:

   (a) the frame is designed with a uniform section,

   (b) the load factor for dead plus superimposed load alone is 1,75, and for dead plus superimposed load plus wind load 1,4.

   Draw the bending moment and shear force diagrams, and determine the axial loads in the members, for the collapse conditions.

   [40 marks]

2. Using the Abridged Version of the Handbook on Hot Rolled Structural Steel Sections, and the Design Recommendations issued, select an appropriate parallel flange I-section for this design. The yield stress is to be taken as 250 MPa.

   Choose your section/sections with respect to the collapse bending moments, shear forces and axial loads. Consider

   (a) whether the section or sections chosen is/are compact,

   (b) whether shear stiffeners are required,

   (c) lateral stability and the points at which lateral bracing is required,

   (d) in-plane buckling.

   35 marks]

3. The moments computed from an elastic analysis with uniform E.I. over the entire frame are given below. Tension on the inside of the frame is taken as positive.

Section	Moment due to vertical loads only (kNm)	Moment due to wind only acting from left to right (kNm)
A	+ 27,00	- 70,91
B	- 13,50	+ 1,93
C	- 54,00	+ 34,77
D	+ 18,00	+ 20,36
E	+ 54,00	+ 5,95
F	+ 54,00	- 8,45
G	+ 18,00	- 22,86
H	- 54,00	- 37,27
I	- 13,50	+ 9,95
J	+ 27,00	+ 57,16

Assume for simplicity that the dead and superimposed load together may or may not act. The wind may act from left to right or from right to left.

For the M_p value calculated in part (a), determine the load factor against failure by alternating plastic deformation at any section.

Do you consider this result to be significant in determining member sizes?

[10 marks]

4.

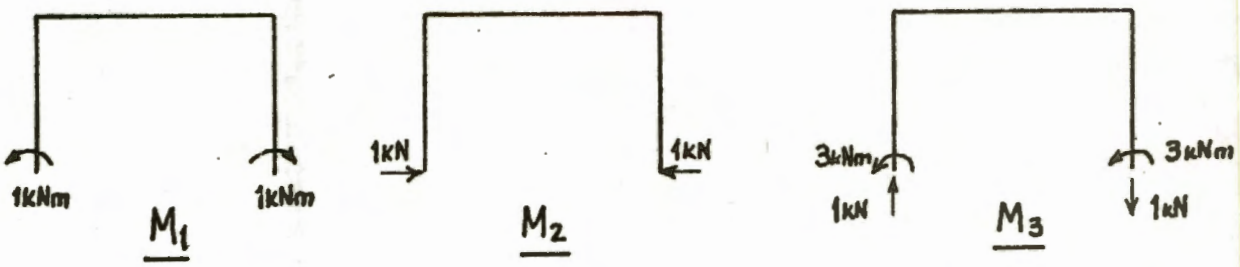

Using the three independent self-stress systems associated with the force systems shown above, write down the compatibility equations for the structure analysed in 1. above at the point of collapse. Assume plastic hinge rotations at each of the hinges in the mechanism.

You may take the following values for the integrals below:

$$\int M_1 \frac{M}{EI} ds = - 0,0076 \text{ kNm}$$

4. (Continued)

$$\int M_2 \frac{M}{EI} ds = - 0{,}0491 \text{ kNm}$$

$$\int M_3 \frac{M}{EI} ds = + 0{,}0240 \text{ kNm}$$

M is the collapse bending moment diagram, and moments causing tension on the inside are positive. The integrals extend over the whole structure.

Hence determine which is the last hinge to form.

[15 marks]

UNIVERSITY OF CAPE TOWN

DEPARTMENT OF CIVIL ENGINEERING

UNIVERSITY EXAMINATION: FEBRUARY, 1977

COURSE CE 511 - SEDIMENT TRANSPORTATION

Note: This is an 'open book' examination. Scripts are to be collected at 5.30 p.m. on Thursday, 24th February 1977 and returned by 9.00 a.m. on Monday, 28th February, 1977. The attached affidavit is to be signed by each student on receipt of the examination script.

Answer ALL questions

1. One criterion for determining whether suspensions will be settling or non-settling is a particle Reynolds number of 2,0. For sand of relative density S_s = 2,65, indicate into which category "average" particles of sand, of mean particle diameter 38, 100, 250, 1000 and 2000 μm at concentrations of 0, 10, 20 and 30%, will fall. Tabulate your results and show how they can be presented graphically. Hence determine for each of the four concentrations, the particle size which designates the boundary between settling and non-settling suspensions.

   (a) Compare the above results with those obtained by two other methods.

   (b) Repeat the above procedure for coal of sphericity 0,7 and relative density as given by Fig. 3.11.

   (c) Repeat the above procedure for iron ore assuming spherical particles and a relative density of 4,0. In this case include particles of size d = 2,5 mm. Assume $\nu = 1{,}14\ mm^2/s$

2. Carry out a feasibility study for transporting 10 million metric tonnes (1 metric tonne = 10^3 kg) of iron ore of relative density 4,0, a distance of 600 km in a horizontal pipeline with a load factor of 95%.

   Assume the pipe roughness is constant at k = 0,06 mm and the kinematic viscosity of water is $\nu = 1{,}14\ mm^2/s$.

   In order to carry out the feasibility study, consider five alternative proposals.

   (i) Assume that the ore is crushed to an average particle size of d = 2,5 mm and the mean drag coefficient can be taken as $C_D = 0{,}44$.

      (a) Which flow regime would you consider as being feasible for transportation of this material and why?

      (b) Assume that the delivered volumetric concentration is C_{vd} = 20%. Determine the limit deposit velocity according to Durand and show that the pipe diameter required to operate at the minimum energy loss is approximately 300 mm.

      (c) What is the total power required per km? Compute this value as the average obtained by four methods.

      (d) Compare the pipe diameter obtained above with that obtained by another method for determining the value of the limit

2. (Continued)

(ii) In order to transport the material in the pseudo homogeneous regime at the same rate and volumetric concentration in a 300 mm diameter pipe it is possible to grind the material finer.

(a) Determine the drag coefficient of the finer material if it is just transported as a pseudo homogeneous mixture at the same rate (i.e. same mixture velocity).

(b) What is the mean particle size of this finer material ? Assume that the analysis for spherical particles applies. Compare this result with the results obtained in (i)(c) above.

(c) What is the total power requirement in this case?

(iii) The finer material can also be transported at a lower mean mixture velocity as a heterogeneous suspension in the 300 mm diameter pipe.

(a) What is the power requirement in this case? Assume that the heterogeneous mixture is transported at the minimum deposit velocity as determined from the Durand equation with the coefficient $F_L = 0,95$. Note that the delivered volumetric concentration will be greater than 20% in this case.

(iv) The material is ground further to give a non-Newtonian suspension at 20% volumetric concentration.

(a) What would the average size of particle have to be in this case?

(b) The rheological properties as determined by means of a capillary tube viscometer, 3 mm in diameter and 3 m long, are as follows:-

Mass Flow (g/s)	0,848	1,69	2,54	4,24	8,48
Pressure Drop (kN/m^2)	4,0	7,2	10,8	16,8	36,0

Determine the power requirement for the same flow rate as in schemes (i) and (ii)

(v) Consider a pipe diameter of 500 mm with the average roughness size of 0,06 mm and for the same mixture flow rate and material concentration as in scheme (iv), determine the power requirement.

Summarise the power requirements, in tabular form, for the five schemes considered above and comment briefly on the feasibility of scheme (v) as compared with the other schemes.

3. Coal of size $d_{50} = 225\ \mu m$ was tested in pipeline test loops of 100 mm and 200 mm diameters at a concentration by weight of $C_w = 53\%$. The relative density of the coal is 1,5 and the kinematic viscosity of water $\nu = 1,14\ mm^2/s$. The following test results were obtained at $V_m = 1,75$ m/s:-

D(mm)	100	200
i_m	0,0457	0,0224

/The pipes .....

3. (Continued)

The pipes were found to be hydraulically smooth.

Determine the head loss in a 300 mm diameter pipe at a mean mixture velocity of 1,75 m/s. Use three different methods of scaling and compare them.

4. Calculate the mixture head loss in units of clear fluid (water) for the coal described above, assuming a heterogeneous flow regime in a pseudo homogeneous mixture (i.e. the method of Wasp et al) in a 300 mm diameter pipe. Compare with the Durand equation.

Assume that the Weltman Green equation $\mu = (\mu_o + A)\, e^{\beta v_r}$ applies

with $u_o = 1,14 \times 10^{-3}$ kg/ms

$A = 0,000064$ kg/ms

$\beta = 4,29.$

Ignore the effect of hindered settling of the particles.